2004

Application of linear parameter varying control synthesis in power systems

Wenzheng Qiu
Iowa State University

NOTE TO USERS

Application of linear parameter varying control synthesis in power systems

by

Wenzheng Qiu

A dissertation submitted to the graduate faculty

in partial fulfillment of the requirements for the degree of

DOCTOR OF PHILOSOPHY

Major: Electrical Engineering (Electric Power)

Program of Study Committee:
Vijay Vittal, Co-major Professor
Mustafa Khammash, Co-major Professor
Wolfgang Kliemann
James McCalley
Venkataramana Ajjarapu

Iowa State University

Ames, Iowa

2004

Graduate College
Iowa State University

This is to certify that the doctoral dissertation of

Wenzheng Qiu

has met the dissertation requirements of Iowa State University

Signature was redacted for privacy.

Co-major Professor

Signature was redacted for privacy.

Co-major Professor

Signature was redacted for privacy.

For the Major Program

TABLE OF CONTENTS

LIST OF TABLES

LIST OF FIGURES

ACKNOWLEDGMENTS

My foremost thanks goes to my co-major advisers Dr. Vijay Vittal and Dr. Mustafa Khammash. I thank them for their their insights and suggestions that helped to shape my research skills. The feedback they gave to me contributed greatly to this dissertation.

I would also like to express my gratitude to my graduate committee members, Drs. James McCalley, Wolfgang Kliemann, and V. Ajjarapu for their generous contributions of time and effort during this research project and for providing me with valuable comments on earlier versions of this dissertation.

My special thanks also go to Dr. Murti Salapaka for helping me further understand concepts in robust control. I appreciate the valuable discussions and suggestions he gave to me.

In addition, I am grateful to all the professors and graduate students in the electric power program at Iowa State University, whose presences and fun-loving spirits made the otherwise gruelling experience tolerable. I enjoyed all the vivid discussions we had on various topics and had lots of fun being a member of this fantastic group. During many discussions regarding my dissertation I received several valuable comments from: Qiming Chen, Badri Ramanathan, and Jialing Liu.

I feel a deep sense of gratitude to my parents who formed part of my vision and taught me the good things that really matter in life. I am grateful for my dear sister,Wenyan Qiu, for rendering me the sense and the value of sisterhood.

Last but not least, I thank my husband, Lu Li, for always being there when I needed him most, and for the love and support he gave to me through all these years.

CHAPTER 1. INTRODUCTION

1.1 Power System Oscillations

Power system oscillations are not a new phenomenon. The earliest recorded incidents in the 1930's were ascribed to governor dead band on hydro-generators. In the mid-1960's, "negative" damping was found during attempts to interconnect the Detroit Edison/Ontario Hydro/Hydro Quebec networks. The reason turned out to be the automatic voltage regulators (AVRs) of turbo-generators. Low frequency oscillations are quite a common problem in most interconnected power systems today. These oscillations are due to the dynamic interactions between the various generators associated with the presence of high gain AVRs and weak connections between distinct areas of a system because of long transmission lines. Unstable or poorly damped oscillations have been observed in power systems around the world (1).

Oscillations are a characteristic of power systems. They are initiated by any small disturbance in the system. Fundamentally, it's an exchange of momentum between the rotating components of the system - mainly the synchronous generators. Power system electromechanical oscillations are usually in the range between 0.1 and 2 Hz depending on the number of generators involved. Local oscillations lie in the upper part of that range and consist of the oscillation of a single generator or a group of generators against the rest of the system. In contrast, inter-area oscillations are in the lower part of the frequency range and comprise the oscillations among groups of generators in different geographical areas of the system. Compared with oscillations found in other dynamic

systems, power system oscillations exhibit low damping.

Local oscillations often occur when a fast exciter is used on the generator, and to stabilize these oscillations, power system stabilizers (PSS) were developed. Inter-area oscillations may appear as the system's load is increased across the weak transmission links in the system which characterize these oscillations (2). If not controlled, these oscillations may lead to total or partial power interruption (3). To ensure safe operation, limits have to be placed on the maximum transfer power over these strategic lines. However, in the present commercial climate of the electric power industry, restricting power transfers is not a preferred option. So the provision of adequate levels of damping for the various oscillations has been of growing concern. There is now a wide choice of devices available to provide additional system damping including: power system stabilizer (PSS), AVR and excitation systems of generators, governors and damping controllers installed on flexible AC transmission system (FACTS) devices, and synchronous condensors. Among them, PSSs remain the method of choice. Also there is an increasing interest in using FACTS devices such as Static var compensators (SVC) and thyristor controlled series capacitors (TCSC) to aid the damping of these oscillations.

1.2 Challenges in Damping Control in Power Systems

1. robustness

   Power system operating conditions vary with system configuration and load level in a complex manner. The system typically operates over a wide range of conditions. A variety of controllers are employed to ensure the system operates in a stable manner within its operating range.

   In the past, many efforts have been made to investigate the application of robust control techniques to power systems, such as Kharitonov's theorem(4), H_∞(5; 6; 7; 8; 9), L_∞(10; 11), and Structured Singular Value(SSV or μ) techniques(13). These

methods mainly use one Linear Time Invariant (LTI) controller to guarantee the robust stability and robust performance after describing the changes of operating condition as uncertainties.

With the increase of competition and deregulation, systems are being operated closer than ever to their limits, which makes it hard to design a LTI controller that performs well at all operating conditions because of the inherent system nonlinearity. The data in (16; 18) shows that power systems have zeros migrating to right half plane (RHP) when system operating conditions change. This kind of non minimum phase (NMP) behavior also poses a challenge to the performance and robustness of the system controllers. A fixed structure controller shows more and more limitations.

2. decentralized design and coordination

   For large power systems, a single local controller is no longer sufficient to stabilize the whole system and to obtain a satisfactory damping property. Centralized design is neither economical nor reliable due to the inherent constraints of large power systems such as geographic dispersion, topology variance, and nonlinearities. Decentralized design becomes a natural consideration. A coordinated action from the various controllers in the system is also needed. The control design method must minimize or prevent deleterious interactions among controllers, ensure the dynamic and steady state performance criteria for the system are satisfied, and provide a simple procedure for tuning the controllers.

1.3 Power System Stabilizer (PSS)

The PSS is often used to provide positive damping for power system oscillations. They are mostly single-loop local controllers, which use speed, power input signal, or

frequency and synthesize a control signal based on appropriate phase-lead compensations to add to the reference voltage signal of the voltage regulator. It is developed to extend stability limits by modulating the generator excitation to provide additional damping to the oscillations of synchronous machine rotors (53). Many methods have been used in the design of PSS, such as root locus and sensitivity analysis (53; 43), pole placement, adaptive control, etc.

The conventional PSS design produces a component of electrical torque in phase with the rotor speed deviations. It is based on a particular operating point. This could lead to non-optimal damping in the entire operating range. When used in a multi-machine system, it even decreases the damping in some cases. The procedure to tune the PSS is also very time consuming.

In recent years, considerable efforts have been placed on the coordinated synthesis of PSSs in large power systems. To achieve both a coordinated action and a better robustness with PSSs, an empirical tuning procedure (which aims to maximize the phase margin in the frequency range where the oscillations are expected to occur) is employed. Naturally, due to its empirical nature, the efficiency of this procedure is limited and depends strongly on the designer's experience and knowledge of the system. The robust control approaches were motivated by a prospect of overcoming the cited drawbacks of tuning. However, the typically high dimensions of the power system models constitute another factor that discourages the application of computationally intensive design techniques and leads to very high order controllers.

1.4 Discussion on Classical Gain Scheduling Control

It is well known that linear analysis techniques have been successfully applied in power systems. Normally each linear model is based on a fixed operating point. When the operating point varies, the original linear model is not applicable anymore because

of the nonlinearity of the system. The wide variations in the characteristics of the power system dynamics throughout the operating envelope make gain scheduling a particularly suitable design strategy to improve the robustness of the system. The classical gain scheduling control scheme is given in Fig.1.1

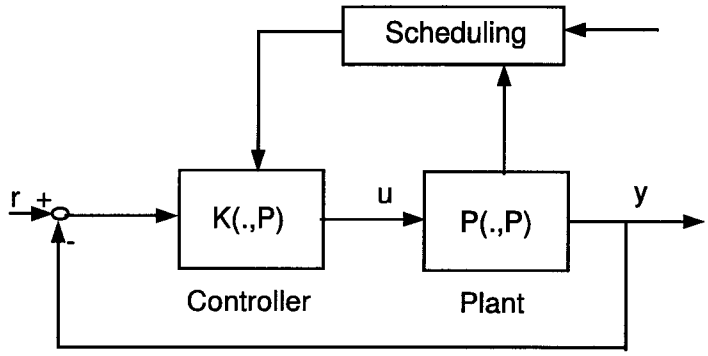

Figure 1.1 Classical gain scheduling control scheme

A typical procedure for classical gain scheduling design consists of the following steps:

1. Select several operating points which cover the range of the plant's dynamics and obtain a linear time-invariant (LTI) approximation to the plant at each operating point;

2. For each linearized plant, design a LTI controller to meet the performance requirements;

3. Then using a scheduling scheme, interpolate or schedule the local linear designs to yield an overall nonlinear controller that covers the entire operating range.

The concept of gain scheduling also has been introduced to power systems(34; 35; 36; 37; 39; 40; 41). The classical design procedure was followed. (34) applied this strategy for Power System Stabilizer (PSS) design for a single machine infinite bus (SMIB) system. The feedback gains are pre-calculated for various real and reactive power output conditions. (35) modelled the generation unit in a multi-machine environment as a single

machine connected to an infinite bus through a transmission line, the transmission line impedance is then used as a scheduling variable. This gain scheduling idea has several practical applications and promising improvement on a wide range of performance. But two disadvantages restrict it. One is the lack of a suitable theoretical guidance as mentioned before, hence, designers decide the scheduling law according to their practical experience and simulation. The other is the complicated control algorithm and requirement of on line model identification. Many new techniques like adaptive control(40), fuzzy logic, artificial neural networks(36; 41) are employed in this field. They do get better results but also pay the extra cost of system identification and/or network training. (39) approximated the single machine infinite bus system as a linear parameter dependent system against both the shunt loads and reference voltage changes. The controller design was applied based on this assumption. However, this assumption will not apply for large variations of operating conditions or large systems.

Although this approach works well in practice, it can not provide stability and performance guarantees except for slowly varying parameters(19; 20) and heuristic rules are followed. The stability of the gain-scheduled system is examined through extensive non-linear simulations. Furthermore, since these operating points are usually indexed by some combination of state or reference state trajectories, the procedure requires a complex parameter identification block to perform the scheduling and has to deal with delicate stability questions in the switching zone.

1.5 A Natural Extension – LPV Method

LPV theory has been developed in the past ten years. It is a natural extension of the conventional gain scheduling approach. The implication that linear parameter varying (LPV) system theory has for gain scheduling is obvious, since gain scheduling conceptually involves a linear, parameter-dependent plant. With real measurable scheduling

variable(s), it can achieve a larger system operating range while guaranteeing the stability and performance not only for slowly changing parameters but also for arbitrarily fast changing parameters. Compared with classical gain scheduling design, not only does it eliminate the strict limitations on the changing rates of scheduling variables, but also has theoretical guarantees for stability and performance instead of rules of thumb. In addition, LPV control theory has been proven useful in simplifying the interpolation and realization problems associated with conventional gain-scheduling. Specifically, it allows us to treat a series of scheduled controllers as a single entity, with the gain scheduling achieved entirely by the parameter dependent controller.

Instead of using a fixed LTI controller, a parameter dependent controller based on a single quadratic Lyapunov function is proposed here to guarantee the LPV system is exponentially stable and achieve an induced L2 norm performance objective from disturbance to error signals. To reduce the conservatism, the known bounds on the parameters' rates of variation are also introduced in the LPV controller design based on a parameter-dependent Lyapunov function. The resulting controller is time varying and smoothly "scheduled" by the measurement of varying parameters. Due to its adaptive nature, such a controller can achieve higher performance than classical robust LTI controllers. Moreover, they can be implemented at little or no extra cost.

Since the LPV theory can guarantee system stability and performance for arbitrarily fast changing scheduling variables, it also has the potential to be applied to the decentralized controller design. Instead of considering the interconnected system model, we just consider each individual machine and represent its interconnection with the rest of the system by arbitrarily fast changing real and reactive power output in some range. All possible dynamics at the interface between the generator and the rest of the system are supposed to be represented by this approach. As a result, the system is decoupled naturally and the order of the plant is decreased dramatically. In addition robustness is considered through the time changing controller whose parameters are dependent on the

scheduling variables, which represent the changes in the system operating conditions. The resulting controllers give satisfactory performance over a wide range of operating conditions.

1.6 Objectives and Scope of Research Work

The main objective of this research project is to apply the LPV techniques to the PSS design. The adaptive nature of a LPV controller is used to improve power system damping in a large operating range. Robustness and performance guarantees are given by the LPV theory. The research conducted develops a procedure for a single PSS design including design setup, selection of weighting functions, realization of the LPV PSS, etc. Inspired by the characteristic of a LPV controller, that it guarantees system stability and performance for arbitrarily fast changing scheduling parameters on a predefined range, further work is done on the application of LPV methods to decentralized PSS design. A systematic procedure for decentralized design is also developed. It accounts for the coordination automatically.

The scope of this research work includes the following:

1. Formulate the power system model as a LPV system in order to apply the LPV approaches. Linearization is applied to the nonlinear differential and algebraic equations at every operating point that is decided by the scheduling variables. The scheduling variables can be many changing parameters that are measurable in real time such as load levels, tie line flows and so on.

2. Develop a systematic procedure to design PSS using LPV synthesis approach. The feedback setup is constructed and guidelines for proper weighting function selection are given.

3. Synthesize a PSS using Single Quadratic Lyapunov Function based LPV method

that considers arbitrarily fast changing parameters. Nonlinear simulations are performed to verify the good damping performance of the LPV PSS. Comparisons with the H_∞ PSS and conventional PSS are made to show that the LPV PSS is more effective.

4. The LPV approach based on a Parameter-dependent Quadratic Lyapunov Function is employed on PSS synthesis to reduce the conservatism from the assumption of the arbitrarily fast changing scheduling parameters. By taking the bounds of parameter rates of change into consideration, the operating range can be extended even larger.

5. Apply curve fitting technique to the realization of LPV controllers. The gridding process in the LPV synthesis leads to a discrete controller. Approximation of the parameter dependence with polynomial or rational functions makes the controller parameters change smoothly with the scheduling variables to guarantee the robustness of the system on a large range.

6. Apply the LPV technique to the decentralized controller design process. Instead of considering the whole system model, we just consider one machine model with arbitrarily fast changing output real and reactive power in some range. All possible dynamics on the interface between the generator and the rest of the system are supposed to be represented by it. By doing this, the system is decoupled naturally and the order of the design plant is decreased dramatically. The resulting controllers give a satisfactory performance on a large range. The design framework and procedure are given. Time domain simulations show that the performance of the LPV PSSs is superior to the conventionally designed PSSs.

1.7 Test Systems

Two test systems are extensively used in this research.

1. The four-machine IEEE generator test system (43) as shown in Figure 1.2. This system was specially designed by Ontario Hydro to study the fundamental nature of inter-area oscillations (43).

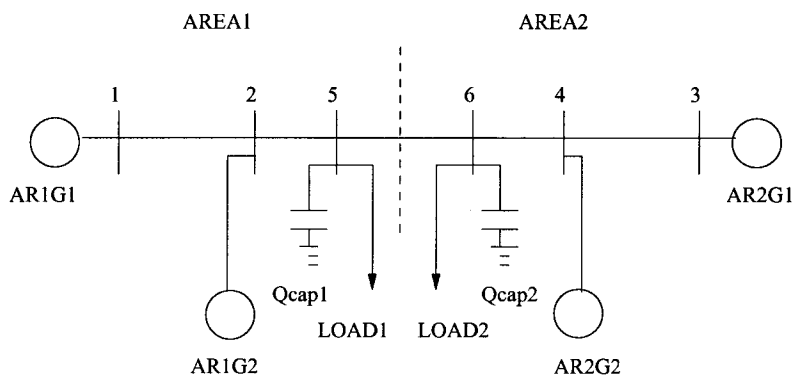

Figure 1.2 Four-machine two-area test system

The Synchronous generators are represented by the two-axis model(42), with the excitation system represented by the IEEE AC-4 model(42). The network is represented by quasi steady-state network parameters with constant impedance load model. By assuming the generator internal reactance to be constant, the network representation is reduced to generator internal buses. We assume local load to be distributed to local generators equally, therefore the system states are precisely based on the tie line flow, which describes the nonlinearity of the system and is the varying parameter. The objective is to design a power system stabilizer (PSS) to stabilize the whole system when it operates at different points.

2. The IEEE 50-generator (50) test system system. This is a moderate sized system which includes all of the modelling features and complexity of large scale power systems. A one-line diagram of the area of interest is shown in Fig. 1.3.

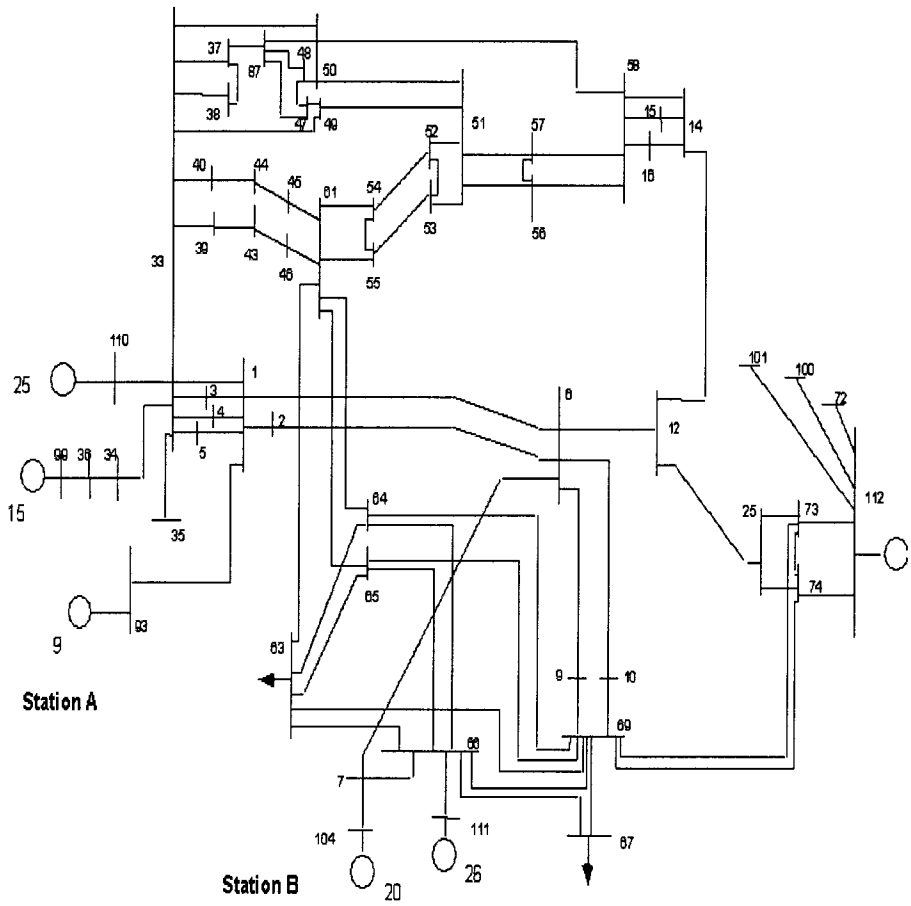

Figure 1.3 IEEE 50-generator system: a one-line diagram of the study area.

This test system contains 44 generators represented by the classical model with uniform damping and 6 generators represented by a two-axis model. The operating point was characterized by setting the real power generation at Buses ♯93 and ♯110.

1.8 Thesis Outline

Chapter 1 gives motivation and background for the research work and introduce the objective and scope of the research. A concise literature review of LPV methodology and a systematic LPV synthesis procedure are given in Chapter 2. Chapter 3 provides a detailed description of the mathematical models of the power system components and overall system dynamic equations and LPV formulation of the power system model. In chapter 4, a systematic procedure to design a LPV PSS is presented. Design setup and weighting function selection are illustrated. The gridding process and LPV controller realization are discussed. Two LPV approaches are investigated in this chapter. One is based on a Single Quadratic Lyapunov Function (SQLF), and the other is based on a Parameter Dependant Lyapunov Function (PDLF). Comparisons are made among conventional PSS, H_∞ PSS, and LPV PSS through frequency domain analysis and non-linear time domain simulation. Chapter 5 proposes a decentralized PSS design scheme using SQLF based LPV approach. Detailed steps for the decentralized synthesis are established. A theoretical proof for closed-loop system stability is provided. Simulation results on the comparison of the controller performance with the conventional PSSs and LPV PSSs are given. Chapter 6 presents conclusions and provides suggestions for future work.

CHAPTER 2. LPV METHODOLOGY

2.1 Literature Review

Over the last ten years, extensive research has focused on developing analysis and synthesis techniques for gain-scheduled controllers for linear parameter varying(LPV) systems (21; 22; 23; 24; 25; 26). The notation of LPV systems was first introduced in (27). This class of systems is different from standard Linear Time Variant (LTV) systems due to the causal dependence of its controller gains on the variations of the plant dynamics. A number of interesting alternative approaches have been proposed in the context of gain scheduling design (for example, Becker et al.1993, Packard 1994, Apkarian and Adams 1998). They are commonly referred to as LPV gain scheduling methods, which are conceptually quite distinct from the conventional gain scheduling approach since they involve the direct synthesis of a controller rather than its construction from a family of local linear controllers designed by LTI methods. Moreover, LPV methods typically use norm based performance measures. All the LPV approaches at present involve some degree of conservativeness.

Using scaled small gain theorem, a systematic gain scheduling control design technique has been developed in (24; 25). H_∞ techniques are extended to the class of LPV systems whose state space matrices are linear fractional functions of the parameters. When the parameter dependency in both plant and controller is linear fractional, the existence of such a gain scheduled controller is fully characterized in terms of linear matrix inequalities (LMIs). Efficient optimization techniques are available for the controller

synthesis (21). It is also demonstrated that the original gain scheduling problem can be reformulated as one of robust performance with structured uncertainties. However, the conservativeness is introduced by assuming the varying parameters are complex and vary arbitrarily fast.

Parallel to the first approach, the use of a single or parameter dependent Lyapunov function in analysis and control design for LPV plants has been studied in the robust control framework (22; 23; 26; 28). The LPV system is allowed to have general parameter-dependence other than trivial continuity requirement. Sufficient conditions are given in (22) that guarantee an LPV system is exponentially stable and achieves an induced L2 norm performance objective from the disturbance to error signals. It generalizes the standard H_∞ methodology and the synthesis process exploits the realness of the varying parameters. This approach is less conservative than the method based on the small gain theorem. A LPV gain scheduling controller was designed in these cases. A single quadratic Lyapunov function is employed here as an analysis base. Since a fixed quadratic Lyapunov function is used in the whole range of parameter variation, potential conservativeness by measuring performance against arbitrarily fast variations in varying parameters is also introduced. In (26) parameter dependent Lyapunov functions are introduced to further reduce the conservativeness. Known bounds on the rate of parameter variation are incorporated into the synthesis procedure. In contrast to scaled small gain approach, the solution to the LPV control synthesis problem is formulated as a parameter dependent LMI optimization problem.

A primary practical difficulty with the foregoing approaches is that the solvability conditions involve an infinite number of constraints and so the task of determining a controller which satisfies these conditions is numerically intractable. This arises because a constraint must be satisfied for every allowable parameter value since there is a continuum of parameter values. An ad hoc gridding method is typically used to divide the parameter space and renders the semi-infinite optimization problem to be finite.

Since the LMI constraints grow rapidly as the parameter number increases, in general, no systematic method for avoiding such gridding exists. Simplifications are possible for some specific classes of plants. For affine LPV systems with parameter values belonging to a convex polytope, the quadratic LPV γ-performance problem can be reduced to a convex problem with a finite number of constraints by imposing the requirement that the allowable parameter set is a convex polytope which has a finite set of extreme points (29; 30). Gain scheduling design tools are given in (21), which are only applicable to time varying and/or nonlinear systems whose linearized dynamics are reasonably approximated by affine parameter-dependent models.

LPV gain scheduling technique has been successfully applied in many engineering applications such as flight and process control (46; 31; 32; 33). In the flight control problem, the LPV approach based on a single quadratic Lyapunov function is generally applied. Different variables such as altitude, attack angle, and Mach number, are taken as scheduling variables in different cases. The approach in (26) is employed in (33) to achieve improvement by introducing the variation rate bound of the scheduling variable and designing multiple LPV controllers over different operating ranges. These applications demonstrate the usefulness of LPV theory for real engineering problems. The promising results obtained and the actual implementation of this approach in safety critical systems like aircrafts and process control highlight the potential of this technique when applied to large power systems.

2.2 Single Quadratic Lyapunov Function (SQLF) Based Method

2.2.1 Definition of the LPV System

First of all, we would like to introduce the definition of the LPV system.

Definition 2.2.1 *Given a compact subset $P \subset \mathbb{R}^s$, the parameter variation set F_p denotes the set of all piecewise continuous mapping R(time) into P with a finite number of discontinuities in any interval.*

Definition 2.2.2 *Assume that the following are given: a compact set $P \subset \mathbb{R}^s$, and continuous functions $A : \mathbb{R}^s \to \mathbb{R}^{n\times n}$, $B : \mathbb{R}^s \to \mathbb{R}^{n\times n_d}$, $C : \mathbb{R}^s \to \mathbb{R}^{n_e\times n}$, $D : \mathbb{R}^s \to \mathbb{R}^{n_e\times n_d}$, These represent an nth order linear parameter varying (LPV) system, whose dynamics evolves as :*

$$\begin{Bmatrix} \dot{X}(t) \\ e(t) \end{Bmatrix} = \begin{Bmatrix} A(\rho(t)) & B(\rho(t)) \\ C(\rho(t)) & D(\rho(t)) \end{Bmatrix} \begin{Bmatrix} X(t) \\ d(t) \end{Bmatrix} Where \rho \in F_P \tag{2.1}$$

The notation Σ_P:=$\{\Sigma_\rho, : \rho \in F_P\}$ represents the LPV system defined above. We will sometimes use $\Sigma(P, A, B, C, D)$ to illustrate the state space data clearly.

2.2.2 Quadratic Stability of LPV System

Quadratic stability is a strong notion of robust stability in the sense that it holds for arbitrarily fast variation in the parameter trajectory ρ, and its definition involves a single quadratic Lyapunov function.

Definition 2.2.3 *Given a compact subset $P \subset \mathbb{R}^s$, a function $A : \mathbb{R}^s \to \mathbb{R}^{n\times n}$, the function A is quadratically stable over P if there exists a matrix $P \in S^{n\times n}$, such that for all $\rho \in P$*

$$A^T(\rho)P + PA_(\rho) < 0 \tag{2.2}$$

For LPV system Σ_P, if A is quadratically stable over P, then Σ_P is a quadratically stable LPV system.

Definition 2.2.4 *Given a quadratic stable LPV system, for zero initial conditions $X(0) = 0$, define induced L_2 norm as :*

$$\| G_{F_P} \|_{i,2} := \sup_{\rho\in F_P, \|d\|_2\neq 0} \sup_{d\in L_2} \frac{\| e \|_2}{\| d \|_2} \tag{2.3}$$

Therefore, the L_2 norm level for a LPV system represents the largest ratio of disturbance norm and error norm over the set of all causal linear operators described by the LPV system.

Theorem 2.2.1 *Given compact set P, the open loop system $\Sigma(P, A, B, C, D)$ and scalar $\gamma > 0$, if there exists an $X \in \mathbb{R}^{n\times n}$, $X = X^T > 0$, such that for all $\rho \in P$,*

$$\begin{Bmatrix} A^T(\rho)X + XA^T(\rho) & XB(\rho) & \gamma^{-1}C^T(\rho) \\ B(\rho)^T X & -I & \gamma^{-1}D^T(\rho) \\ \gamma^{-1}C(\rho) & \gamma^{-1}D(\rho) & -I \end{Bmatrix} < 0 \tag{2.4}$$

then the function A is quadratically stable over P, and there exists $\beta < \gamma$ such that induced L_2 norm $\|GF_P\| \leq \beta$.

2.2.3 SQLF LPV Controller Synthesis

Given a compact set $P \subset \mathbb{R}^s$, consider the open-loop LPV system

$$\begin{Bmatrix} \dot{x}(t) \\ e(t) \\ y(t) \end{Bmatrix} = \begin{Bmatrix} A(\rho(t)) & B_1(\rho(t)) & B_2(\rho(t)) \\ C_1(\rho(t)) & D_{11}(\rho(t)) & D_{12}(\rho(t)) \\ C_2(\rho(t)) & D_{21}(\rho(t)) & D_{22}(\rho(t)) \end{Bmatrix} \begin{Bmatrix} x(t) \\ d(t) \\ u(t) \end{Bmatrix} \tag{2.5}$$

Where $\rho \in F_P$.

We restrict the matrix function D_{12} to be full column rank and D_{12} to be full row rank. To simplify the derivation of the control synthesis result, the following restrictive assumption is made : D_{12} and D_{21} are constant matrices. $D_{11} = 0$,$D_{22} = 0$, $D_{12}^T D_{12} = I$, $D_{21}D_{21}^T = I$, $D_{12}^T C_1(\rho) = 0$ and $B_1(\rho)D_{21}^T = 0$ for all $\rho \in P$. The solution to the synthesis problem is conceptually the same when these assumptions are relaxed, however, the algebra is considerably more complicated. Under these assumptions, after suitable norm preserving transformations on d and e, and invertible transformations on u and y, the

LPV system can be written as:

$$\begin{Bmatrix} \dot{x}(t) \\ e_1(t) \\ e_2(t) \\ y(t) \end{Bmatrix} = \begin{Bmatrix} A(\rho(t)) & B_1(\rho(t)) & 0 & B_2(\rho(t)) \\ C_1(\rho(t)) & 0 & 0 & 0 \\ 0 & 0 & 0 & I \\ C_2(\rho(t)) & 0 & I & 0 \end{Bmatrix} \begin{Bmatrix} x(t) \\ d_1(t) \\ d_2(t) \\ u(t) \end{Bmatrix} \tag{2.6}$$

Then the ρ dependent feedback controller can be written as:

$$\begin{Bmatrix} \dot{x}(t) \\ u(t) \end{Bmatrix} = \begin{Bmatrix} A_k(\rho(t)) & B_k(\rho(t)) \\ C_k(\rho(t)) & D_k(\rho(t)) \end{Bmatrix} \begin{Bmatrix} x_k(t) \\ y(t) \end{Bmatrix} \tag{2.7}$$

Let $x_{clp}^T(t) = [x^T(t), x_k^T(t)]$, $e^T(t) = [e_1^T(t),\ e_2^T(t)]$ and $d^T = [d_1^T(t),\ d_2^T(t)]$, then the closed-loop system becomes

$$\begin{Bmatrix} \dot{x}_{clp}(t) \\ e(t) \end{Bmatrix} = \begin{Bmatrix} A_{clp}(\rho(t)) & B_{clp}(\rho(t)) \\ C_{clp}(\rho(t)) & D_{clp}(\rho(t)) \end{Bmatrix} \begin{Bmatrix} x_{clp}(t) \\ d(t) \end{Bmatrix} \tag{2.8}$$

Definition 2.2.5 *Given the LPV system, satisfying the assumption in (2.6), and $\gamma > 0$, the quadratic LPV γ-performance problem is solvable if there exist an $m \geq 0$, a finite-dimensional m-state controller (2.7), and an $X \in \mathbb{R}^{(n+m)\times(n+m)}$, $X = X^T > 0$ such that for all $\rho \in P$*

$$\begin{Bmatrix} A_{clp}^T(\rho)X + XA_{clp}^T(\rho) & XB_{clp}(\rho) & \gamma^{-1}C_{clp}^T(\rho) \\ B_{clp}(\rho)^T X & -I & \gamma^{-1}D_{clp}^T(\rho) \\ \gamma^{-1}C_{clp}(\rho) & \gamma^{-1}D_{clp}(\rho) & -I \end{Bmatrix} < 0 \tag{2.9}$$

Theorem 2.2.2 *Given P, the open loop system (2.6) and scalar $\gamma > 0$, the quadratic LPV γ-performance problem is solvable if and only if there exist matrices $X_{11} \in \mathbb{R}^{n\times n}$, $X_{11} = X_{11}^T > 0$, and $Y_{11} \in \mathbb{R}^{n\times n}$, $Y_{11} = Y_{11}^T > 0$, such that for all $\rho \in P$:*

$$\begin{Bmatrix} A_1(\rho)Y_{11} + Y_{11}A^T(\rho) - B_2(\rho)B_2(\rho) & Y_{11}C_1^T(\rho) & \gamma^{-1}B_1(\rho) \\ C_1(\rho)Y_{11} & -I & 0 \\ \gamma^{-1}B_1^T(\rho) & 0 & -I \end{Bmatrix} < 0 \tag{2.10}$$

$$\left\{ \begin{array}{ccc} A^T(\rho)X_{11} + X_{11}A(\rho) - C_2^T(\rho) & C_2(\rho)X_{11}B_1\rho & \gamma^{-1}C_1^T(\rho) \\ B_1(\rho)^T X_{11} & -I & 0 \\ \gamma^{-1}C_1(\rho) & 0 & -I \end{array} \right\} < 0 \qquad (2.11)$$

$$\left\{ \begin{array}{cc} X_{11} & \gamma^{-1}I_n \\ \gamma^{-1}I_n & Y_{11} \end{array} \right\} \geq 0 \qquad (2.12)$$

then the function A is quadratically stable over P, and there exists $\beta < \gamma$ *such that* $\|GF_P\| \leq \beta$.

Let $Z := (X_{11} - \gamma^{-1}Y_{11})^{-1}$,

$H(\rho) = -[Y_{11}^A(\rho) + A(\rho)^T Y_{11}^{-1} - Y_{11}B_2(\rho)B_2(\rho)^T Y_{11}^{-1} + C_1(\rho)^T C_1(\rho) + \gamma^{-2}Y_{11}^{-1}B_1(\rho)B_1(\rho)^T Y_{11}^{-1}]$

Then the LPV controller should be:

$A_k(\rho) := A(\rho) + \gamma^{-2}B_1(\rho)B_1(\rho)^T Y_{11}^{-1} - B_2(\rho)B_2(\rho)^T - Z[C_2(\rho)^T C_2(\rho) + \beta^{-2}H(\rho)]$,

$B_k(\rho) := ZC_2(\rho)T$,

$C_k(\rho) = -B_2(\rho)^T Y_{11}^{-1}$,

$D_k(\rho) := 0$.

2.3 Parameter Dependent Lyapunov Function (PDLF) Based Method

2.3.1 Definition of Parameter Dependent LPV System

The controller derived from the method in section 2.2.3 considers arbitrarily fast parameter change. In other words, it uses a single quadratic Lyapunov function (SQLF) for all cases, which leads to much conservatism. The conservatism can be reduced through a parameter dependent Lyapunov function (26) (PDLF) if the bounds on the parameter's rate of variation are known.

Definition 2.3.1 *Given a compact subset $P \subset \mathbb{R}^s$, finite non-negative numbers $\{\nu_i\}_{i=1}^s$ with $\nu := [\nu_1 \dots \nu_s]^T$. We define the parameter ν-variation set as* $F_P^\nu := \{\rho \in C^1(\mathbb{R}, \mathbb{R}^s) : \rho(t) \in P, |\dot{\rho}_i| \leq \nu_i, i = 1, \dots, s\}$ *where $C^1(\mathbb{R}, \mathbb{R}^s)$ stands for the class of piecewise continuously differentiable functions from $\mathbb{R}$ to $\mathbb{R}^s$.*

The LPV systems studied in this section are slightly different because of their state space data dependence on parameters and their derivatives. The definition is as follows:

Definition 2.3.2 *Given a compact set $P \subset \mathbb{R}^s$, and the continuous functions $(A, B, C, D) : \mathbb{R}^s \times \mathbb{R}^s \to (\mathbb{R}^{n\times n}, \mathbb{R}^{n\times n_d}, \mathbb{R}^{n_e\times n}, \mathbb{R}^{n_e\times n_d})$. An n-th order LPV system with bounded parameter variation rates Σ_P is given by*

$$\begin{Bmatrix} \dot{X}(t) \\ e(t) \end{Bmatrix} = \begin{Bmatrix} A(\rho(t), \dot{\rho}(t)) & B(\rho(t), \dot{\rho}(t)) \\ C(\rho(t), \dot{\rho}(t)) & D(\rho(t), \dot{\rho}(t)) \end{Bmatrix} \begin{Bmatrix} X(t) \\ d(t) \end{Bmatrix} Where \rho \in F_P \qquad (2.13)$$

where $\rho \in F_P^\nu, x(t) \in \mathbb{R}^n, d(t) \in \mathbb{R}^{n_d}$, and $e(t) \in \mathbb{R}^{n_e}$.

2.3.2 Parameter Dependant Stability

Definition 2.3.3 *Given a compact subset $P \subset \mathbb{R}^s$, finite non-negative numbers $\{\nu_i\}_{i=1}^s$, and a function $A : \mathbb{R}^s \times \mathbb{R}^s \to \mathbb{R}^{n\times n}$, the function A is parametrically-dependent stable over P if there exists a continuously differentiable function $P : \mathbb{R}^s \to S^{n\times n}$, such that, $P(\rho) > 0$ and for all $\rho \in P$ and $|\beta_i| \leq \nu_i, i = 1, 2, \dots, s$*

$$A^T(\rho, \beta)P(\rho) + P(\rho)A_(\rho, \beta) + \sum_{i=1}^{s}(\beta_i \frac{\partial P}{\partial \rho_i}) < 0 \qquad (2.14)$$

If no bounds apply to parameter variation ($\nu_i \to \infty$ *for* $i = 1, 2, \dots, s$), by restricting P to be a constant matrix, the notation for parameter-dependant stability goes to quadratic stability.

Definition 2.3.4 *Given a parametrically-dependent stable LPV system, for zero initial conditions $X(0) = 0$, define induced L_2 norm as :*

$$\| G_{F_P} \|_{i,2} := \sup_{\rho \in F_P^\nu, \|d\|_2 \neq 0} \sup_{d \in L_2} \frac{\| e \|_2}{\| d \|_2} \qquad (2.15)$$

2.3.3 LPV γ-Performance/ν-Variation Problem

Definition 2.3.5 *Given the open-loop LPV system Σ_P in above definition, and the performance level $\gamma > 0$. The parameter-dependent γ-performance problem is solvable if there exist an integer $m \geq 0$, a funciton $W \in C^1(\mathbb{R}_s, S^{(n+m)\times(n+m)})$, and continuous matrix functions $(A_K, B_K, C_K, D_K) : \mathbb{R}^s \times \mathbb{R}^s \to (\mathbb{R}^{m\times m}, \mathbb{R}^{m\times n_y}, \mathbb{R}^{n_u\times m}, \mathbb{R}^{n_u\times n_y})$, such that $W(\rho) > 0$ and*

$$\left\{ \begin{array}{ccc} A_{clp}^T(\rho,\beta)W(\rho) + W(\rho)A_{clp}^T(\rho,\beta) + \sum i = 1s(\beta_i \frac{\partial W}{\partial \rho_i}) & W(\rho)B_{clp}(\rho,\beta) & \gamma^{-1}C_{clp}^T(\rho,\beta) \\ B_{clp}(\rho,\beta)^T W(\rho) & -I & \gamma^{-1}D_{clp}^T(\rho,\beta) \\ \gamma^{-1}C_{clp}(\rho,\beta) & \gamma^{-1}D_{clp}(\rho,\beta) & -I \end{array} \right\} < 0 \qquad (2.16)$$

for all $\rho \in P$ and $|\beta_i| \leq \nu_i, i = 1, \cdots, s$.

This is also a generalized sub-optimal H_∞ optimal control problem. It conceptually expands the applicability of the H_∞ control methodology.

Theorem 2.3.1 *Given a compact set $P \subset \mathbb{R}^s$, non-negative numbers $\{\nu_i\}_{i=1}^s$, performance level $\gamma > 0$, and the open loop LPV system in (2.6), the LPV synthesis γ-performance/ν-variation problem is solvable if and only if there exist continuously differentiable matrix functions $X : \mathbb{R}^s \to \varphi^{n\times n}$ and $Y : \mathbb{R}^s \to \varphi^{n\times n}$, such that for all $\rho \in P$, $X(\rho)$,$Y(\rho) > 0$,and*

$$\left\{ \begin{array}{ccc} Y(\rho)\hat{A}^T(\rho) + \hat{A}(\rho)Y(\rho) - \sum_{i=1}^s \pm(\nu_i \frac{\partial Y}{\partial \rho_i}) - \gamma B_2(\rho)B_2^T(\rho) & Y(\rho)C_{11}^T(\rho) & B_1(\rho) \\ C_{11}(\rho)Y(\rho) & -\gamma I_{n_{e1}} & 0 \\ B_1^T(\rho) & 0 & -\gamma I_{n_d} \end{array} \right\} < 0 \qquad (2.17)$$

$$\left\{ \begin{array}{ccc} X(\rho)\bar{A}(\rho) + \bar{A}^T(\rho)X(\rho) - \sum_{i=1}^s \pm(\nu_i \frac{\partial X}{\partial \rho_i}) - \gamma C_2^T(\rho)C_2(\rho) & X(\rho)B_{11}(\rho) & C_1^T(\rho) \\ B_{11}(\rho)X(\rho) & -\gamma I_{n_{d1}} & 0 \\ C_1(\rho) & 0 & -\gamma I_{n_e} \end{array} \right\} < 0 \qquad (2.18)$$

$$\left\{ \begin{array}{cc} X(\rho) & I_n \\ I_n & Y(\rho) \end{array} \right\} \geq 0 \qquad (2.19)$$

where

$\hat{A}(\rho) := A(\rho) - B_2(\rho)C_{12}(\rho)$, $B_1(\rho) = [B_{11}(\rho)B_{12}(\rho)]$,

$\bar{A}(\rho) := A(\rho) - B_{12}(\rho)C_2(\rho)$, $C_1^T(\rho) = [C_{11}^T(\rho)C_{12}^T(\rho)]$

Define the following:

$Q(\rho) := X(\rho) - Y^{-1}(\rho)$,

$F(\rho) := -[\gamma B_2^T(\rho) + C_{12}(\rho)]$,

$L(\rho) := -[\gamma X^{-1}(\rho) C_2^T(\rho) + B_{12}(\rho)]$.

$H(\rho, \dot{\rho}) := -[A_F^T(\rho) Y^{-1}(\rho) A_F(\rho) + \sum_{i=1}^{s} (\dot{\rho}_i \frac{\partial Y^{-1}}{\partial \rho_i}) + \gamma^{-1} C_F^T(\rho) C_F(\rho) + \gamma^{-1} Y^{-1}(\rho) B_1(\rho) B_1^T(\rho) Y^{-1}(\rho)]$

$A_F(\rho) := A(\rho) + B_2(\rho) F(\rho)$ and $C_F^T(\rho) := [C_{11}^T(\rho) C_{12}^T(\rho) + F^T(\rho)]$.

Then the resulting LPV controller can be defined as:

$A_K(\rho, \dot{\rho}) := A(\rho) + \gamma^{-1}[Q^{-1}(\rho) X(\rho) L(\rho) B_{12}^T(\rho) + B_1(\rho) B_1^T(\rho)] Y^{-1}(\rho)$

$+ B_2(\rho) F(\rho) + Q^{-1}(\rho) X(\rho) L(\rho) C_2(\rho) - Q^{-1}(\rho) H(\rho, \dot{\rho})$

$B_K(\rho) := -Q^{-1}(\rho) X(\rho) L\rho$

$C_K(\rho) := F(\rho)$

$D_K(\rho) := 0$

To solve LMIs in 2.17-2.19, an ad hoc approach is employed here. Let $\{f_i\}_{i=1}^N$ and $\{g_i\}_{i=1}^N$ be user defined sets of continuously differentiable functions from $\mathbb{R}^s to \mathbb{R}$.

$X(\rho) := \sum_{i=1}^N f_i(\rho) X_i$, $Y(\rho) := \sum_{i=1}^N g_i(\rho) Y_i$

are continuously differentiable on $\mathbb{R}_s \rightarrow \varphi^{n \times n}$. So once the basis functions f_i and g_i are chosen, the original synthesis LMIs are solvable by optimizing over the matrices X_i, $Y_i \in \varphi^{n \times n}$.

The rate-bound LPV controllers are a function of the scheduling variables as well as their derivatives. We can either simulate the LPV controller by feeding in the scheduling derivative or eliminate them from the controllers. Eliminating the derivative usually has no effect on the controller performance.

2.4 PSS Design Procedure

The resulting controller can achieve a larger system operating range while guaranteeing the stability and performance not only for slow changing parameters but also for arbitrarily fast changing parameters. The LPV synthesis procedure consists of the following steps:

1. Choose scheduling variables, which are measurable in real time and can characterize system operating conditions, such as tie-line power flow, real and reactive power output of generators;

2. Fix the range of the scheduling variables according to the actual operating range of the system and grid the scheduling variable ranges. Get the corresponding system model (Matrices A, B, C,and D) at each gridding point;

3. Build the controller design setup according to system requirements and control objectives. At each gridding point, weighting functions are chosen; then form the LPV model for the generator.

4. Solve the set of LMIs and get the A_k, B_k, C_k, and D_k at each operating point;

5. Use a curve fitting technique to form the LPV controller, as detailed in Section 2.8.

More details are discussed below.

2.5 PSS Design Setup

Mixed sensitivity setup is employed for the LPV PSS design. The weighted interconnection of LPV design is shown in Fig. 2.1. The main objective of the PSS is to make the output $\Delta\omega$, the relative frequency as small as possible in the presence of the disturbance signal $d = \Delta V_{ref}$. The controller design is done over a wide range of operating conditions. As a result, the ΔV_{ref} setting will change. Since the oscillations of concern typically occur in the frequency range of approximately $0.2Hz$ to $2Hz$, W_{perf} is chosen as a high pass filter. The fictitious input *noise* is applied to avoid a singularity problem and to achieve the form of (2.6) for the open loop plant. W_{noise} could be chosen as any small constant. W_u can be chosen as a limitation on the controller output, which is impractical if it is too large.

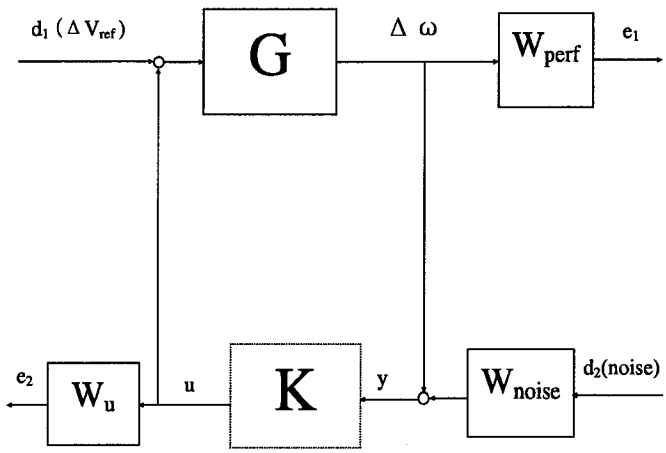

Figure 2.1 LPV PSS design setup

2.6 Solving the Infinite Dimension LMIs

The solution of the LPV γ-performance problem is governed by the set of LMIs being satisfied for all $\rho \in P$, so it is a convex problem. In practical design cases, in order to avoid solving the above infinite dimensional LMIs (2.10-2.12,2.17-2.19), an alternative approximate problem is set up by gridding the parameter space and solving the set of LMIs that hold on the subset of P formed by gridding points. If this approximate problem does not have a solution, neither does the original infinite dimension problem. Even if the solution is found, it does not guarantee that the solution satisfies the original constraints for all $\rho \in P$. However, since the matrix functions are continuous with respect to ρ, after checking on a dense enough subset of P, we can expect that the LMIs hold for all $\rho \in P$. The result shows that this assumption is feasible.

2.7 Gridding Process

Experience in flight control design and process control design has shown that if the gridding is fine enough, stability/performance with the implemented LPV controller is

generally not an issue. The number of grid points depends on the system operating range chosen and the nonlinearity of the system. The gridding is not necessarily even. The more nonlinear the system is, the denser the gridding should be. Too dense gridding could bring unnecessary computational burden, while too sparse gridding could lead to a poor design.

In the approaches followed in the research, a set of grid points based on the tie line real power is formed. In all the cases we studied, it is found that a grid at every $100MW$ interval provides accurate results. At each grid point the power flow solution is obtained. From the obtained solution the system model (matrices A, B, C, and D) is derived.

2.8 Realization of the LPV Controller

The parameter space gridding necessary to numerically solve for the LPV controller leads to a discrete controller. Instead of getting a fixed dependence of $A(\rho)$, $B(\rho)$, $C(\rho)$ and $D(\rho)$ on ρ, the matrices are only known at a discrete set of ρ values. Implementation of the LPV controller requires storing the values of the controller at each grid point and interpolating between these points during close-loop operation. The relationship can be approximated by polynomial or rational functions through curve fitting. The approximation procedure essentially consists of setting up an over determined system of linear equations for the coefficients at various points on a grid of varying parameters. These equations are then solved using a least square minimization approach. Approximation of the parameter dependence with polynomial or rational functions makes the controller parameters change with the scheduling variables to guarantee the robustness of the system on a large range.

CHAPTER 3. POWER SYSTEM MODELS

The power system is a highly nonlinear system. The dynamic behavior of the system is dominated by its components (generator, exciter, load, etc.), which are coupled implicitly with the network model. So the mathematical model of the power system can be represented by two sets of equations: one set of differential equations and one set of algebraic equations.

$$\begin{aligned} \dot{X} &= F(X,Y) \\ 0 &= G(X,Y) \end{aligned} \tag{3.1}$$

where X is the vector of state variables by the differential equation, and Y is the vector of network variables.

3.1 Load Model

All of the loads are represented by constant impedance in this research. The load nodes and the terminal voltage nodes of the generators are eliminated, so the resulting network contains only the internal generator nodes (numbered from 1 to n). The generator reactance and the constant impedance loads are included in the bus admittance matrix Y_{bus} of the reduced network.

3.2 Generator Model

The complete mathematical description of the synchronous machines is too complicated to be used directly for system analysis and synthesis. Different degrees of approximations are adopted to simplify the generator model. Two kinds of generator models are used in this dissertation, which are the two-axis model and the classical model (14). We assume that in a n generator system, the first m generators are represented by the two-axis model and equipped with exciters and the remaining $n - m$ generators are represented using the classical model.

3.2.1 Classical Model

The classical model represents a generator without excitation(see Chapter 2 of (14)). It is the simplest model for generators and it assumes the following :

1. Mechanical power input is constant.
2. Damping or asynchronous power is negligible.
3. Constant-voltage-behind-transient-reactance model for the synchronous machines is valid.
4. The mechanical rotor angle of a machine coincides with the angle of the voltage behind the transient reactance.

The dynamic equations for the classical model are given by

$$M_i\dot{\omega}_i = P_i - P_{ei} \tag{3.2}$$

$$\dot{\delta}_i = \omega_i - \omega_S \qquad i = m+1, m+2, ..., n \tag{3.3}$$

where,

$$P_i = P_{mi} - E_i^2 G_{ii}$$

$$P_{ei} = \sum_{j=1, j\neq i}^{n} [E_i E_j B_{ij} \sin(\delta_i - \delta_j) + E_i E_j G_{ij} \cos(\delta_i - \delta_j)]$$

and

E_i: internal bus voltage of generator i

M_i: inertia constant of generator i

P_{mi}: mechanical power input of generator i

G_{ii}: driving point conductance of node i

$G_{ij} + jB_{ij}$: the transfer admittance between node i and node j in the reduced network

ω_i: rotor speed of generator i (with respect to the synchronous frame)

ω_S: synchronous speed

3.2.2 Two-axis Model

Generators with excitation control are described by the two-axis model (see chapter 4 of (14)) in this work. In the two-axis model the transient effects are accounted for and the following assumptions are required.

1. In the stator voltage equations the variation of flux linkages of d-q axes are negligible compared to the speed voltage terms.

2. $\omega \cong \omega_S = 1$ p.u.

The resultant dynamic equations are given by

$$\tau'_{d0i}\dot{E}'_{qi} = E_{FDi} - E'_{qi} + (x_{di} - x'_{di})I_{di} \tag{3.4}$$

$$\tau'_{q0i}\dot{E}'_{di} = -E'_{di} - (x_{qi} - x'_{qi})I_{qi} \tag{3.5}$$

$$M_i\dot{\omega}_i = P_{mi} - (I_{di}E'_{di} + I_{qi}E'_{qi}) + (x'_{qi} - x'_{di})I_{qi}I_{di} - D_i(\omega_i - \omega_S) \tag{3.6}$$

$$\dot{\delta}_i = \omega_i - \omega_S \qquad i = 1, 2, ..., m \tag{3.7}$$

where,

E'_d, E'_q: direct and quadrature axes stator EMFs corresponding to rotor transient flux components, respectively

I_d, I_q: the d and q axes stator currents

τ'_{d0}, τ'_{q0}: open-circuit direct and quadrature axes transient time constants

x_d, x'_d: direct axis synchronous and transient reactances

x_q, x'_q: quadrature axis synchronous and transient reactances

E_{FD}: stator EMF corresponding to the field voltage

D_i: damping coefficient of generator i

3.2.3 Angle Reference

In (3.3) and (3.7) above, the absolute rotor angles (δ_i, $i = 1, 2, \ldots, n$) are used as state variables. In order to make state variables independent, we introduce the relative rotor angles as new state variables. Without loss of generality, δ_1 is chosen as reference, then the relative rotor angles are defined as:

$$\delta_{i1} = \delta_i - \delta_1, \qquad i = 2, 3, \ldots, n$$

The dynamic equations (3.2) — (3.7) remain unchanged with each δ_i replaced by δ_{i1} and ω_S replaced by ω_1. Therefore (3.3) and (3.7) becomes

$$\dot{\delta}_{i1} = \omega_i - \omega_1 \qquad i = 2, 3, \ldots, n \tag{3.8}$$

3.3 Excitation System Model

The block diagram of the exciter model, which is IEEE AC-4 (15), is shown in Figure 3.1. The state variables are E_{FD}, X_{E1}, and X_{E2}, and the dynamic equations

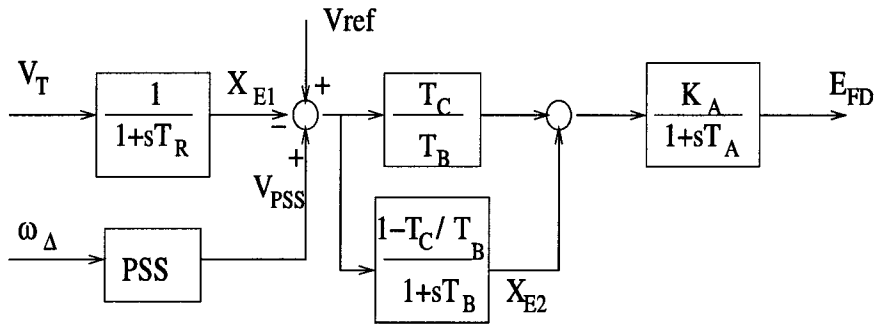

Figure 3.1 Excitation system model: IEEE AC-4.

are given by

$$\dot{E}_{FDi} = \frac{K_{Ai}}{T_{Ai}} X_{E2i} - \frac{1}{T_{Ai}} E_{FDi} + \frac{aK_{Ai}}{T_{Ai}} (V_{REFi} - X_{E1i}) \tag{3.9}$$

$$\dot{X}_{E1i} = -\frac{1}{T_{Ri}} X_{E1i} + \frac{1}{T_{Ri}} V_{Ti} \tag{3.10}$$

$$\dot{X}_{E2i} = -\frac{1}{T_{Bi}} X_{E2i} + \frac{1-a}{T_{Bi}} (V_{REFi} - X_{E1i}) \tag{3.11}$$

where,

V_{REF}: exciter reference voltage

$a = T_{Ci}/T_{Bi}$, T_{Bi} and T_{Ci} are time constants

V_T: generator terminal voltage

$$\begin{aligned} V_T &= V_{Tq} + jV_{Td} \\ &= (E_q^{'} + x_d^{'} I_d) + j(E_d^{'} - x_q^{'} I_q) \qquad i = 1, 2, ..., m \end{aligned} \tag{3.12}$$

A power system stabilizer (PSS) is used to add damping for the system through the modulation signal to a generator's voltage reference input.

3.4 Network Modelling

The reduced network contains only the generator internal buses. The bus admittance matrix Y_{bus} consists of $Y_{ij}\angle\gamma_{ij} = G_{ij} + jB_{ij}$.

Since generators are reduced to their internal buses, the associated currents and voltages are usually in the $d-q$ axis reference frame, as shown in (3.2) — (3.6). Following the procedure in Chapter 9 of (14), the generator currents are given in the following form:

$$I_{qi} = \sum_{j=1}^{m}[F_{G+B}(\delta_{ij})E'_{qj} - F_{B-G}(\delta_{ij})E'_{dj}] + \sum_{k=m+1}^{n} F_{G+B}(\delta_{ik})E_k \tag{3.13}$$

$$I_{di} = \sum_{j=1}^{m}[F_{B-G}(\delta_{ij})E'_{qj} + F_{G+B}(\delta_{ij})E'_{dj}] + \sum_{k=m+1}^{n} F_{B-G}(\delta_{ik})E_k \tag{3.14}$$

$$i = 1, 2, ..., n$$

where

$$F_{G+B}(\delta_{ij}) = G_{ij}\cos(\delta_{ij}) + B_{ij}\sin(\delta_{ij}) \tag{3.15}$$

$$F_{B-G}(\delta_{ij}) = B_{ij}\cos(\delta_{ij}) - G_{ij}\sin(\delta_{ij}) \tag{3.16}$$

$$\delta_{ij} = \delta_i - \delta_j \tag{3.17}$$

3.5 Overall System Equation

From the above discussions, the dynamic equations governing the generators and exciters could be cast in the following form:

$$\dot{X} = f(X, Y, u) \tag{3.18}$$

where,

$X^T = [X_{SM}^T, X_{ES}^T]$, the vector of state variables

$X_{SM} = [E'_{q1}, E'_{d1}, \omega_1, ..., E'_{qm}, E'_{dm}, \omega_m, \delta_{m1}, \omega_{m+1}, \delta_{(m+1)1}, ..., \omega_n, \delta_{n1}]^T$

$X_{ES} = [E_{FD1}, X_{E11}, X_{E21}, ..., E_{FDm}, X_{E1m}, X_{E2m}]^T$

$Y = [I_{q1}, I_{d1}, ..., I_{qm}, I_{dm}, I_{m+1}, ...I_n, V_{T1}, ...V_{Tn}]^T$,

the vector of non-state (network) variables

$u = [V_{REF1}, \ldots, V_{REFm}]$, the vector of control inputs

and **f** is the vector of nonlinear functions summarized below:

$$\begin{aligned}
f_{1i} &= \dot{E}'_{qi} \\
&= \frac{1}{\tau'_{d0i}}[E_{FDi} - E'_{qi} + (x_{di} - x'_{di})I_{di}] \qquad i = 1, ..., m \qquad (3.19) \\
f_{2i} &= \dot{E}'_{di} \\
&= \frac{1}{\tau'_{q0i}}[-E'_{di} - (x_{qi} - x'_{qi})I_{qi}] \qquad i = 1, ..., m \qquad (3.20) \\
f_{3i} &= \dot{\omega}_i \qquad i = 1, ..., m \\
&= \frac{1}{M_i}[P_{mi} - (I_{di}E'_{di} + I_{qi}E'_{qi}) + (x'_{qi} - x'_{di})I_{qi}I_{di} - D_i(\omega_i - \omega_S)] \qquad (3.21) \\
f_{3i} &= \dot{\omega}_i \qquad i = m+1, ..., n \\
&= \frac{1}{M_i}[(P_{mi} - E'_i I_{qi} - D_i(\omega_i - \omega_S)] \qquad (3.22) \\
f_{4i} &= \dot{\delta}_{i1} \\
&= \omega_i - \omega_1 \qquad i = 2, ..., n \qquad (3.23) \\
f_{5i} &= \dot{E}_{FDi} \\
&= \frac{K_{Ai}}{T_{Ai}}X_{E2i} - \frac{1}{T_{Ai}}E_{FDi} + \frac{aK_{Ai}}{T_{Ai}}(V_{REFi} - X_{E1i}) \qquad i = 1, ..., m \qquad (3.24) \\
f_{6i} &= \dot{X}_{E1i} \\
&= -\frac{1}{T_{Ri}}X_{E1i} + \frac{1}{T_{Ri}}V_{Ti} \qquad i = 1, ..., m \qquad (3.25)
\end{aligned}$$

$$\begin{aligned} f_{7i} &= \dot{X}_{E2i} \\ &= -\frac{1}{T_{Bi}}X_{E2i} + \frac{1-a}{T_{Bi}}(V_{REFi} - X_{E1i}) \qquad i = 1, ..., m \end{aligned} \tag{3.26}$$

We also have the network algebraic equation

$$g(X, Y) = 0 \tag{3.27}$$

From (3.13) and (3.14), we have

$$I_{qi} = \sum_{j=1}^{m}[F_{G+B}(\delta_{ij})E'_{qj} - F_{B-G}(\delta_{ij})E'_{dj}] + \sum_{k=m+1}^{n} F_{G+B}(\delta_{ik})E_k \tag{3.28}$$

$$I_{di} = \sum_{j=1}^{m}[F_{B-G}(\delta_{ij})E'_{qj} + F_{G+B}(\delta_{ij})E'_{dj}] + \sum_{k=m+1}^{n} F_{B-G}(\delta_{ik})E_k \tag{3.29}$$

$$i = 1, 2, ..., n$$

For the exciter input voltage V_T:

$$V_T^2 - (E'_q + x'_d I_d)^2 + (E'_d - x'_q I_q)^2 = 0 \tag{3.30}$$

3.6 Linearization Model

Linearization of (3.18) leads to

$$\Delta\dot{X} = \frac{\partial f}{\partial X}\Delta X + \frac{\partial f}{\partial Y}\Delta Y + \frac{\partial f}{\partial u}\Delta u \tag{3.31}$$

Similarly, Linearization of (3.27) results in

$$\frac{\partial g}{\partial X}\Delta X + \frac{\partial g}{\partial Y}\Delta Y = 0 \tag{3.32}$$

$$\Delta Y = -(\frac{\partial g}{\partial Y})^{-1}\frac{\partial g}{\partial X}\Delta X \tag{3.33}$$

Substituting 3.33 into 3.31, the representation of the whole system in the state space form can be obtained as following:

$$\Delta\dot{X} = A\Delta X + B\Delta u \tag{3.34}$$

Where

$$A = \frac{\partial f}{\partial X} - \frac{\partial f}{\partial Y}(\frac{\partial g}{\partial Y})^{-1}\frac{\partial g}{\partial X} \tag{3.35}$$

$$B = \frac{\partial f}{\partial u} \tag{3.36}$$

3.7 LPV Model

The above linearization process is applied to every operating point (ρ). For each given operating condition, specified in terms of real and reactive power load, real power generation schedules at generator buses, and voltage magnitude at certain buses, a power flow solution is obtained. This solution provides the voltage magnitude and angles at all of the buses. With the voltage solution and the power injection at each generator bus, initial conditions for the state variables are calculated. The state equations and the network equations are then linearized, and a set of state-space equations whose entries depend on the operating conditions (ρ) are obtained in the following form:

$$\Delta\dot{X} = A(\rho)\Delta X + B(\rho)u \tag{3.37}$$

Where ΔX is the vector of incremental state variables, u is the vector of incremental control variables, and $A(\rho)$, and $B(\rho)$ are varying coefficient matrices with proper dimensions. ρ is time varying vector. It is bounded and its trajectory is unknown in advance, but we can measure it in real time. At each specific ρ, A and B are constant.

The linearization process is straightforward, but it is not feasible to achieve the complete LPV model as 3.38 in practice due to an infinite number of operating points (ρ) during the operating range. However, the complete form of the LPV model is not necessary at all in the LPV synthesis. Section 2.7 discussed details in solving the infinite dimension LMIs involved in the synthesis. A gridding process is employed to solve the approximated problem, which only needs the information of state space matrices A_ρ, B_ρ, C_ρ, and D_ρ on the grid points. For example, if there are two gridding points ρ_1 and

ρ_2, the linearization is only needed to be done on these two points. The resulting A_{ρ_1}, B_{ρ_1}, C_{ρ_1}, D_{ρ_1}, A_{ρ_2}, B_{ρ_2}, C_{ρ_2}, and D_{ρ_2} supply enough information for the LPV controller synthesis.

The linearized system models, including the generators, exciters, governors and the networks, have the following state space representation:

$$\begin{aligned} \dot{X} &= A(\rho)X + B(\rho)u + B(\rho)d \\ y &= C(\rho)X + D(\rho)u \end{aligned} \tag{3.38}$$

where X is a vector of the state variables, u is the control input, d is the disturbance, and y is the output variable. For PSS design case, they are defined as follows:

$$\begin{aligned} X^T &= [Generator\ states, Exciter\ states, etc.] \\ u &= [\Delta V_{PSS} : PSS\ voltage\ output] \\ d &= [\Delta V_{ref} : Exciter\ voltage\ reference] \\ y &= [\Delta\omega :\ the\ relative\ rotor\ speed] \end{aligned}$$

where A, B, C and D are coefficient matrices which depend on the operating condition ρ. At each gridding point, the state matrices A and B can be derived through the formula 3.35, Where

$$\left[\frac{\partial f}{\partial X}\right] = \begin{array}{c} \\ \dot{E}'_{q(1-m)} \\ \dot{E}'_{d(1-m)} \\ \dot{\omega}_{(1-n)} \\ \dot{\delta}_{(21-n1)} \\ \dot{E}_{FD(1-m)} \\ \dot{X}_{E1(1-m)} \\ \dot{X}_{E2(1-m)} \end{array} \begin{bmatrix} \frac{\partial f_{1i}}{\partial E'_{qj}} & 0 & 0 & 0 & \frac{\partial f_{1i}}{\partial E_{FDj}} & 0 & 0 \\ 0 & \frac{\partial f_{2i}}{\partial E'_{dj}} & 0 & 0 & 0 & 0 & 0 \\ \frac{\partial f_{3i}}{\partial E'_{qj}} & \frac{\partial f_{3i}}{\partial E'_{dj}} & \frac{\partial f_{3i}}{\partial \omega_j} & 0 & 0 & 0 & 0 \\ 0 & 0 & \frac{\partial f_{4i}}{\partial \omega_j} & 0 & 0 & 0 & 0 \\ 0 & 0 & \frac{\partial f_{5i}}{\partial \omega_j} & 0 & \frac{\partial f_{5i}}{\partial E_{FDj}} & \frac{\partial f_{5i}}{\partial X_{E1j}} & \frac{\partial f_{5i}}{\partial X_{E2j}} \\ 0 & 0 & 0 & 0 & 0 & \frac{\partial f_{6i}}{\partial X_{E1j}} & 0 \\ 0 & 0 & \frac{\partial f_{7i}}{\partial \omega_j} & 0 & 0 & \frac{\partial f_{7i}}{\partial X_{E1j}} & \frac{\partial f_{7i}}{\partial X_{E2j}} \end{bmatrix} \tag{3.39}$$

$$\left[\frac{\partial f}{\partial Y}\right] = \begin{matrix} \dot{E}'_{q(1-m)} \\ \dot{E}'_{d(1-m)} \\ \dot{\omega}_{(1-n)} \\ \dot{\delta}_{(21-n1)} \\ \dot{E}_{FD(1-m)} \\ \dot{X}_{E1(1-m)} \\ \dot{X}_{E2(1-m)} \end{matrix} \begin{bmatrix} 0 & \frac{\partial f_{1_i}}{\partial I_{dj}} & 0 \\ \frac{\partial f_{2_i}}{\partial I_{qj}} & 0 & 0 \\ \frac{\partial f_{3_i}}{\partial I_{qj}} & \frac{\partial f_{3_i}}{\partial I_{dj}} & 0 \\ 0 & 0 & 0 \\ 0 & 0 & 0 \\ 0 & 0 & \frac{\partial f_{6_i}}{\partial V_{Tj}} \\ 0 & 0 & 0 \end{bmatrix} \tag{3.40}$$

$$\left[\frac{\partial G}{\partial Y}\right] = \begin{matrix} I_{q(1-m)} \\ I_{d(1-m)} \\ V_{T(1-m)} \end{matrix} \begin{bmatrix} \frac{\partial I_{qi}}{\partial I_{qj}} & 0 & 0 \\ 0 & \frac{\partial I_{di}}{\partial I_{dj}} & 0 \\ \frac{\partial V_{Ti}}{\partial I_{qj}} & \frac{\partial V_{Ti}}{\partial I_{dj}} & \frac{\partial V_{Ti}}{\partial V_{Tj}} \end{bmatrix} \tag{3.41}$$

$$\left[\frac{\partial g}{\partial X}\right] = \begin{matrix} I_{q(1-m)} \\ I_{d(1-m)} \\ V_{T(1-m)} \end{matrix} \begin{bmatrix} \frac{\partial I_{qi}}{\partial E'_{qj}} & \frac{\partial I_{qi}}{\partial E'_{dj}} & 0 & \frac{\partial I_{qi}}{\partial \delta_{r1}} & 0 & 0 & 0 \\ \frac{\partial I_{di}}{\partial E'_{qj}} & \frac{\partial I_{di}}{\partial E'_{dj}} & 0 & \frac{\partial I_{di}}{\partial \delta_{r1}} & 0 & 0 & 0 \\ \frac{\partial V_{Ti}}{\partial E'_{qj}} & \frac{\partial V_{Ti}}{\partial E'_{dj}} & 0 & 0 & 0 & 0 & 0 \end{bmatrix} \tag{3.42}$$

$$\left[\frac{\partial f}{\partial u}\right] = \begin{matrix} \dot{E}'_{q(1-m)} \\ \dot{E}'_{d(1-m)} \\ \dot{\omega}_{(1-n)} \\ \dot{\delta}_{(21-n1)} \\ \dot{E}_{FD(1-m)} \\ \dot{X}_{E1(1-m)} \\ \dot{X}_{E2(1-m)} \end{matrix} \begin{bmatrix} 0 \\ 0 \\ 0 \\ 0 \\ \frac{\partial f_{5i}}{\partial V_{REFj}} \\ 0 \\ \frac{\partial f_{7i}}{\partial V_{REFj}} \end{bmatrix} \tag{3.43}$$

The details of 3.39-3.43 can be found in Appendix A.

In this research, the rotor speed is chosen as the control input for PSS. Then C, and D can be written in the following form.

$$C = [0...0, 1, 0...0] \tag{3.44}$$

$$D = 0 \tag{3.45}$$

This LPV model enables us to apply the promising LPV theories to power systems. The information of varying parameters is used in controller design and scheduling to stabilize the large range of plants and provide higher performance.

CHAPTER 4. CONTROLLER DESIGN APPLICATION

LPV synthesis approach will first be applied to the four-machine, two-area sample system. The objective is to design a power system stabilizer (PSS) to stabilize the whole system when it operates at different points. The PSS is supposed to be installed at generator 2.

4.1 Discussion on Classical PSS Design

As we mentioned before, PSS is used to provide positive damping for power system oscillations. The conventional PSS design is to produce a component of electrical torque in phase with the rotor speed deviations. Much study has been done in this area(53). The following diagram illustrates the relationship between the applied torques on the turbine-generator shaft and the resulting generator rotor speed and the rotor angular displacement. The transfer function $GEP(S)$ includes the dynamics of the generator, excitation system, and the power system.

An ideal stabilizer characteristic would therefore be inversely proportional to $GEP(S)$, i.e. :

$$PSS_{ideal}(s) = D_{deire}/GEP(s) \tag{4.1}$$

In practice, the PSS uses its lead/lag stages to compensate for phase lags in $GEP(s)$ over the frequency range of interest. It is normally of second or third order. Also a washout stage is included to prevent steady-state voltage offsets as system frequency changes.

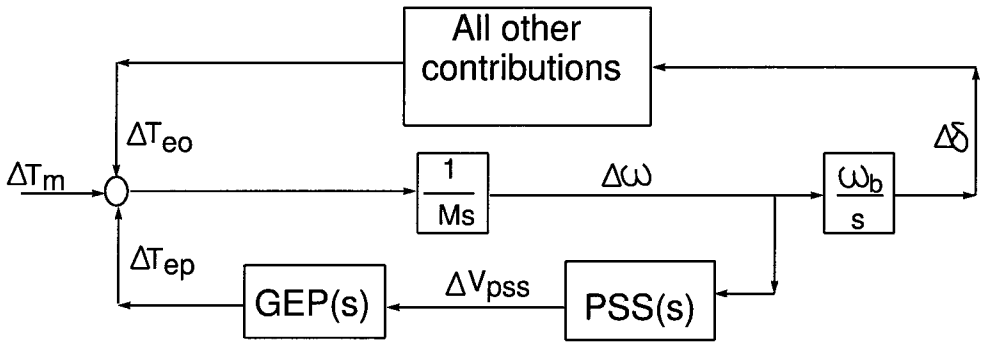

Figure 4.1 PSS with speed input–system block diagram

Filters are normally required for limiting noise and minimizing torsional interaction.

$$PracticalPSS(s) = K_(s)\frac{T_w s}{(1+T_w s)}\frac{(1+sT_1)(1+sT_3)}{(1+sT_2)(1+sT_4)}FILT(s) \tag{4.2}$$

The conventional design procedure for multi-machine systems is detailed in (52; 53). First, the complete state space model for the system is built. Then the state space model of the modified system is obtained by eliminating the columns and rows which correspond to the angles and speeds of the generators. The ideal phase lead curve is derived from the modified model. Conventional design uses lead/lag blocks to approximate the ideal compensating phase curve over a frequency range from $0.1Hz$ to $2Hz$. The curve comes from a single generator infinite bus equivalent, where all generator speeds and angles remain constant. Normally a $2nd$ or $3rd$ order lead/lag block will be good enough to match the ideal phase curve.

For the 4-machine test system, a conventional PSS installed at generator 2 was designed based on the above rule to improve the stability and damp the oscillations. The tie line real power flow of $0MW$ is chosen as the nominal point. The $3rd$ order conventional PSSs are employed here. The comparison between the phase lead of conventionally designed PSSs and ideal phase lead are shown in Fig. 4.2. The ideal phase curves at dif-

ferent operating points considering the dynamics of other generators instead of assuming them as constants are shown in Fig. 4.3 and Fig. 4.4.

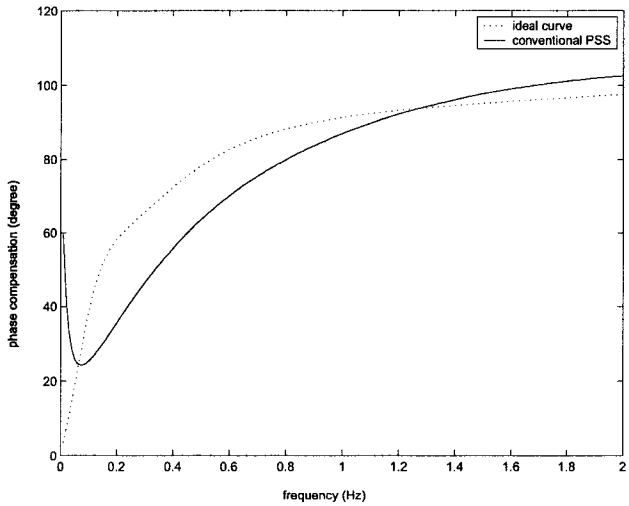

Figure 4.2 Comparison of PSS phase lead with the ideal phase compensation for generator at Bus ♯2 for 0MW tie line real power

From the above comparison, the following observations are made:

1. A lower order PSS is not enough to approximate the ideal phase compensation curve which considers the dynamics of other generators in the system.

2. A conventional PSS is designed at a nominal operating point, which could lead to non-optimal phase compensation at other operating points in the operating range. The ideal phase compensation curve changes with the operating points, the fixed PSS can't guarantee the robustness for a large operating range.

3. The ideal phase curve (GEP(s)) is based on the assumption that the dynamics of other generators in the system do not influence the PSS behavior by setting the speed and angle states constant. The simplification may introduce some errors in

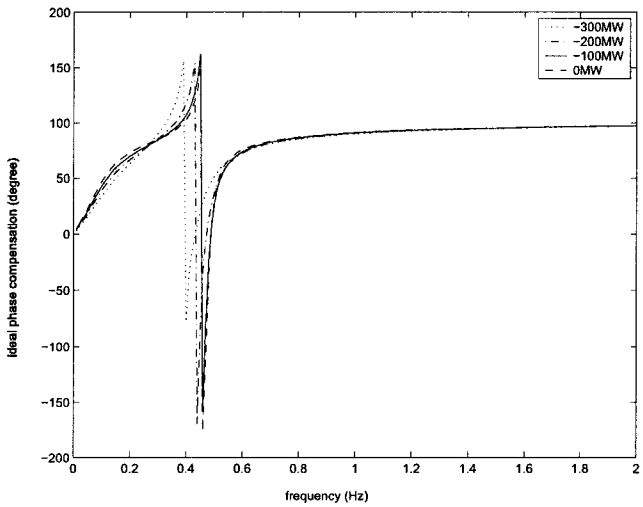

Figure 4.3 Ideal phase compensation curves for tie line real power at -300MW, -200MW, -100MW and 0MW.

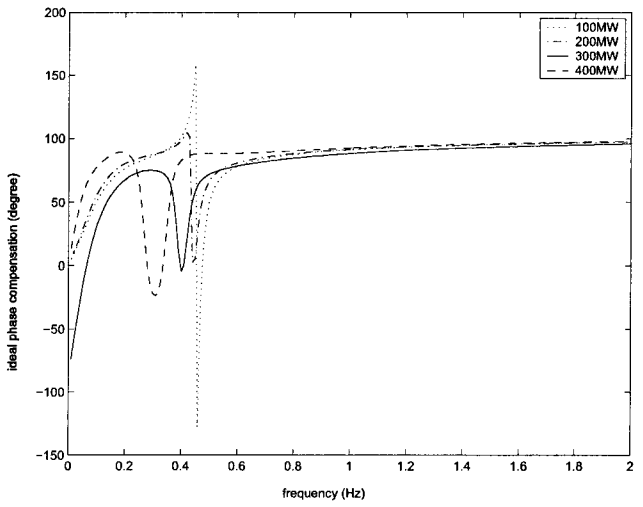

Figure 4.4 Ideal phase compensation curves for tie line real power at 100MW, 200MW, 300MW and 400MW.

the ideal phase lead curve, which can lead to deteriorating performance at some frequency points.

4. A complex tuning process is essential to be taken in selecting the gain for conventionally designed PSS to balance the damping between local modes and inter-area modes. It involves of on-line and off-line tuning procedures.

For the multi-PSS case that will be discussed in the next chapter, the situation is even more complicated. The phase compensation for one stabilizer is independent of the others since the speed and angle states are held constant for the ideal phase determination. Different PSSs may have conflicting influence on some modes. Further tuning is needed to coordinate them to reach a compromise (54; 16). In summary, the conventional PSS design for large power systems is very complicated and time consuming. Manual tuning is a necessary step to guarantee the coordination among PSSs.

4.2 SQLF LPV Design

4.2.1 Closed-loop H_∞ Norm Comparison with Optimal H_∞ Design

For the 4-machine system, the tie line real power flow is chosen as the scheduling variable, which is supposed to vary in the range of $[-200, 200]MW$. The Load1 varies in the range of $[1340, 1740]MW$ while Load2 varies in the range of $[1200, 1600]MW$. Five gridding points chosen are $-200MW$, $-100MW$, $0MW$, $100MW$ and $200MW$. The weighting function are : $W_{perf} = 10/(s+5)$, $W_u = 0.01$,$W_{noise} = 0.001$, respectively. Using the method based on the single quadratic Lyapunov function described in section 2.2.3, the resulting LPV controller at five gridding points is of 28th order.

At each of the five gridding points, one optimal H_∞ controller is designed for the corresponding LTI plant. Also the optimal H_∞ PSS designed for the nominal plant ($P = 0MW$) controller is applied for all 5 points. The closed-loop H_∞ norms in these three

cases are compared in Table 4.1. The closed-loop H_∞ norms with the LPV controller at the frozen points range from 0.024 to 0.028, which are larger than those achieved by the H_∞ optimal design. This is natural since the LPV controller is a suboptimal problem and designed with respect to all the possible parameter trajectories in the parameter variation set. When the H_∞ optimal controller designed at nominal plant $P = 0MW$ is applied for all the plants, we can observe that the closed loop system loses stability at $P = -200MW$, while the LPV controller maintains the system stability and performance in the whole range.

P(MW)	H_∞ I	H_∞ II	LPV
-200	0.014	unstable	0.028
-100	0.012	0.014	0.026
000	0.012	0.012	0.026
100	0.012	0.016	0.025
200	0.012	0.019	0.024

Table 4.1 Comparison of closed-loop H_∞ norm at the gridding points

4.2.2 Damping Ratio from MASS

At different operating points, within the whole operating range, the eigenvalues are computed using MASS. In Table 4.2, the eigenvalues corresponding to the inter-area mode and local modes and their damping ratios are compared among the cases without PSS, with conventional PSS, with optimal H_∞ PSS and with LPV PSS. The conventional PSS is tuned using the procedure described in (52; 53) at the operating point, where the tie line real power is $0MW$. The matches between the phase lead of the designed PSS and ideal phase lead are shown in Fig. 4.2. Without PSS, the five plants are all stable but have poorly damped inter-area modes. With optimal H_∞ PSS, the plant works well at its designed operating point, but when the operating point changes, the PSS even destabilizes the system. It also can be observed from the table that LPV PSS effectively

damped both inter-area mode and local modes by a larger damping ratio over the whole range than conventionally designed PSS.

4.2.3 Nonlinear Time Domain Simulation Results

Nonlinear time domain simulation is performed using ETMSP(42). First, a $0.1pu$ reference terminal voltage change is applied to generator 2, the output frequency of generator 2 is monitored. Then a three-phase short circuit fault is applied at bus 6 for $100ms$; the tie line real and reactive power flow are monitored. In the simulation results, the comparisons are made among cases with LPV PSS, with optimal H_∞ PSS and LPV PSS.

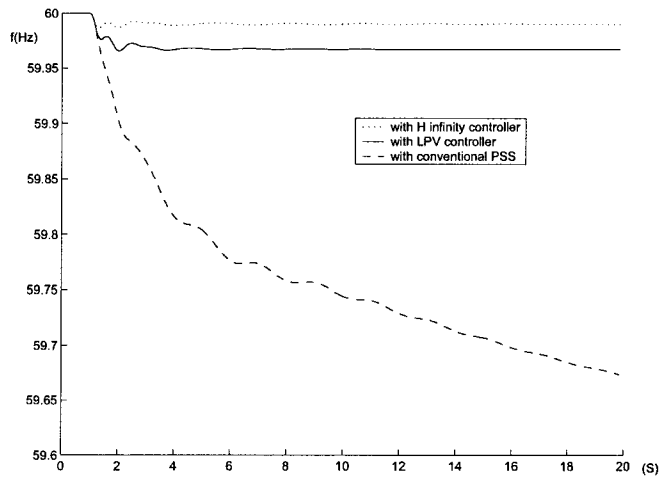

Figure 4.5 0.1pu change of reference terminal voltage at generator 2 (at $200MW$).

From the above comparison, we can see that LPV PSS has a larger operational range and improves system robustness and performance. It damps the oscillations for the whole operational range very well, even better than the optimal H_∞ PSS controller. What's more, the LPV synthesis technique allows us to design a gain-scheduled controller in one

Table 4.2 Comparison of damping ratios for different cases at the gridding points

Operating Conditions		Inter-area		Local	
		Mode	DR	Mode	DR
$P_{tie} = 200MW$	No PSS	$-0.07815 \pm 2.933i$	0.0266	$-1.039 \pm 7.927i$	0.1299
				$-1.117 \pm 7.865i$	0.1406
	Conv.	$-0.1452 \pm 2.994i$	0.0484	$-1.118 \pm 7.866i$	0.1407
				$-1.596 \pm 7.838i$	0.1996
	LPV	$-0.3901 \pm 3.097i$	0.1250	$-1.118 \pm 7.866i$	0.1407
				$-1.118 \pm 7.866i$	0.3918
	H_∞	$-0.1473 \pm 2.428i$	0.0606	$-1.118 \pm 7.866i$	0.1407
				$-1.427 \pm 6.735i$	0.2072
$P_{tie} = 100MW$	No PSS	$-0.08519 \pm 3.052i$	0.0279	$-1.030 \pm 7.936i$	0.1287
				$-1.087 \pm 7.870i$	0.1368
	Conv.	$-0.2059 \pm 3.075i$	0.0668	$-1.090 \pm 7.870i$	0.1371
				$-1.605 \pm 7.784i$	0.2005
	LPV	$-0.6397 \pm 2.960i$	0.2113	$-1.089 \pm 7.871i$	0.1371
				$-3.536 \pm 8.193i$	0.3963
	H_∞	$-0.1659 \pm 2.403i$	0.0689	$-1.089 \pm 7.871i$	0.1371
				$-1.416 \pm 6.776i$	0.2045
$P_{tie} = 0MW$	No PSS	$-0.0904 \pm 3.904i$	0.0292	$-1.033 \pm 7.942i$	0.1290
				$-1.072 \pm 7.871i$	0.1349
	Conv.	$-0.2708 \pm 3.087i$	0.0840	$-1.075 \pm 7.872i$	0.1353
				$-1.617 \pm 7.840i$	0.2020
	LPV	$-0.7811 \pm 2.433i$	0.3046	$-1.075 \pm 7.871i$	0.1353
				$-1.585 \pm 6.827i$	0.2262
	H_∞	$-0.2570 \pm 2.459i$	0.1040	$-1.075 \pm 7.872i$	0.1353
				$-0.2570 \pm 2.459i$	0.2038
$P_{tie} = -100MW$	No PSS	$-0.09386 \pm 3.068i$	0.0306	$-1.047 \pm 7.943i$	0.1307
				$-1.070 \pm 7.943i$	0.1348
	Conv.	$-0.3471 \pm 3.027i$	0.1139	$-1.073 \pm 7.876i$	0.1352
				$-1.632 \pm 7.835i$	0.2039
	LPV	$-0.5167 \pm 2.063i$	0.5299	$-1.073 \pm 7.867i$	0.1351
				$-3.284 \pm 8.117i$	0.3751
	H_∞	$-0.184 \pm 2.4901i$	0.0737	$-1.073 \pm 7.867i$	0.1351
				$-1.423 \pm 6.795i$	0.2049
$P_{tie} = -200MW$	No PSS	$-0.0936 \pm 2.949i$	0.0317	$-1.073 \pm 7.941i$	0.1340
				$-1.086 \pm 7.855i$	0.1370
	Conv.	$-0.4533 \pm 2.844i$	0.1574	$-1.087 \pm 7.856i$	0.1371
				$-1.649 \pm 7.828i$	0.2062
	LPV	$-0.2795 \pm 1.905i$	0.1452	$-1.087 \pm 7.856i$	0.1371
				$-2.887 \pm 8.064i$	0.3371
	H_∞	$0.009263 \pm 1.784i$	0.3729	-	-
				-	-

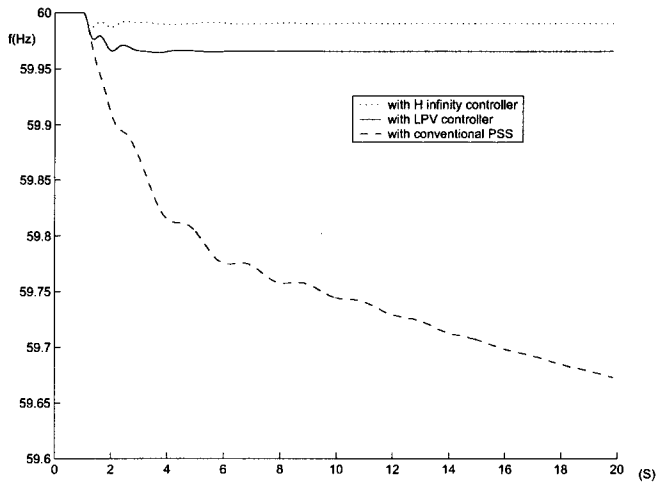

Figure 4.6 0.1pu change of reference terminal voltage at generator 2 (at $100MW$).

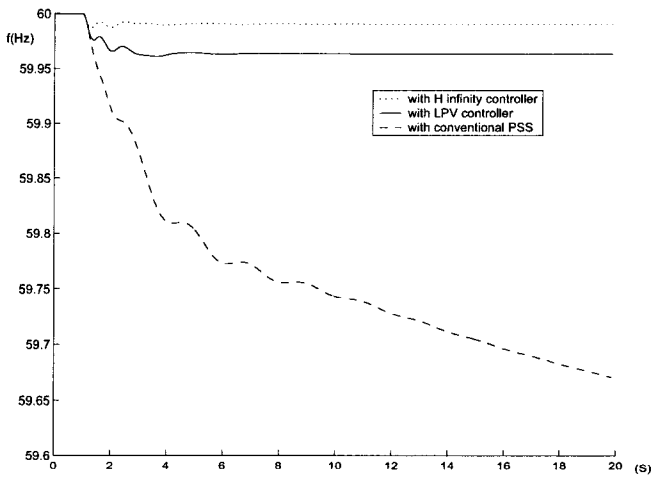

Figure 4.7 0.1pu change of reference terminal voltage at generator 2 (at $0MW$).

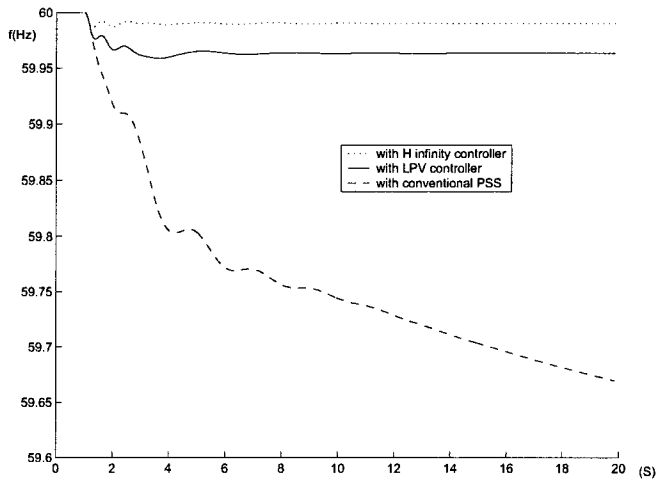

Figure 4.8 0.1pu change of reference terminal voltage at generator 2 (at $-100MW$).

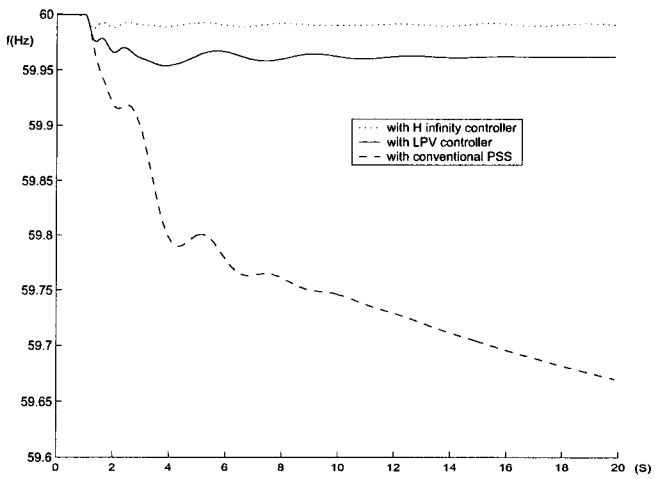

Figure 4.9 0.1pu change of reference terminal voltage at generator 2 (at $-200MW$).

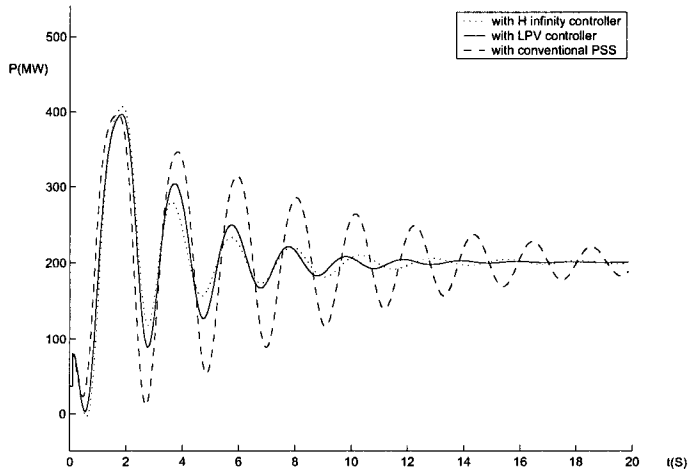

Figure 4.10 Tie line real power comparison among the LPV PSS, optimal H_∞ PSS and the conventional PSS (at $P_{tie} = 200MW$).

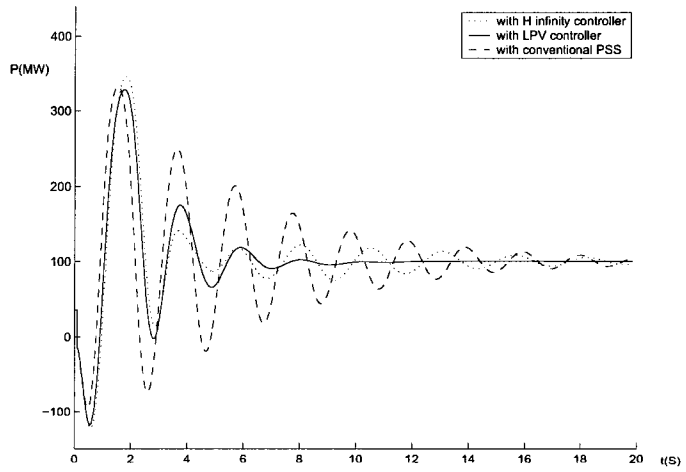

Figure 4.11 Tie line real power comparison among the LPV PSS, optimal H_∞ PSS and the conventional PSS (at $P_{tie} = 100MW$).

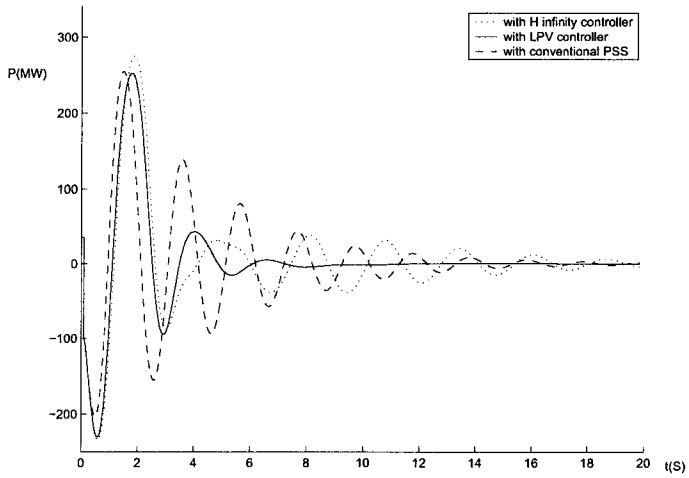

Figure 4.12 Tie line real power comparison among the LPV PSS, optimal H_∞ PSS and the conventional PSS (at $P_{tie} = 0MW$).

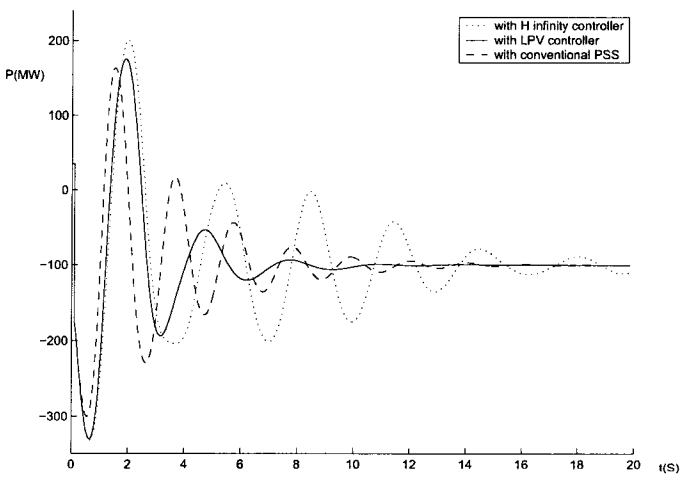

Figure 4.13 Tie line real power comparison among the LPV PSS, optimal H_∞ PSS and the conventional PSS (at $P_{tie} = -100MW$).

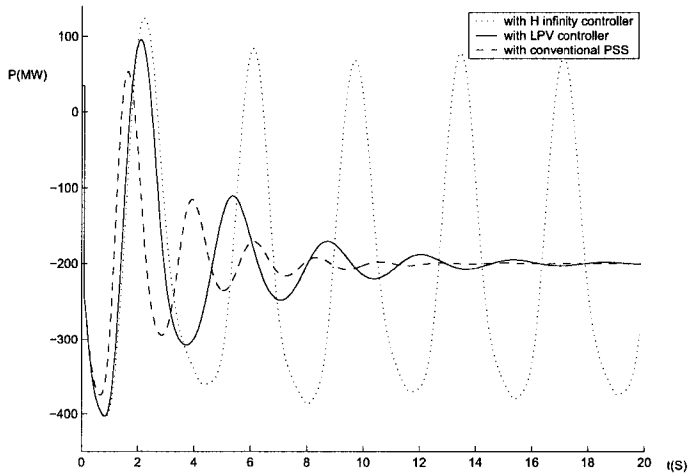

Figure 4.14 Tie line real power comparison among the LPV PSS, optimal H_∞ PSS and the conventional PSS (at $P_{tie} = -200MW$).

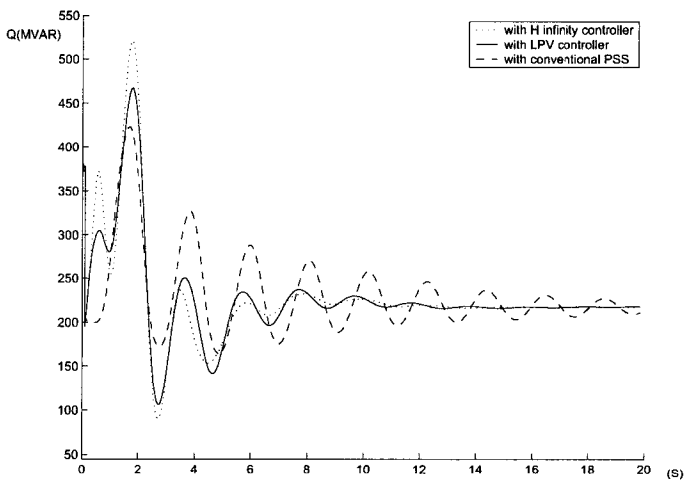

Figure 4.15 Tie line reactive power comparison among the LPV PSS, optimal H_∞ PSS and the conventional PSS (at $P_{tie} = 200MW$).

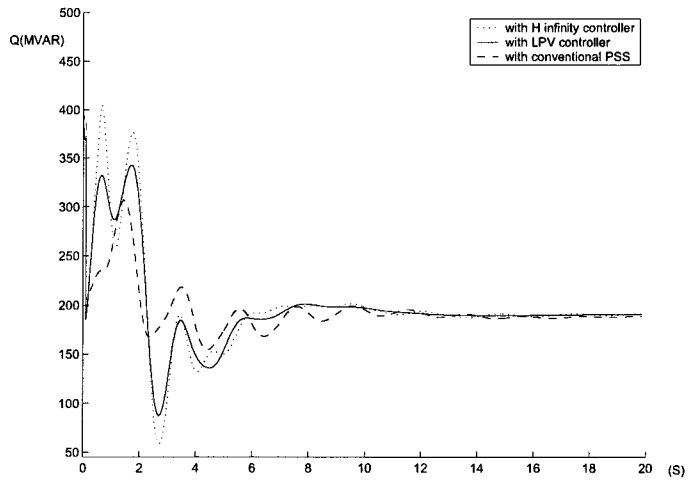

Figure 4.16 Tie line reactive power comparison among the LPV PSS, optimal H_∞ PSS and the conventional PSS (at $P_{tie} = 100MW$).

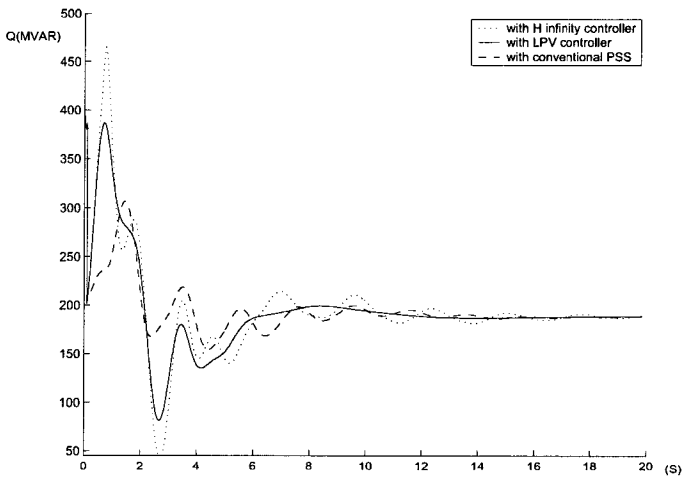

Figure 4.17 Tie line reactive power comparison among the LPV PSS, optimal H_∞ PSS and the conventional PSS (at $P_{tie} = 0MW$).

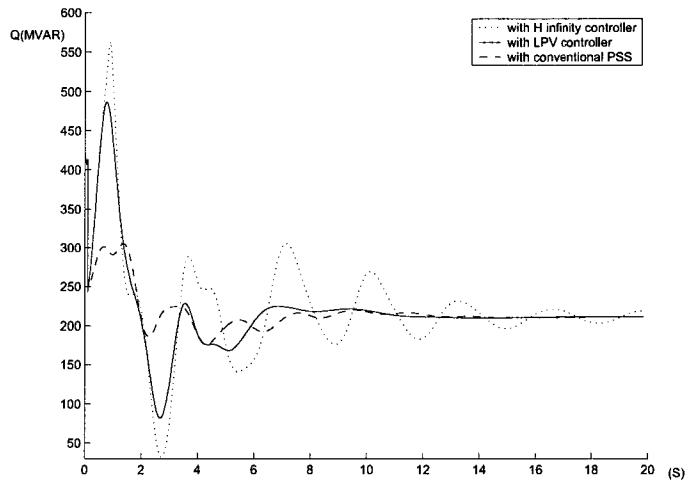

Figure 4.18 Tie line reactive power comparison among the LPV PSS, optimal H_∞ PSS and the conventional PSS (at $P_{tie} = -100MW$).

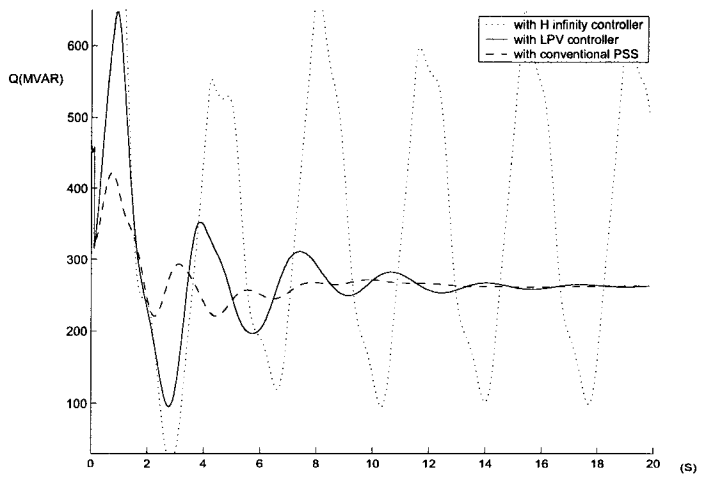

Figure 4.19 Tie line reactive power comparison among the LPV PSS, optimal H_∞ PSS and the conventional PSS (at $P_{tie} = -200MW$).

step,that is, to design the local LTI controllers and the scheduling strategy simultaneously. The LPV controller not only provides guarantees regarding the global behavior and sustaining performance, but also maintains stability and performance specifications for both slow varying parameters and rapidly changing parameters.

4.2.4 Realization of LPV PSS

It is shown in Fig.4.21-4.25 that each entry of the state space matrices of the LPV controller could be well approximated by the first order polynomial in P_{tie} at each of the gridding points through the least-squares estimation. The controller space matrices can be written as:

$$\begin{aligned} A_k(P_{tie}) &\doteq A_0 + P_{tie}A_1 \\ B_k(P_{tie}) &\doteq B_0 + P_{tie}B_1 \\ C_k(P_{tie}) &\doteq C_0 + P_{tie}C_1 \\ D_k(P_{tie}) &\doteq D_0 + P_{tie}D_1 \end{aligned} \tag{4.3}$$

The dynamics of the LPV controller can be expressed in the diagram as Fig. 4.20. During the big disturbance, P_{tie} might be out of the design range $[-200MW, 200MW]$.

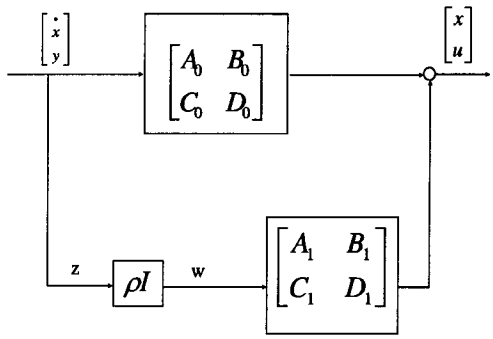

Figure 4.20 Diagram of the LPV dynamics.

If P_{tie} is less than $-200MW$, $A_k(P_{tie}) = A_k(-200)$. If P_{tie} is greater than $200MW$, $A_k(P_{tie}) = A_k(200)$. The same rule applies to B_k, C_k, and D_k.

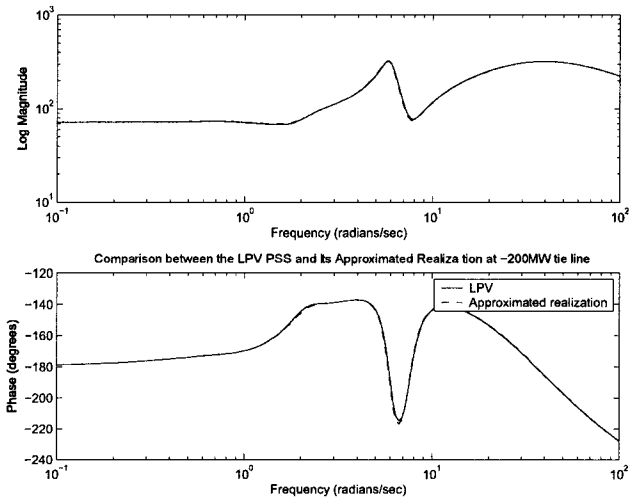

Figure 4.21 Comparison between the LPV PSS and its approximated realization (at $-200MW$).

4.3 Results For PDQF LPV Design

The single quadratic Lyapunov function based method gives good results. But its limit comes from the big conservatism considering arbitrary variation of parameter change. For the example above, we can't extend the range ([-200,200]) any more for the same weighting setup. In the real case, the load change rate always has some bounds. Motivated by the available bound information, a new synthesis formulation described in section 4.3 based on parameter dependent quadratic Lyapunov function can be employed to reduce conservatism and extend the operating range. The range [-300,400] is investigated here. We assume the tie line real power changes at a rate between $[-50MW/sec, 50MW/sec]$. The same weighting functions are chosen: $W_{perf} = 10/(s+5)$, $W_u = 0.01$, $W_{noise} = 0.001$. The basis functions f_i, g_i are chosen as

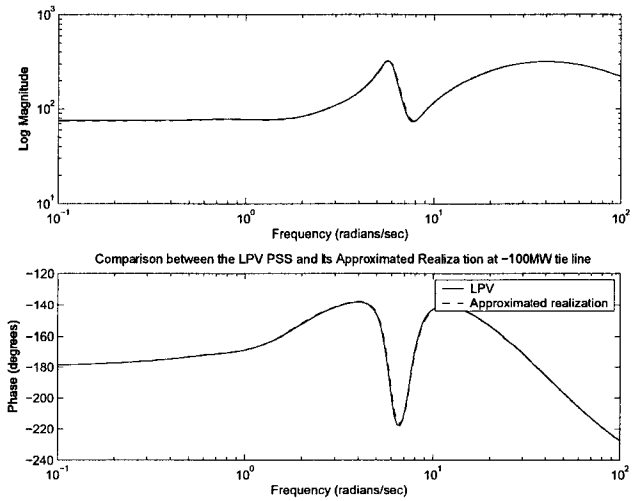

Figure 4.22 Comparison between the LPV PSS and its approximated realization(at $-100MW$).

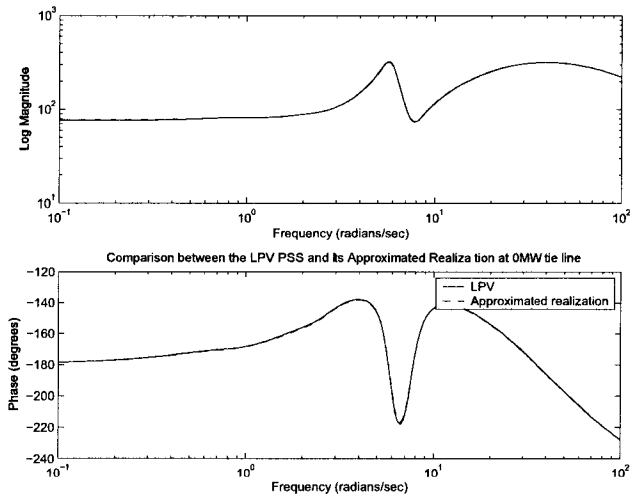

Figure 4.23 Comparison between the LPV PSS and its approximated realization(at $0MW$).

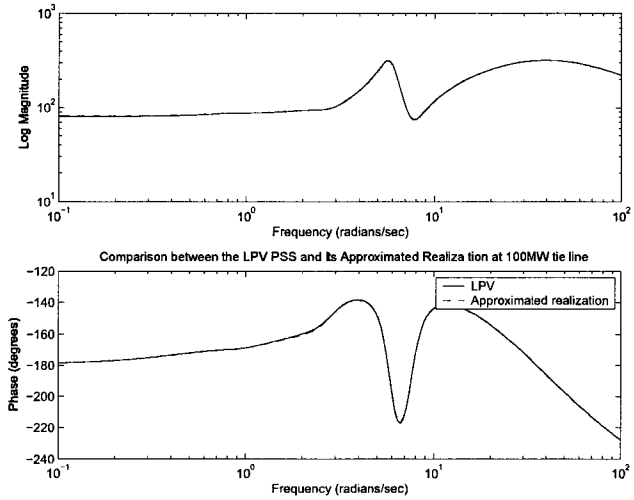

Figure 4.24 Comparison between the LPV PSS and its approximated realization(at $100MW$).

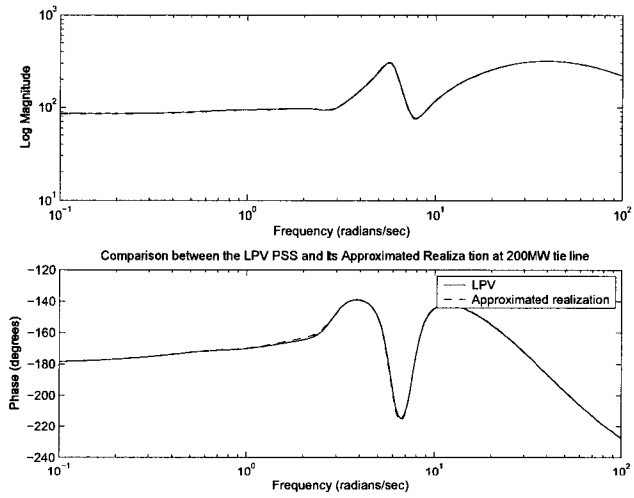

Figure 4.25 Comparison between the LPV PSS and its approximated realization(at $200MW$).

follows (let $i = 2$):

$f_1(P_{tie}) = g_1(P_{tie}) = 1$, which are constant.

$f_2(P_{tie}) = g_2(P_{tie}) = P_{tie}$, which are linear.

The resulting rate bounded LPV controller at the eight gridding points is of 28th order and the achieved closed loop induced L_2 norm from $[\Delta V_{ref}\ noise]^T$ to $[W_{perf}\ W_u]^T$ is 0.9000. Similarly, the optimal H_∞ controller's corresponding LTI plants are designed. The closed loop H_∞ norms at each gridding point are compared in Table 4.3. We can see the optimal H_∞ PSS can not stabilize the system at operating points $P_{tie} = -200 and -300 MW$, while the rate bounded LPV controller works well for maintaining system stability and performance.

P(MW)	H_∞ I	H_∞ II	LPV(bounded rates)
-300	0.056	unstable	0.110
-200	0.014	unstable	0.038
-100	0.012	0.014	0.025
000	0.012	0.012	0.020
100	0.012	0.016	0.017
200	0.012	0.019	0.017
300	0.012	0.021	0.018
400	0.013	0.024	0.028

Table 4.3 Comparison of closed-loop H_∞ norm at the gridding points

4.3.1 Inter-area Mode and Damping Ratio from MASS

Small signal stability is evaluated through mode analysis. MASS is employed to compute the eigenvalues at different operating points within the whole operating range. The eigenvalue corresponding to the inter-area mode and its damping ratios are compared with the case with conventional PSS designed based on the nominal point where the tie line real power is $0MW$ in Table 4.4. It can seen from the table that the rate bounded

LPV PSS effectively damped the inter-area mode by a larger damping ratio over the whole range than conventionally designed PSS.

P(MW) on tie line	with LPV PSS		with Conv. PSS	
	Inter-area mode(Hz)	DR	Inter-area mode(Hz)	DR
400	0.5001	0.1695	0.3904	0.0102
300	0.4870	0.1501	0.4577	0.0297
200	0.4606	0.1794	0.4765	0.0484
0	0.3788	0.1505	0.4913	0.0840
−200	0.3018	0.1174	0.4526	0.1574
−300	0.2550	0.2929	0.3401	0.2145

Table 4.4 Inter-area mode and damping ratio

4.3.2 Realization of LPV PSS

A piece-wise quadratic approximation can provide satisfactory precision. For the piece-wise approximation we find two quadratic curves intersecting at an intermediate point $P_{tie} = 0MW$. It is shown in Fig.4.26-4.33 that the LPV controller could be well approximated. The controller space matrices can be written as:

When $-300 \leq P_{tie} \leq -100$,

$$\begin{aligned} A_k(P_{tie}) &\doteq A_{10} + P_{tie}A_{11} + P_{tie}^2 A_{12} \\ B_k(P_{tie}) &\doteq B_{10} + P_{tie}B_{11} + P_{tie}^2 B_{12} \\ C_k(P_{tie}) &\doteq C_{10} + P_{tie}C_{11} + P_{tie}^2 C_{12} \\ D_k(P_{tie}) &\doteq D_{10} + P_{tie}D_{11} + P_{tie}^2 D_{12} \end{aligned} \tag{4.4}$$

When $-100 < P_{tie} \leq 400P_{tie}$

$$\begin{aligned} A_k(P_{tie}) &\doteq A_{20} + P_{tie}A_{21} + P_{tie}^2 A_{22} \\ B_k(P_{tie}) &\doteq B_{20} + P_{tie}B_{21} + P_{tie}^2 B_{22} \\ C_k(P_{tie}) &\doteq C_{20} + P_{tie}C_{21} + P_{tie}^2 C_{22} \\ D_k(P_{tie}) &\doteq D_{20} + P_{tie}D_{21} + P_{tie}^2 D_{22} \end{aligned} \tag{4.5}$$

During the big disturbance, P_{tie} might be out of the design range $[-300MW, 400MW]$. If P_{tie} is less than $-300MW$, $A_k(P_{tie}) = A_k(-300)$. If P_{tie} is greater than $400MW$, $A_k(P_{tie}) = A_k(400)$. The same rule applies to B_k, C_k, and D_k.

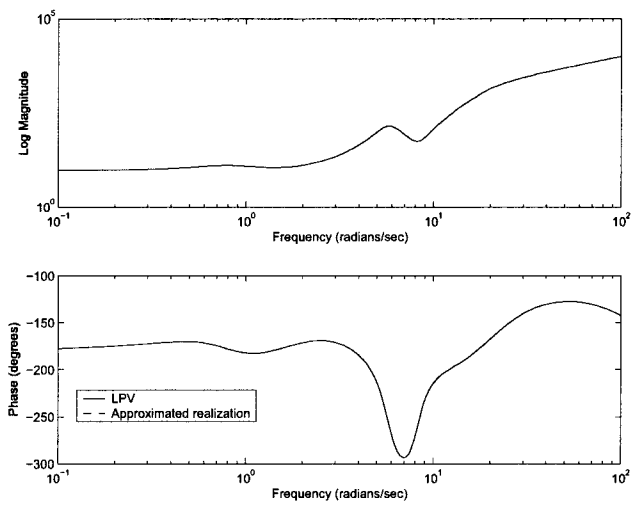

Figure 4.26 Comparison between the LPV PSS and its approximated realization (at $-300MW$).

4.4 Time Domain Simulation Results

Nonlinear time domain simulations are performed for different operating conditions to test the efficacy of the rate bounded LPV PSS. A three phase fault is applied to Bus ♯6 for 0.1s and the tie line real power is monitored, as shown in Fig.4.34-4.37. The performance of the rate bounded LPV PSS is compared with that of the conventional PSS designed at the nominal operating point where the tie line exporting power is $0MW$. It is observed that the rate bounded LPV PSS provides good damping in the operating range while the damping characteristic of the conventional PSS deteriorates when the system becomes more stressed.

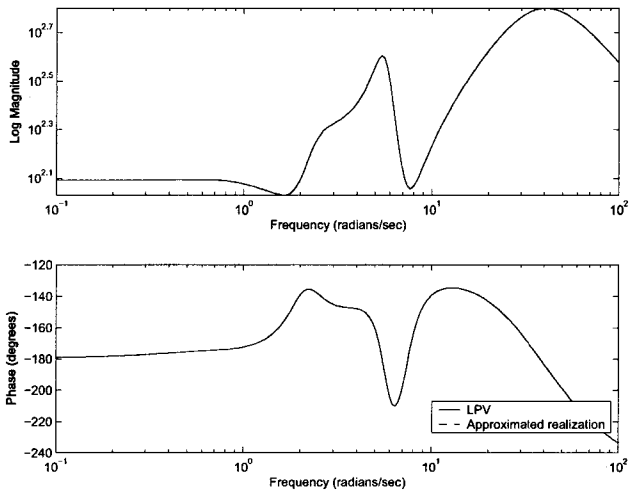

Figure 4.27 Comparison between the LPV PSS and its approximated realization (at $-200MW$).

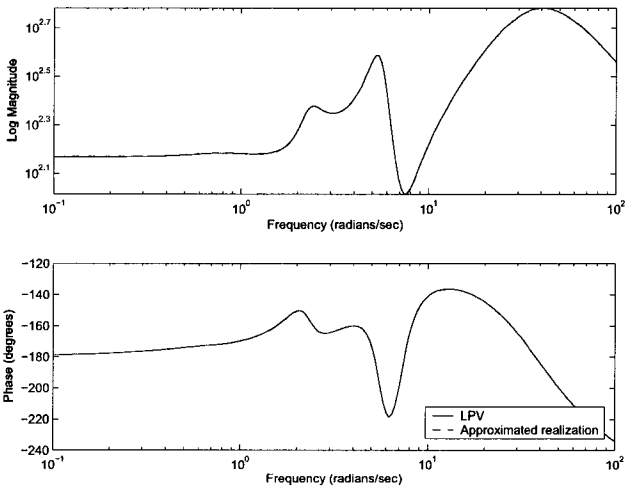

Figure 4.28 Comparison between the LPV PSS and its approximated realization(at $-100MW$).

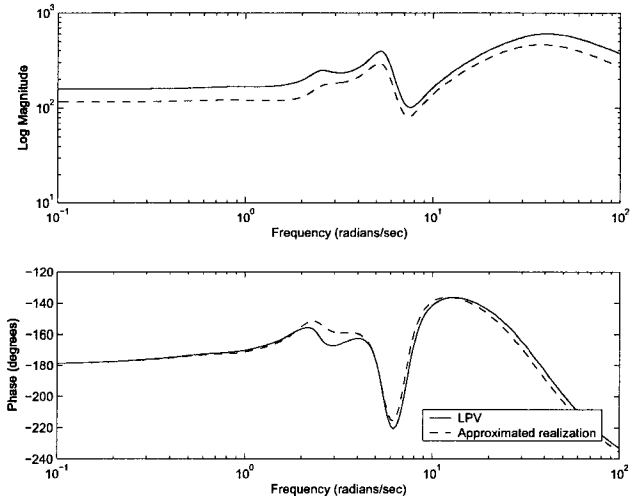

Figure 4.29 Comparison between the LPV PSS and its approximated realization(at $0MW$).

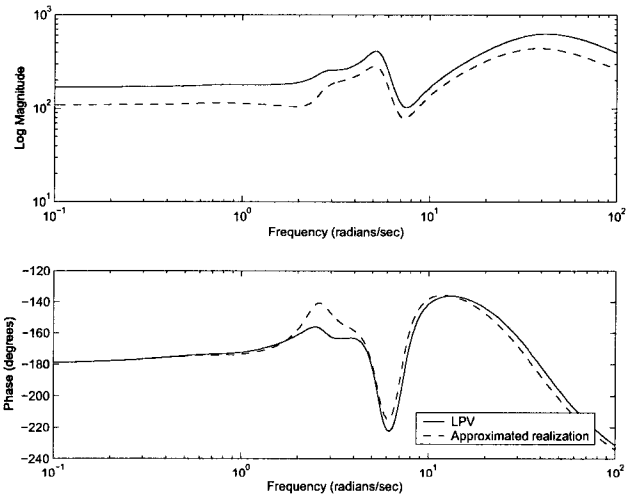

Figure 4.30 Comparison between the LPV PSS and its approximated realization(at $100MW$).

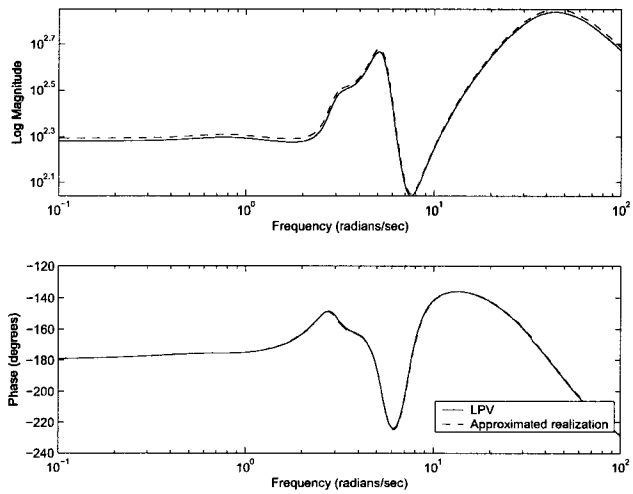

Figure 4.31 Comparison between the LPV PSS and its approximated realization(at $200MW$).

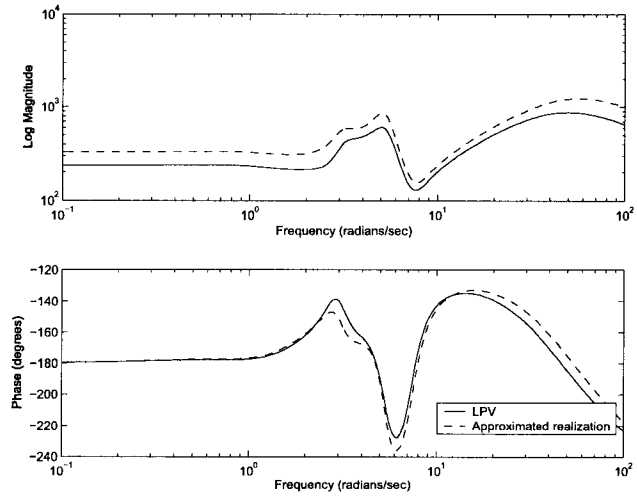

Figure 4.32 Comparison between the LPV PSS and its approximated realization(at $300MW$).

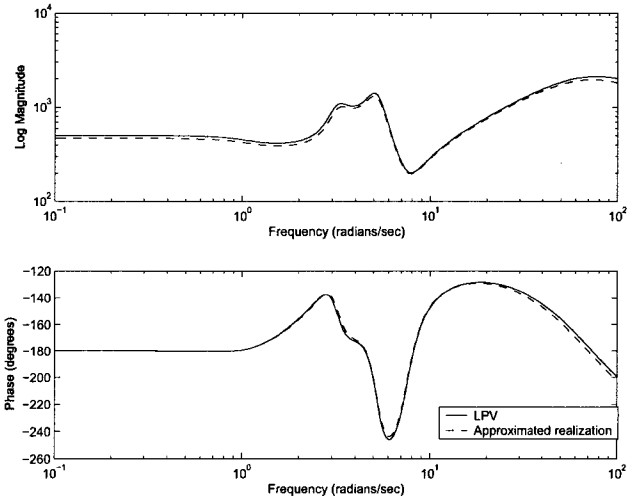

Figure 4.33 Comparison between the LPV PSS and its approximated realization(at $400MW$).

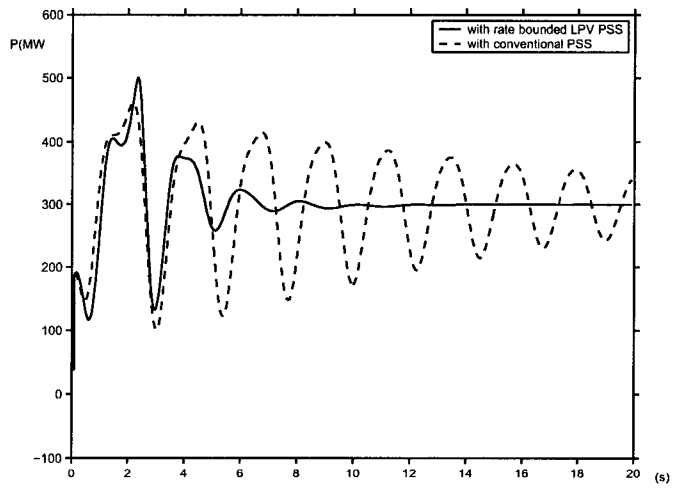

Figure 4.34 Comparison between the rate bounded LPV PSS and conventional PSS (at $300MW$).

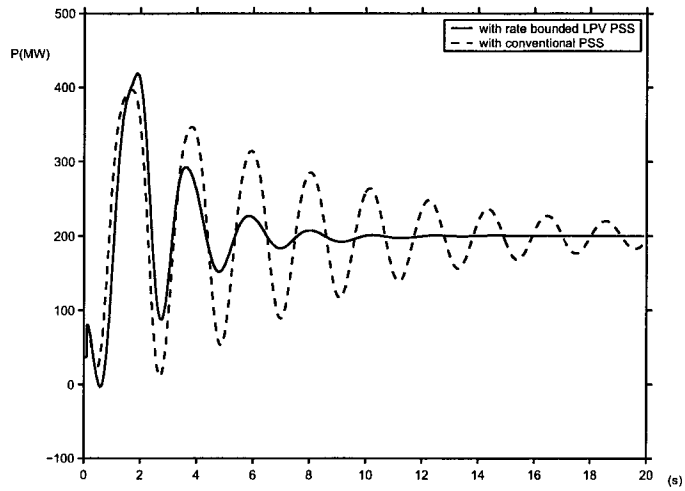

Figure 4.35 Comparison between the rate bounded LPV PSS and conventional PSS (at $200MW$).

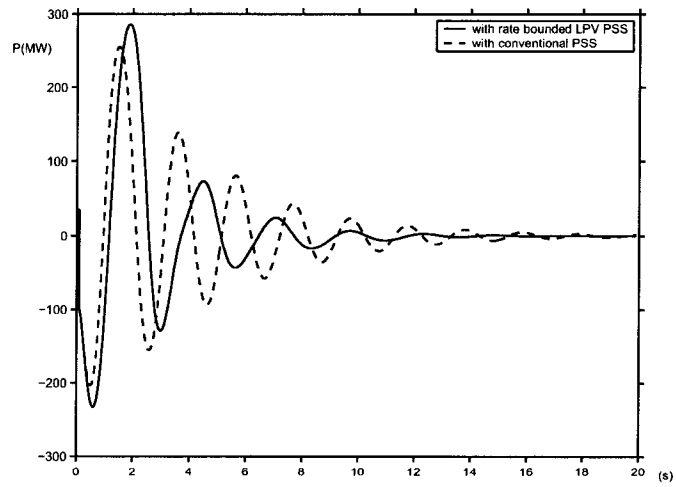

Figure 4.36 Comparison between the rate bounded LPV PSS and conventional PSS (at $0MW$).

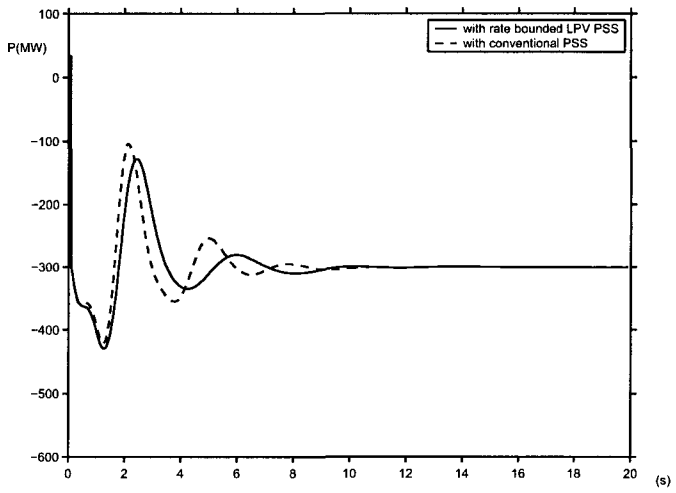

Figure 4.37 Comparison between the rate bounded LPV PSS and conventional PSS (at $-300MW$).

CHAPTER 5. DECENTRALIZED PSS DESIGN WITH LPV METHOD

5.1 Introduction

For large power systems, a single local controller is no longer sufficient to stabilize the whole system and to obtain a satisfactory damping property. Centralized design is neither economical nor reliable due to the inherent constraints of large power systems such as geographic dispersion, topology variance, and nonlinearities. Decentralized design becomes a natural consideration(48; 49). A coordinated action from the various controllers in the system is also needed. The control design method must minimize or prevent deleterious interactions among controllers, ensure that the dynamic and steady state performance criteria for the system are satisfied, and provide a simple procedure for tuning the controllers.

In recent years, considerable efforts have been placed on the coordinated synthesis of PSSs in large power systems. To achieve both a coordinated action and a better robustness with PSSs, an empirical procedure called tuning (which aims to maximize the phase margin in the frequency of interest) is employed. Naturally, due to its empirical nature, the efficiency of this procedure is limited and depends strongly on the designers' experience and knowledge of the system. The robust control approaches were motivated by the prospect of overcoming the cited drawbacks of tuning. However, typically high dimensions of power system models constitute another factor that discourages the application of computationally intensive design techniques and leads to very high order

controllers.

In this work, the LPV technique is applied to the decentralized controller design for PSS. Instead of considering the interconnected system model, we just consider each individual machine and represent its interconnection with the rest of the system by arbitrarily fast changing real and reactive power output in some range. All possible dynamics at the interface between the generator and the rest of the system are supposed to be represented by this approach. As a result, the system is decoupled naturally and the order of the plant is decreased dramatically. In addition robustness is considered through the time changing controller whose parameters are dependent on the scheduling variables, which represent the changes in the system operating conditions. The resulting controllers give satisfactory performance over a wide range of operating conditions.

5.2 Decentralized Design Steps

The SQLF LPV method can guarantee the stability and performance not only for slow changing parameters but also for arbitrarily fast changing parameters. That is to say, it automatically takes care of the dynamics of the changing parameters. In any power system network, each generator is connected with the rest of the system through its terminal bus. In addition the real and reactive power output of each generator characterizes the generator's interaction with the rest of the system through the transmission network. The real and reactive power variations also capture changes in network topology, network solution, and generator variables like voltage and rotor angles. Given these unique characteristics, the output real and reactive power of each generator where the local PSS will be installed are chosen as scheduling variables. As a result of this choice, each generator can then be decoupled from the rest of the system. The single generator subsystem includes only one generator and the influence of the rest of the system will be taken care of by the scheduling variables, its output real and reactive power. All possible

dynamics at the interface between the generator and the rest of the system are supposed to be represented by the scheduling variables. It can be seen that this decoupling leads to a decentralized design for the localized controller and results in lower order PSSs.

The grid points are obtained based on the scheduling variables, which vary on a fixed range. The design procedure for the decentralized PSSs include the following steps:

1. For each grid point obtain the power flow solution for the interconnected system and determine the matrices $A(\rho)$, $B(\rho)$,$C(\rho)$, and $D(\rho)$. This solution also determines the generator bus voltage and the real and reactive power output of each generator, this then determines the interaction with the rest of the system;

2. Choose the generator where a PSS should be installed. Optimum potential location is chosen using existing techniques such as combined damping torque technique and High order residues (51);

3. Using the real and reactive power output of the chosen generator from step 1 as scheduling variables form the decoupled single generator subsystem using the scheduling variables as a representative of the system interface;

4. Using the LPV synthesis procedure described in Section 2.4, synthesize the LPV controller;

5. Repeat the above steps to design another PSS for the next generator until the system performance is satisfied.

It is to be noted that when the PSSs at other generators are designed only the initial output of the machine is used. The effect of the PSS at the other generators is not represented. The reason we can do this is that the adding PSS to a generator won't change the range of real and reactive power output of other generators. Hence the design is indeed decentralized. The framework for the multi-machine decentralized PSS design is given in Fig. 5.1

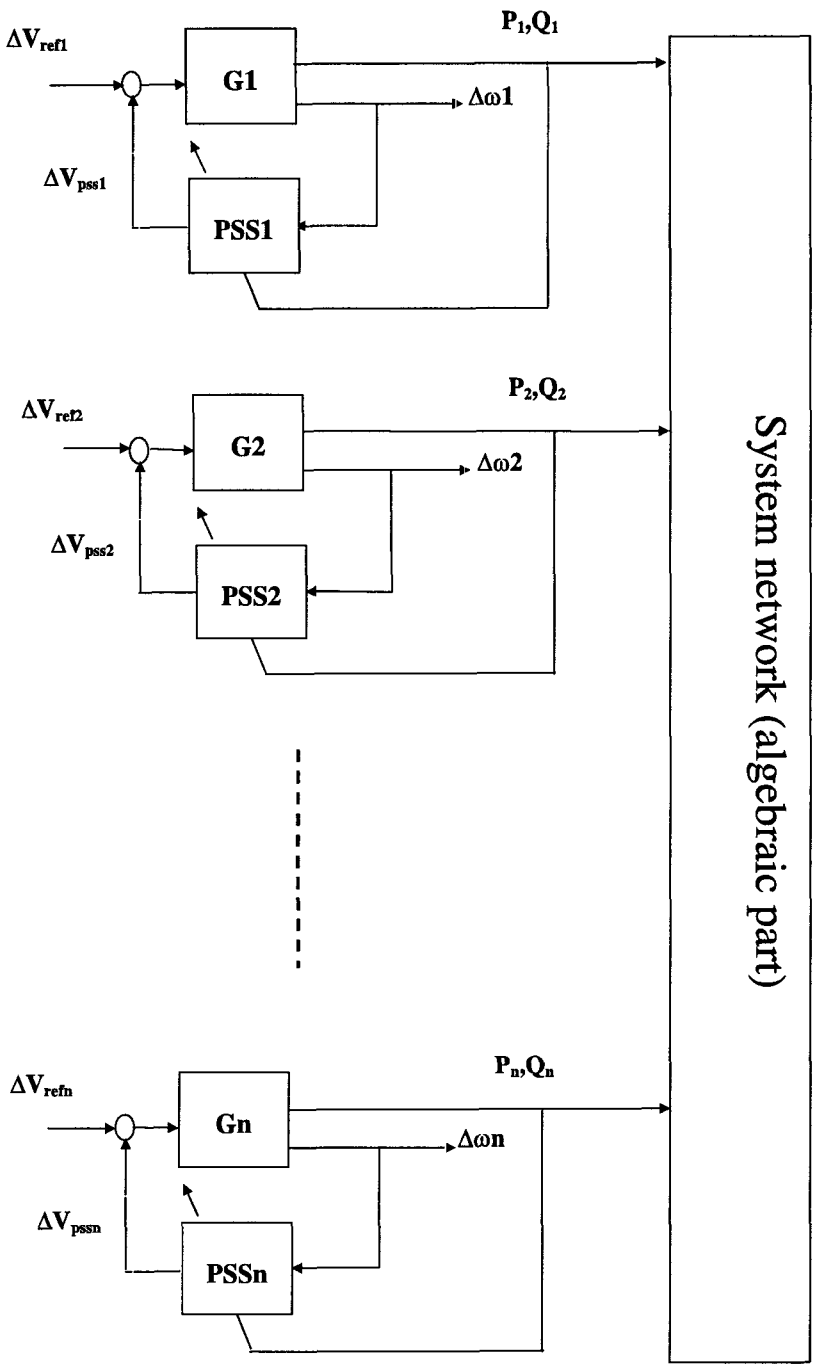

Figure 5.1 LPV synthesis framework for decentralized PSS design

5.3 PSS Design for a Four-Machine System

The proposed LPV decentralized design procedure is first applied to the 4-machine system. Again, the exporting power from Area1 is chosen as the changing parameter, which is allowed to vary in the range of $[0, 400MW]$. 5 grid points are chosen and they are evenly spaced. Four PSSs installed at each generator in the system are designed independently following the above procedure. The same weighting functions

$$W_{perf} = \frac{0.05s + 400}{s + 40}$$

$$W_u = 0.01$$

$$W_{noise} = 0.01$$

are chosen for each PSS design. the resulting PSSs are of $7th$ order.

5.3.1 Small Signal Analysis

At each grid point, the small signal stability analysis is done using MASS. The eigenvalue corresponding to the least damped inter-area mode and its damping ratio are given in the Table 5.1. It can be seen from the table that the decentralized PSSs damped the inter-area mode well over the whole operating range.

Table 5.1 Least damped inter-area mode and its damping ratio

P_{5-6}(MW)	Least damped inter-area mode	DR
0	$-0.6320 \pm 0.7342j$	0.6523
100	$-0.4169 \pm 2.7770j$	0.1485
200	$-0.4271 \pm 2.9140j$	0.1450
300	$-0.4063 \pm 3.0690j$	0.1312
400	$-0.3568 \pm 0.3980j$	0.6675

5.3.2 Time Domain Simulation

Time domain simulations are run for different operating conditions. A three phase fault is applied at Bus ♯5 for a period of 100ms. The simulation results are shown in Fig.5.2-5.6. In all five figures, decentralized LPV PSSs are able to hold the system stable and have good damping performance.

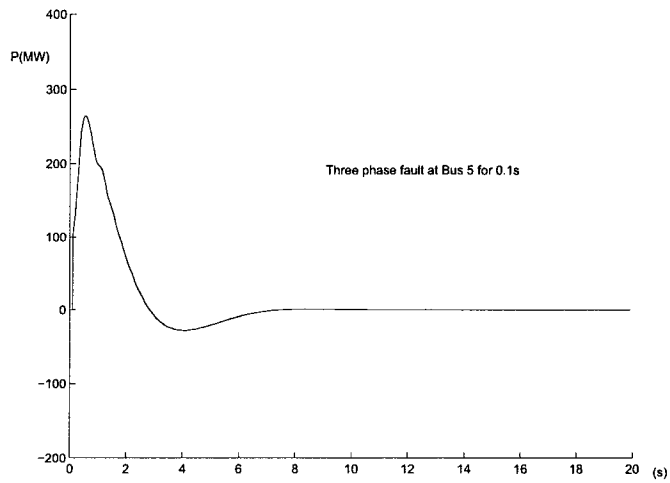

Figure 5.2 Time response of tie line real power ($0MW$) in the case of a 100ms three phase fault at Bus 5.

5.4 PSS Design for a Fifty-Machine System

The LPV decentralized design is then applied to the 50-generator IEEE test system (50). the performance of the decentralized LPV PSSs and conventionally designed PSSs are compared. The studies includes small signal stability study, time domain simulations and transient stability study.

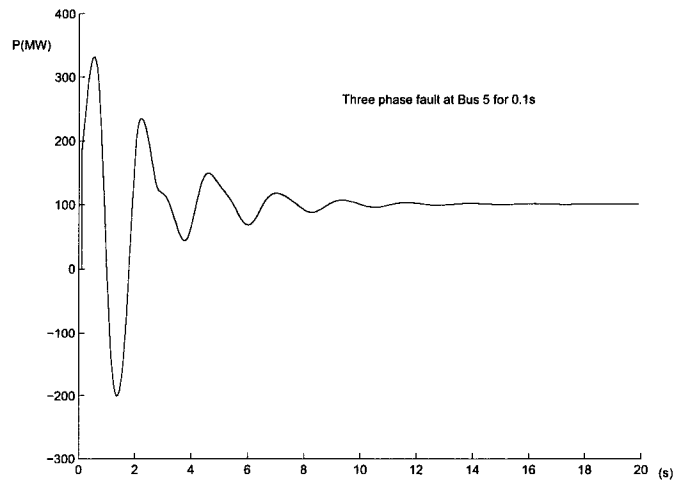

Figure 5.3 Time response of tie line real power ($100MW$) in the case of a 100ms three phase fault at Bus 5.

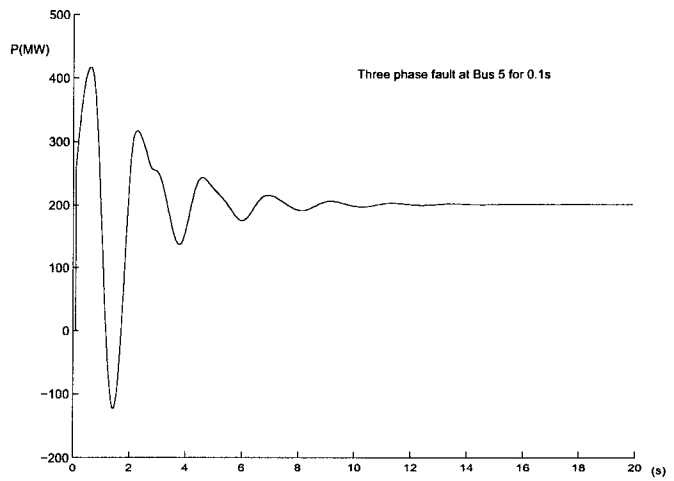

Figure 5.4 Time response of tie line real power ($200MW$) in the case of a 100ms three phase fault at Bus 5.

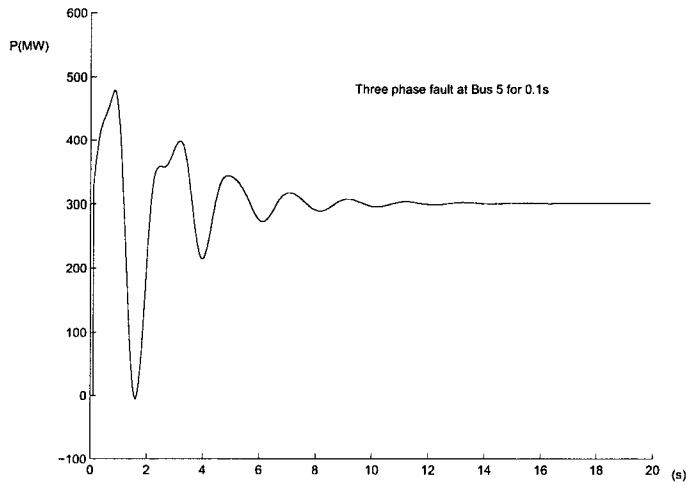

Figure 5.5 Time response of tie line real power ($300MW$) in the case of a 100ms three phase fault at Bus 5.

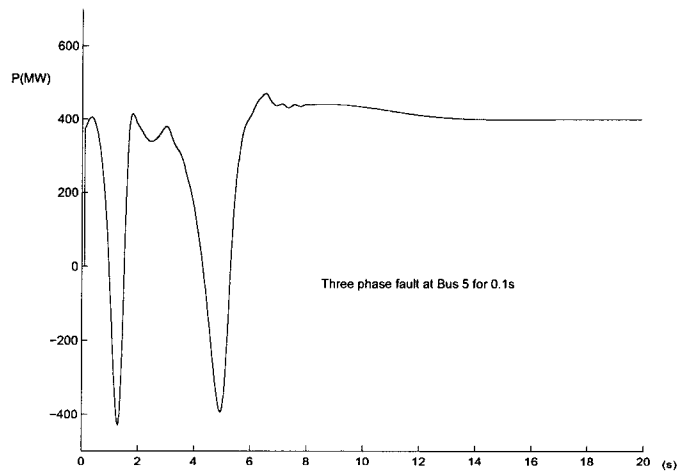

Figure 5.6 Time response of tie line real power ($400MW$) in the case of a 100ms three phase fault at Bus 5.

5.4.1 Gridding Process

The operating point is characterized by setting the real power generation at Buses ♯93 and ♯110. This generation varies in the range $[2 \times 1150 - 2 \times 1750]MW$. Seven gridding points are chosen for each generator. They correspond to $2 \times 1150MW$, $2 \times 1250MW$, $2 \times 1350MW$, $2 \times 1450MW$, $2 \times 1550MW$, $2 \times 1650MW$ and $2 \times 1750MW$ of generation at Buses ♯93 and ♯110. For each gridding point, the power flow for the interconnected system is solved and the real and reactive power output of each generator can be determined as shown in Table5.2.

P(MW) at Bus♯93 and Bus♯110	93		104		110		111	
	P(MW)	Q(MVAR)	P(MW)	Q(MVAR)	P(MW)	Q(MVAR)	P(MW)	Q(MVAR)
2×1150	1150	469.67	2000	500	1150	612.04	2000	663.99
2×1250	1250	500.79	2000	500	1250	642.41	2000	692.11
2×1350	1350	537.37	2000	500	1350	677.69	2000	726.84
2×1450	1450	579.28	2000	500	1450	717.81	2000	767.14
2×1550	1550	627.33	2000	500	1550	763.49	2000	814.79
2×1650	1650	708.22	2000	500	1650	766.00	2000	878.87
2×1750	1650	766.00	2000	500	1750	766.00	2000	971.58

Table 5.2 Real and reactive power output of generators where PSSs are installed at gridding points

First, the scheduling variables for each PSS include real and reactive power output of the generator where the PSS is located. In the case where the real power is fixed by dispatcher's order such as generator ♯111, the reactive power still varies. It will give the operating information of the system to the PSS to correspondingly adjust.

When both real and reactive powers of a generator are fixed such as generator ♯104, the corresponding single PSS won't schedule itself. It doesn't mean decentralized PSSs can't deal with the situation. Since the new control strategy involves multiple PSSs distributed at different locations, the coordination among them gives the control for the whole system. In this case, other PSSs will take care of the system changed dynamics

and the control coordination.

5.4.2 Design Details

Four independently designed PSSs following the procedures described in Section ?? are located on generators at Bus ♯93, ♯104, ♯110 and ♯111 respectively. Single Quadratic Lyapunov Function based LPV approach is adopted and the same design setup as in Section 2.5 is applied. The same weighting functions

$$W_{perf} = \frac{0.05s + 400}{s + 40}$$

$$W_u = 0.01$$

$$W_{noise} = 0.01$$

are chosen for each PSS design. Since the design is based on the decoupled single machine system, the resulting PSSs are all $7th$ orders, which is much lower in comparison with other robust design methods where the whole system model has to be considered.

For the purpose of comparison, four conventional PSSs at the same locations as the LPV PSSs, are designed at the nominal operating point where the generation at Bus ♯93 and ♯110 is $2\times1350MW$. The conventional design procedure is detailed in (52; 53). First, the complete state space model for the system is built. Then the state space model of the modified system is obtained by eliminating the columns and rows which correspond to the angles and speeds of the generators. The ideal phase lead curve is derived from the modified model. Conventional design uses lead/lag blocks to approximate the ideal compensating phase curve over a frequency range from $0.1Hz$ to $2Hz$. The curve comes from a single generator infinite bus equivalent, where all generator speeds and angles remain constant. Normally a $3rd$ order lead/lag block will be good enough to match the ideal phase curve. The $3rd$ order conventional PSSs are employed here. The comparison

between the phase lead of conventionally designed PSSs and ideal phase lead are shown in Fig. 5.7-5.10. The transfer functions of the PSSs are given as $G_c(s) = \frac{N_c(s)}{D_c(s)}$. For the PSSs installed at generators ♯93 and ♯110,

$$\begin{aligned} N_c(s) &= 12.3s^3 + 162.3s^2 + 150s \\ D_c(s) &= 0.004s^3 + 0.4004s^2 + 10.04s + 1 \end{aligned}$$

For the PSSs installed at generators ♯104 and ♯111,

$$\begin{aligned} N_c(s) &= 8.88s^3 + 131.1s^2 + 150s \\ D_c(s) &= 0.004s^3 + 0.4004s^2 + 10.04s + 1 \end{aligned}$$

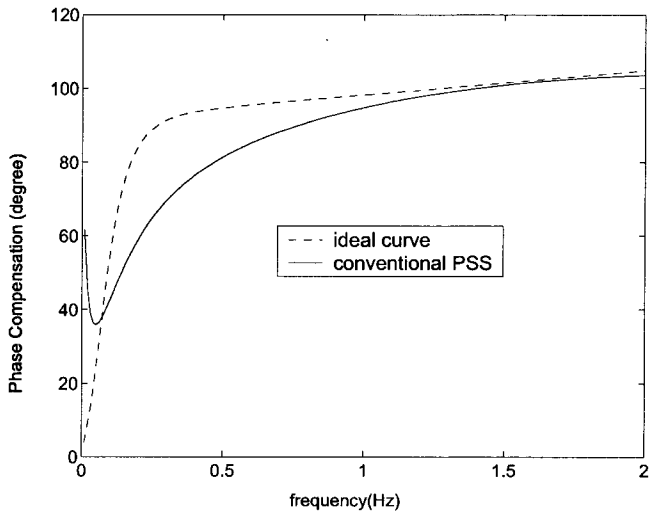

Figure 5.7 Comparison of PSS phase lead with the ideal phase compensation for generator at Bus ♯93

The LPV synthesis yields a higher order controller than the conventional design. Since a H_∞ design is involved in the LPV synthesis, it gives a controller of the same order as the open-loop plant. The LPV technique decouples the single generator from the whole system, so the open-loop plant just includes the generator and the weighting

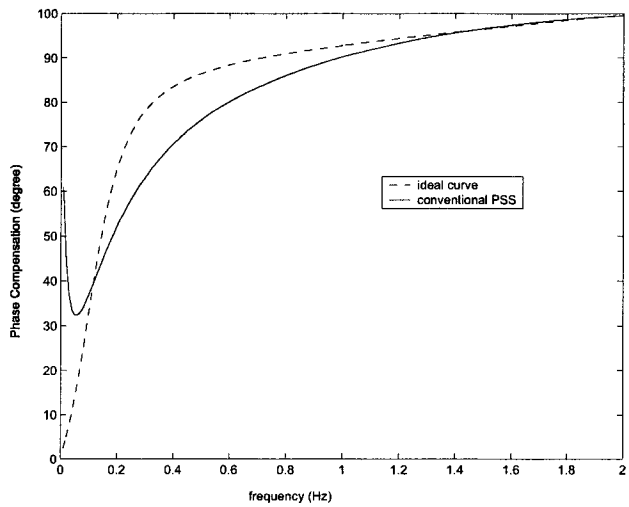

Figure 5.8 Comparison of PSS phase lead with the ideal phase compensation for generator at Bus ♯104

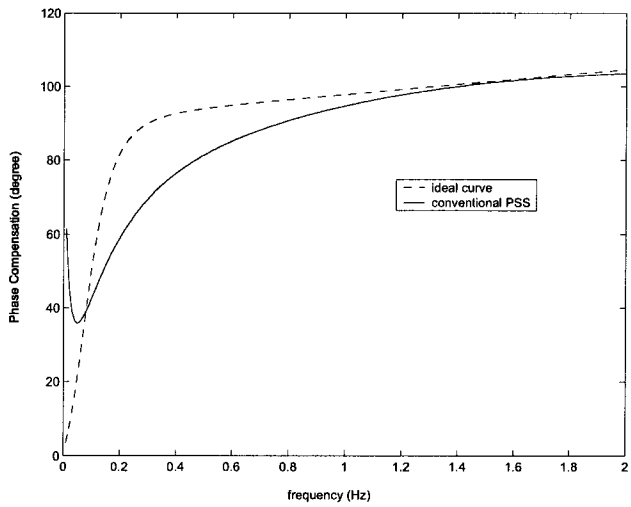

Figure 5.9 Comparison of PSS phase lead with the ideal phase compensation for generator at Bus ♯110

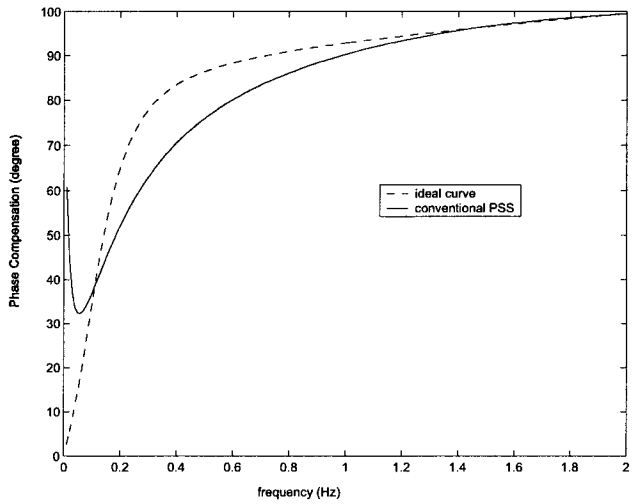

Figure 5.10 Comparison of PSS phase lead with the ideal phase compensation for generator at Bus ♯111

functions. In our case, the two-axis generator model and the first order weighting compose the $7th$ order open-loop plant. Then a $7th$ order LPV controller is introduced. To further illustrate the adaptive characteristic of LPV controllers, the transfer functions at different operating points of the LPV PSS at generator ♯111 are given as $G_k(s) = \frac{N(s)}{D(s)}$.

At the operating point characterized by $P = 1150MW$ and $Q = 470MVAR$ at Bus ♯93 and $P = 1150MW$ and $Q = 470MVAR$ at Bus ♯110 respectively

$$\begin{aligned} N(s) &= 6.188e4s^6 + 1.132e7s^5 + 6.192e8s^4 + \\ &\quad 1.087e10s^3 + 2.385e10s^2 + 2.053e10s + 6.494e9 \\ D(s) &= s^7 + 248.4s^6 + 2.279e4s^5 + 9.764e5s^4 + \\ &\quad 1.965e7s^3 + 1.545e8s^2 + 2.337e8s + 9.79e7 \end{aligned}$$

At the operating point characterized by $P = 1350MW$ and $Q = 537MVAR$ at Bus

♯93 and $P = 1350MW$ and $Q = 678MVAR$ at Bus ♯110 respectively

$$\begin{aligned} N(s) &= 6.188e4s^6 + 1.132e7s^5 + 6.204e8s^4 + \\ &\quad 1.094e10s^3 + 2.49e10s^2 + 2.2e10s + 7.024e9 \\ D(s) &= s^7 + 247.1s^6 + 2.254e4s^5 + 9.622e5s^4 + \\ &\quad 1.951e7s^3 + 1.59e8s^2 + 2.421e8s + 1.017e8 \end{aligned}$$

At the operating point characterized by $P = 1750MW$ and $Q = 766MVAR$ at Bus ♯93 and $P = 1750MW$ and $Q = 766MVAR$ at Bus ♯110 respectively

$$\begin{aligned} N(s) &= 6.188e4s^6 + 1.133e7s^5 + 6.222e8s^4 + \\ &\quad 1.103e10s^3 + 2.649e10s^2 + 2.421e10s + 7.82e9 \\ D(s) &= s^7 + 245.2s^6 + 2.216e4s^5 + 9.41e5s^4 + \\ &\quad 1.929e7s^3 + 1.656e8s^2 + 2.545e8s + 1.073e8 \end{aligned}$$

Further discussion is needed regarding the design of a conventional PSS. First, a conventional PSS is designed at a nominal operating point, which could also lead to non-optimal phase compensation at other operating points in the operating range. Another important point is that the ideal phase curve is based on the assumption that the dynamics of other generators in the system do not influence the PSS behavior by setting the speed and angle states constant. This simplification may introduce some errors in the ideal phase lead curve, which can lead to deteriorating performance at some frequency points. Also, a complex tuning process is essential to be taken in selecting the gain for conventionally designed PSS to balance the damping between inter-area modes and inter-area modes. It involves a lot of on-line and off-line tuning procedures.

For the multi-PSS case, the phase compensation for one stabilizer is independent of the others since the speed and angle states are held constant for the ideal phase

determination. Different PSSs may have conflict influence on some modes. Further tuning is needed to coordinate them to reach a compromise (54; 17). In summary, the conventional PSS design for large power systems is very complicated and time consuming. Manual tuning is a necessary step to guarantee the coordination among PSSs. The ideal phase curve considering the dynamics of other generators instead of assuming them as constants is shown in Fig. 5.11. It is obvious that a low order lead/lag block can't match the curve anymore. For example, at the system critical frequencies, $0.27Hz$ and $1Hz$ which can be observed in the simulation results, see Fig. 5.14- 5.19, conventional PSS can not give good compensation any more since in the simplified model, these important phase changes are ignored.

The LPV PSS takes care of the dynamics of the other generators through the scheduling variables, which interface with the rest of the system, so the decentralized LPV PSSs coordinate with each other automatically through their adaptive parameters, which are dependent on the scheduling variables. Similarly, the LPV PSSs give uniform performance during the whole operating range by changing parameters according to the operating conditions. The design is relatively straightforward. It does not need the complicated tuning process. Designers can define closed-loop performance by adjusting the system setup and weighting functions.

The LPV PSS phase lead at the operating point characterized by generation at Bus 93&110 at $2 \times 1350MW$ is compared with the ideal phase lead without ignoring any dynamics in Fig. 5.12 and the conventionally PSS phase lead. The LPV PSS gives much better compensation than conventional PSS at the system critical frequencies while relaxes the compensation at uncritical frequencies. Moreover, the LPV design is more straightforward. It does not need to the complicated tuning process. Designers can define closed-loop performance by adjusting the system setup and weighting functions.

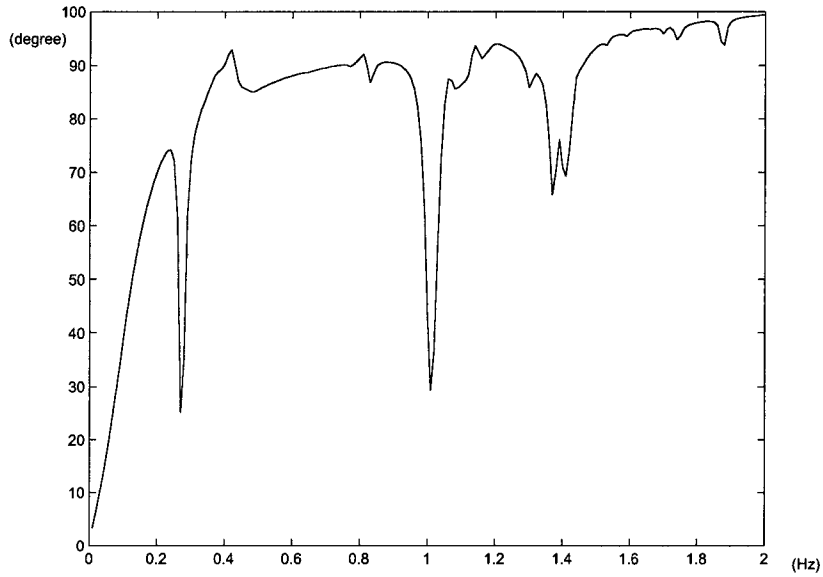

Figure 5.11 Ideal phase compensation for generator 111 without ignoring the dynamics of other generators (at $1350MW$).

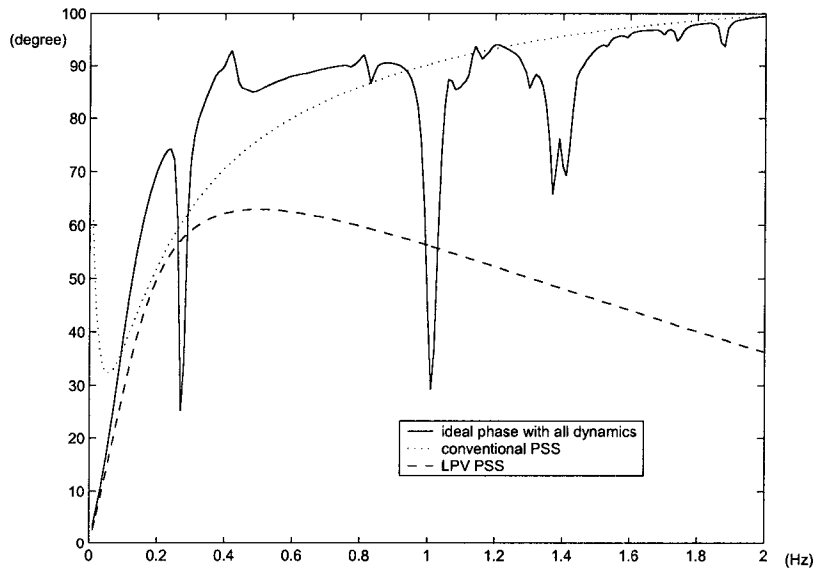

Figure 5.12 Comparison between LPV PSS phase lead and ideal phase lead for generator 111 without ignoring the dynamics of other generators (at $1350MW$).

5.4.3 Small Signal Analysis

At different operating conditions within the whole operating range, the eigenvalues of the linearized system are computed. The critical modes and their damping ratios are given in Table 5.3. It can be seen from the table that both conventional PSSs and LPV PSSs can improve system damping while the LPV PSSs can provide a higher damping ratio than the conventional PSSs.

Table 5.3 Comparison of damping ratio

P(MW) at	w/o PSS		with Conv. PSS		with LPV PSS	
Bus 93&110	f(Hz)	DR	f(Hz)	DR	f(Hz)	DR
2×1150	1.6454	0.0266	1.4843	0.3754	1.1272	0.9975
	1.0556	0.0370	0.9950	0.0593	1.5385	0.2597
	0.3021	0.0268	0.3075	0.1347	0.1252	0.3848
2×1350	1.6420	0.0269	1.4839	0.3729	1.8597	0.9752
	1.0006	0.0314	0.9923	0.0584	1.5835	0.2877
	0.2919	0.0060	0.2939	0.1532	0.1289	0.3590
2×1750	1.6283	0.0278	1.4814	0.3631	1.7695	0.9773
	1.0690	0.0224	0.9549	0.0646	1.6444	0.3141
	0.2533	-0.1083	0.2346	0.0882	0.1397	0.2714

5.4.4 Transient Stability

The effect of LPV PSSs in enhancing transient stability performance is verified by evaluating the critical clearing time (CCT) at three different operating points for a three-phase fault at Bus ♯1, Bus ♯7 and Bus ♯33 respectively. The results given in Table 5.4 further illustrate the advantages of LPV PSSs in comparison with the conventional PSSs. With the power production of $2 \times 1750MW$ at Buses ♯93 and ♯110, a 3-phase fault is applied at Bus ♯7 for $100ms$. The relative rotor angles of the generator at Bus ♯95 are given for the cases when generators are equipped with conventional PSSs and LPV PSSs. Results are given in Fig. 5.13. Apparently, for this fault LPV PSSs provide stability for the system while conventional PSSs can not.

Table 5.4 Comparison of critical clearing time

Power Generation at Generators 93 & 110	Fault Location	CCT(ms) with Conv. PSS	CCT(ms) with LPV PSS
$2 \times 1750MW$	Bus 1	119	130
	Bus 7	94	113
	Bus 33	134	148
	Bus 7 trip line 6-7	63	88
$2 \times 1350MW$	Bus 1	213	218
	Bus 7	137	151
	Bus 33	245	251
	Bus 7 trip line 6-7	97	116
$2 \times 1150MW$	Bus 1	265	269
	Bus 7	150	162
	Bus 33	309	314
	Bus 7 trip line 6-7	105	121

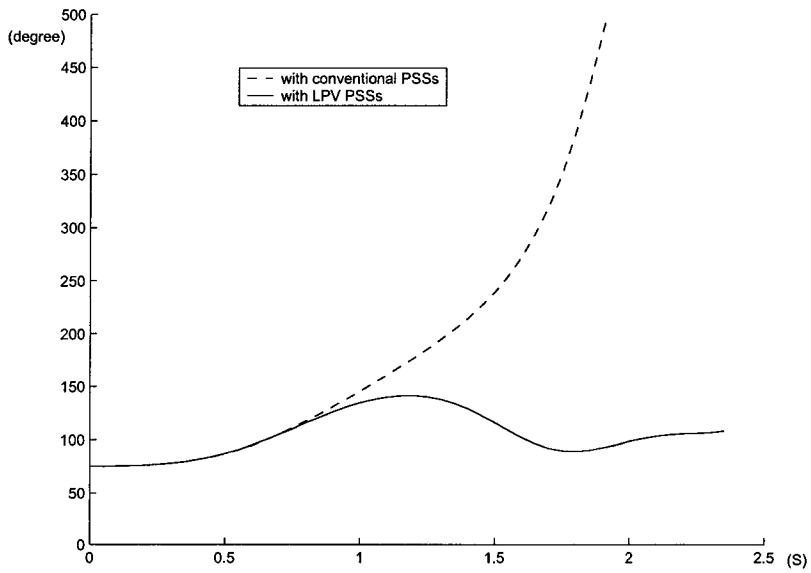

Figure 5.13 Relative rotor angles of the generator at Bus ♯95.

A three-phase fault with fixed clearing time of $0.15s$ is applied to verify the performance of the LPV PSSs under transient conditions. The results are shown in Table 5.5 . With LPV PSSs, the system transient stability is enhanced in terms of the maximal power generation at both both Bus ♯93 and Bus ♯110 to keep the system stable after the fault.

Table 5.5 Comparison of critical power generation

Fault Location	Maximal Transfer P(MW) with Conv. PSS	Maximal Transfer P(MW) with LPV PSS
Bus 1	2×1620	2×1661
Bus 7	2×1150	2×1366
Bus 33	2×1696	2×1742

5.4.5 Time Domain Simulation

Nonlinear simulation studies are performed using ETMSP (42). A three-phase short circuit is applied at Bus ♯33 and cleared after $100ms$. The real and reactive power of generators at Bus ♯104 are monitored. First, the generation at Bus ♯93 and Bus ♯110 is set at $1150MW$ each. At this operating point, the system is dominated by the plant modes (50). Comparisons are made between the conventionally designed PSSs and the LPV PSSs in Fig. 5.14-5.15. LPV PSSs and conventionally designed PSSs demonstrate similar performance in this case. In Fig. 5.17-5.16, the performance of the designed controllers is also compared with that of the conventional controllers when the generation at Bus ♯93 and Bus ♯110 is set at $1750MW$ each, where the inter-area modes dominate the system (50). LPV PSSs show better damping than conventionally designed PSSs.

Fig. 5.18 and 5.19 show results of comparison between LPV PSSs and conventional PSSs for a more severe fault, which leads to inter-area oscillations. The real power output of both generator ♯93 and generator ♯110 are set at $1750MW$ and a three phase fault

applied to Bus ♯7 for $60ms$, then the fault is cleared by opening the line between Bus ♯6 and Bus ♯7. It can be seen from the figures that the LPV PSSs demonstrates much better robustness and performance than the conventional PSSs. Comparison between outputs of LPV PSS and conventionally designed PSS at different locations are given in Fig 5.22- 5.25. It can be observed that LPV PSSs exert more control effort than conventionally designed PSSs for the first few seconds after the disturbance.

Four optimal H_∞ PSSs are also synthesized with the same setup as LPV PSSs at the same locations. Even for each single machine system, the stability is guaranteed. The closed-loop system is not even stable at the designed point. This also demonstrates in another way that LPV methods take care of the coordination automatically among different decoupled sub-systems by considering interface variables as scheduling variable.

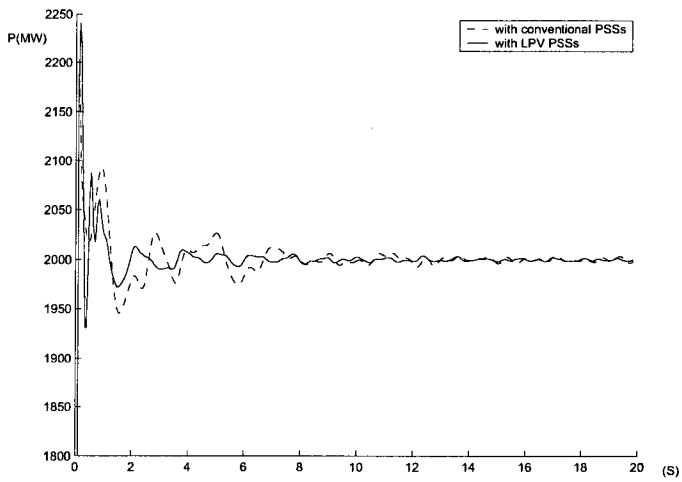

Figure 5.14 Real power output of generator at Bus ♯104 with 0.1s fault at Bus ♯33(at $1150MW$).

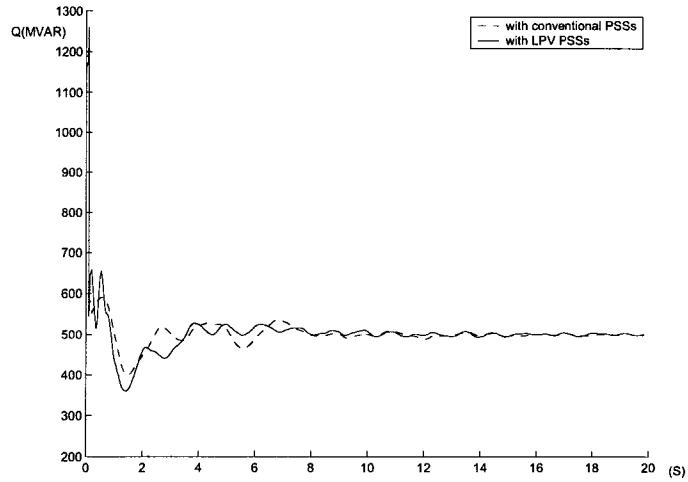

Figure 5.15 Reactive power output of generator at Bus ♯104 with 0.1s fault at Bus ♯33(at $1150MW$).

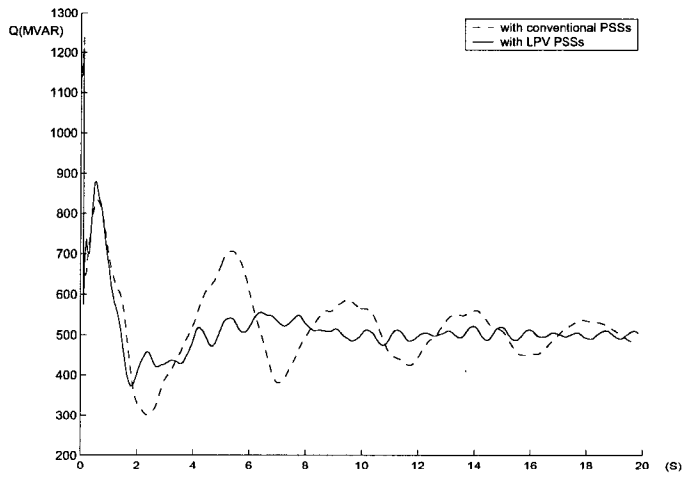

Figure 5.16 Reactive power output of generator at Bus ♯104 with 0.1s fault at Bus ♯33 (at $1750MW$).

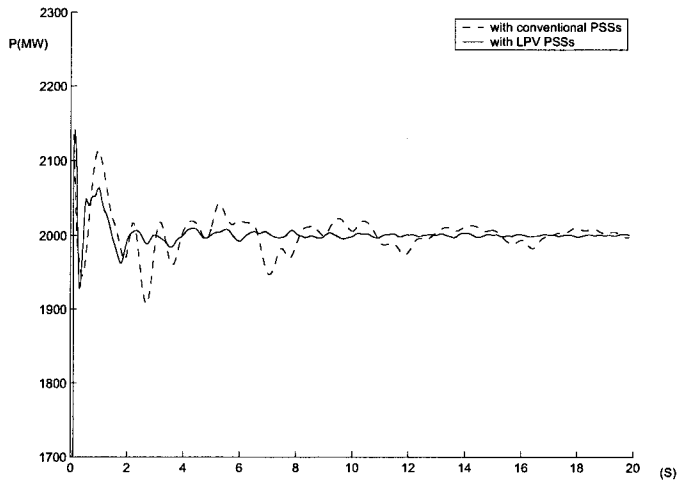

Figure 5.17 Real power output of generator at Bus ♯104 with 0.1s fault at Bus ♯33 (at $1750MW$).

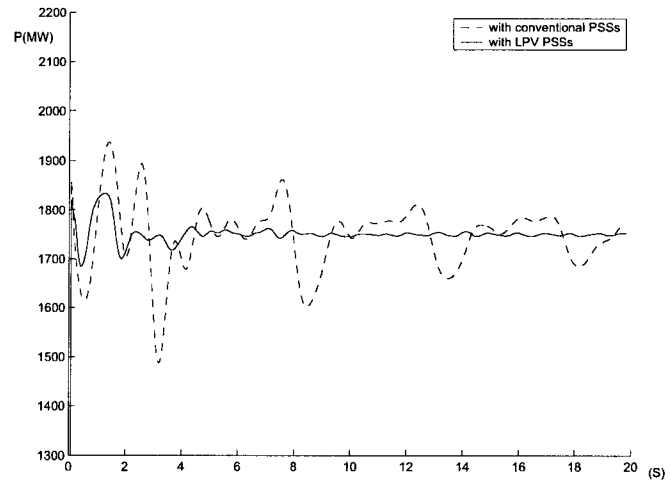

Figure 5.18 Real power of the generator at Bus ♯110: 3-phase fault at Bus ♯7 and clear the fault by opening the line between Bus ♯6 and Bus ♯7 (at $1750MW$).

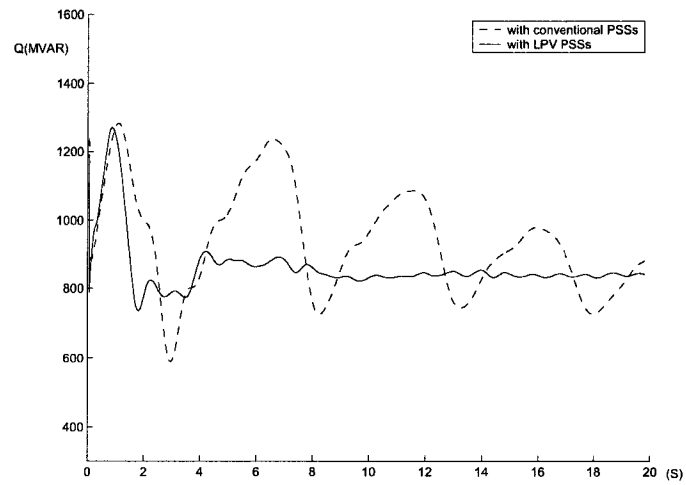

Figure 5.19 Reactive power of the generator at Bus ♯110: 3-phase fault at Bus ♯7 and clear the fault by opening the line between Bus ♯6 and Bus ♯7 (at $1750MW$).

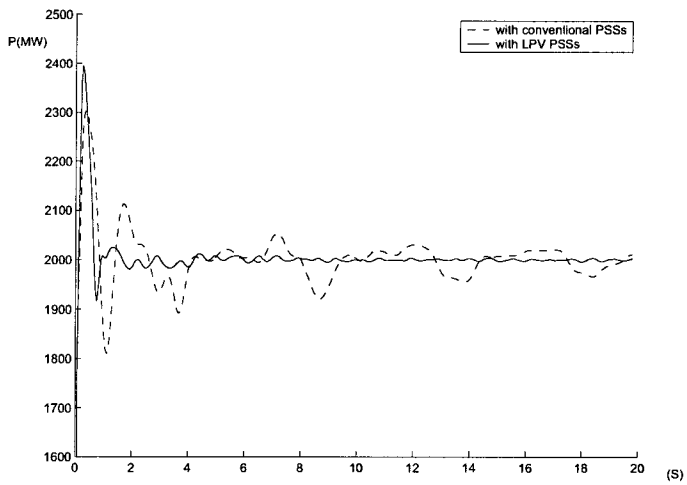

Figure 5.20 Real power of the generator at Bus ♯104: 3-phase fault at Bus ♯7 and clear the fault by opening the line between Bus ♯6 and Bus ♯7 (at $1750MW$).

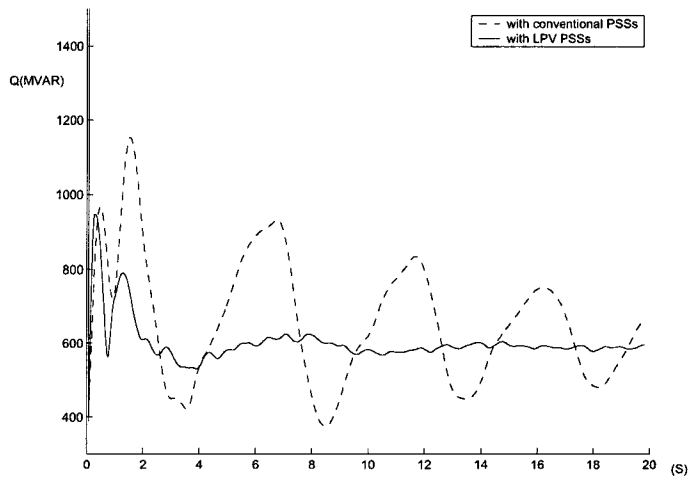

Figure 5.21 Reactive power of the generator at Bus ♯104: 3-phase fault at Bus ♯7 and clear the fault by opening the line between Bus ♯6 and Bus ♯7 (at $1750MW$).

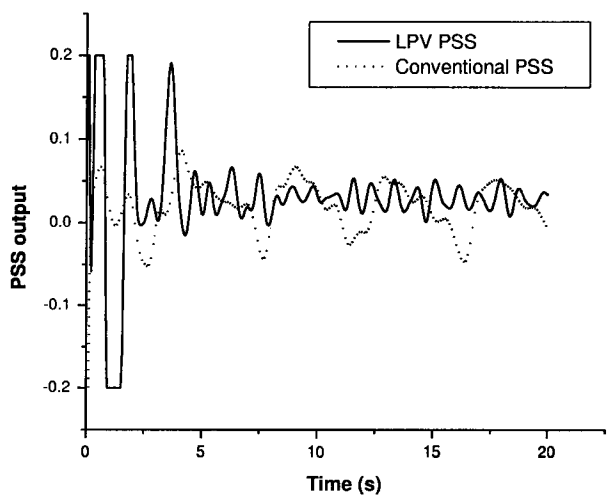

Figure 5.22 Comparison of the PSS output at generator ♯93: 3-phase fault at Bus ♯7 and clear the fault by opening the line between Bus ♯6 and Bus ♯7 (at $1750MW$).

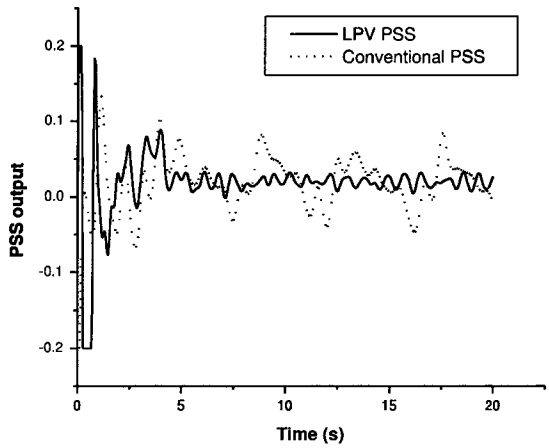

Figure 5.23 Comparison of the PSS output at generator ♯104: 3-phase fault at Bus ♯7 and clear the fault by opening the line between Bus ♯6 and Bus ♯7 (at $1750MW$).

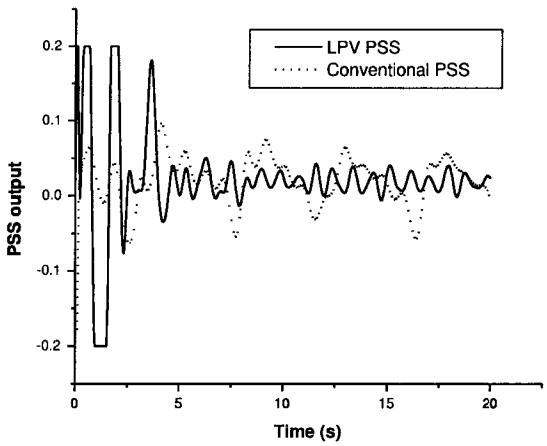

Figure 5.24 Comparison of the PSS output at generator ♯110: 3-phase fault at Bus ♯7 and clear the fault by opening the line between Bus ♯6 and Bus ♯7 (at $1750MW$).

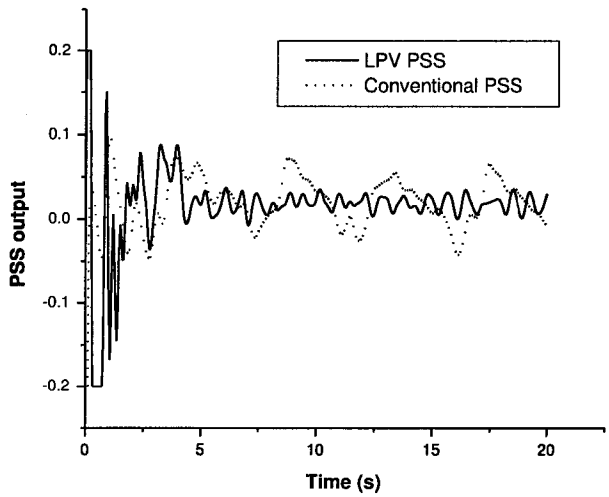

Figure 5.25 Comparison of the PSS output at generator ♯111: 3-phase fault at Bus ♯7 and clear the fault by opening the line between Bus ♯6 and Bus ♯7 (at $1750MW$).

5.5 Theoretical Proof for Stability

The heuristic method works well in both 4-machine and 50-machine systems and the results are very promising. In the following a theoretical proof is developed to show that the decentralized LPV design guarantees the stability of the interconnected system.

Without losing generality, assume the system operating condition is characterized by setting the real power of some tie line (P_{tie}) and P_{tie} varies in the range $[\underline{P_{tie}}, \overline{P_{tie}}]$. For the ith generator in the system, the state space description is as the following:

$$\tau'_{d0i}\dot{E}'_{qi} = E_{FDi} - E'_{qi} + (x_{di} - x'_{di})I_{di} \tag{5.1}$$

$$\tau'_{q0i}\dot{E}'_{di} = -E'_{di} - (x_{qi} - x'_{qi})I_{qi} \tag{5.2}$$

$$M_i\dot{\omega}_i = P_{mi} - (I_{di}E'_{di} + I_{qi}E'_{qi}) + (x'_{qi} - x'_{di})I_{qi}I_{di} - D_i(\omega_i - \omega_S) \tag{5.3}$$

$$\dot{\delta}_i = \omega_i - \omega_S \tag{5.4}$$

where

$$I_{qi} = \sum_{j=1}^{m}[F_{G+B}(\delta_{ij})E'_{qj} - F_{B-G}(\delta_{ij})E'_{dj}] + \sum_{k=m+1}^{n} F_{G+B}(\delta_{ik})E_k \tag{5.5}$$

$$I_{di} = \sum_{j=1}^{m}[F_{B-G}(\delta_{ij})E'_{qj} + F_{G+B}(\delta_{ij})E'_{dj}] + \sum_{k=m+1}^{n} F_{B-G}(\delta_{ik})E_k \tag{5.6}$$

where

$$\delta_{ij} = \delta_i - \delta_j \tag{5.7}$$

The power flow solution is determined by P_{tie}. So

$$\delta_j = \delta_j(P_{tie}) \tag{5.8}$$

$$E'_{qj} = E'_{qj}(P_{tie}) \tag{5.9}$$

$$E'_{dj} = E'_{dj}(P_{tie}) \tag{5.10}$$

for $j \neq i$ and $j = 1, ..., n$.

Then 5.5 and 5.6 can be written as:

$$I_{qi} = I_{qi}(\delta_i, E'_{qi}, E'_{di}, P_{tie}) \tag{5.11}$$

$$I_{di} = I_{di}(\delta_i, E'_{qi}, E'_{di}, P_{tie}) \tag{5.12}$$

Substitute 5.11 and 5.12 into 5.1-5.3, we have:

$$\tau'_{d0i}\dot{E}'_{qi} = E_{FDi} - E'_{qi} + (x_{di} - x'_{di})I_{di}(\delta_i, P_{tie}) \tag{5.13}$$

$$\tau'_{q0i}\dot{E}'_{di} = -E'_{di} - (x_{qi} - x'_{qi})I_{qi}(\delta_i, P_{tie}) \tag{5.14}$$

$$M_i\dot{\omega}_i = P_{mi} - (I_{di}(\delta_i, P_{tie})E'_{di} + I_{qi}(\delta_i, P_{tie})E'_{qi}) + (x'_{qi} - x'_{di})I_{qi}(\delta_i, P_{tie})I_{di}(\delta_i, P_{tie}) - D_i(\omega_i - \omega_S) \tag{5.15}$$

$$\dot{\delta}_i = \omega_i - \omega_S \tag{5.16}$$

It can be seem from 5.13-5.16 that the generator is decoupled from the other generators in the system as shown in Fig. 5.26.

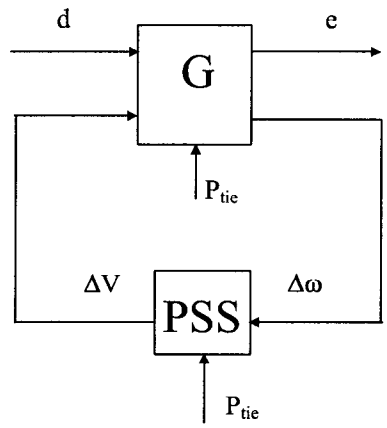

Figure 5.26 Decoupled single machine frame.

The system is linearized to form the LPV model as follows:

$$\begin{aligned} \dot{X} &= A(P_{tie})X + B(P_{tie})u \\ y &= C(P_{tie})X + D(P_{tie})u \end{aligned} \tag{5.17}$$

where

$$\begin{aligned} X^T &= [\Delta E'_{qi}, \Delta E'_{di}, \Delta\omega_i, \Delta\delta i] \\ u &= [controller\ output] \\ y &= [controller\ input] \end{aligned}$$

Then apply the SQLF based LPV synthesis to this single machine system. The resulting closed-loop system can be written as

$$\dot{X} = A_{cls}(P_{tie})X \tag{5.18}$$

where

$$X^T = [\Delta E'_{qi}, \Delta E'_{di}, \Delta\omega_i, \Delta\delta i, X_{Ki}]$$

where X_{Ki} represents the states of the controller installed at *ith* generator.

It is quadratically stable over $[\underline{P_{tie}}, \overline{P_{tie}}]$ (by Theorem 2.2.1).

Lemma 5.5.1 *Given a compact set P, and a quadratically stable LPV system*

$$\dot{x}(t) = A(\rho(t))x(t) \tag{5.19}$$

where $\rho \in F_P$. *There exist constant scalar* $\gamma_1, \gamma_2 > 0$ *such that the state transition matrix* $\Phi_\rho(t, t_0)$, *which characterizes all solutions to equation 5.19, satisfies*

$$\|\Phi_\rho(t, t_0)\| \leq \gamma_1 e^{[-\gamma_2(t-t_0)]} \tag{5.20}$$

for all $\rho \in F_P$

The proof of Lemma 5.5.1 is shown in (55).

By lemma 5.5.1, the closed-loop system 5.18 is asymptotically stable in the range $[\underline{P_{tie}}, \overline{P_{tie}}]$.

As a state of the closed-loop system 5.18, $\Delta\delta i \to 0$, as $t \to \infty$.

This applies for $i = 1, ..., n$.

Then, $\Delta\delta ij \to 0$, as $t \to \infty$ for $i, j = 1, ..., n$.

So the whole system is stable.

CHAPTER 6. CONCLUSIONS AND FUTURE WORK

6.1 Conclusions

In this dissertation, the application of linear parameter varying synthesis to power system controller design is investigated. The study is motivated by the inevitable limitation of a LTI controller on the nonlinear power systems in a large operating range and successful implementation of this approach in safety critical systems like aircrafts and process control. The main goal is to apply the LPV techniques to the Power System Stabilizer synthesis. A summary of some significant contribution is as follows:

1. Development of the LPV model of power systems. The LPV model is the basis for the LPV controller synthesis process. The model uses real time information of measurable varying parameters in power systems to improve system robustness and performance.

2. A systematic procedure to design PSS using LPV synthesis is presented. The feedback setup is constructed and a general guidelines for proper weighting function selecting is given. The LPV design technique also allows us to design a gain-scheduled controller in one step. That includes the design of the local LTI controllers and the design of the scheduling scheme simultaneously.

3. Apply Single Quadratic Lyapunov Function based LPV synthesis. The resulting PSS can guarantee the stability and performance over a large range of plants with arbitrarily fast changing parameters. The performance of the PSS is tested in

both the frequency domain and the time domain. Comparisons are made to the conventionally designed PSS and the H_∞ optimal PSS. LPV PSS is more effective.

4. Applying the Parameter Dependant Lyapunov Function based LPV synthesis. The bounds on the rate of variation of the parameters are used in LPV controller design to reduce the conservativeness and expand the operating range of the system further. Simulation is done to check the performance of the implemented closed-loop system. The resulting LPV PSS damps the inter-area oscillations for a wide range of operating conditions and is superior to the conventional PSS.

5. Solving infinite dimension LMI through a gridding process. Theoretically, infinite grid points are needed to capture the entire dynamics following any type of disturbance. But this is intractable in practice. An approximate problem is set up by gridding the parameter space and solving the set of LMIs that hold on the subset of P formed by gridding points. A rule for gridding is proposed.

6. Realization of LPV controllers. The gridding process leads to a discrete controller. The controller state matrices are only known at a discrete set of ρ values. During closed-loop operation, the continuous controller is approximated by polynomial or rational functions through curve fitting.

7. Casting the LPV control theories into a framework applicable to large power systems in a decentralized controller frame. The design framework and procedure are given. By taking generator real and reactive power as scheduling variables, the generator is decoupled from the rest of the system. The design for a given PSS is independent of the design of the others and all the PSSs cooperate with each other automatically. The decoupling also leads to a relatively low order PSS design. The numerical examples further illustrate that LPV approach is useful for designing decentralized controllers in power systems. The nonlinear simulations show that

these independently designed decentralized PSSs cooperate well in a wide operating range and have better damping characteristics than conventionally designed PSSs. The disturbances tested have been selected to be different in nature and are at different locations. The performance of the LPV PSSs is superior to the conventionally designed PSSs.

8. A theoretical proof for stability is given for the decentralized controller design.

The adaptive nature of LPV controllers overcomes the limitation on LTI controllers and it guarantees robust performance for a wide operating range. The primary results from this research clearly demonstrate the great potential of LPV synthesis application in power systems.

6.2 Future Work

In the future work, the following issues should be addressed:

1. Investigate the design of a robust LPV controller, which would consider not only the changing parameters that can be measured on line, but also the varying parameters that can't be measured in real time. Instead of setting them to the nominal values, they can be represented as uncertainties. So the LPV synthesis problem can be converted into H_∞ problem with more inputs and outputs. The process could be shown as the Fig.6.1. Then the same LPV synthesis procedure can be applied to design the robust LPV controller, which not only can deal with measurable changing parameters, but also achieve robust stability and robust performance for uncertainties.

2. In this dissertation, all the discussed LPV controllers have the same performance requirement for all operating points. This is not necessary for all the cases. LPV

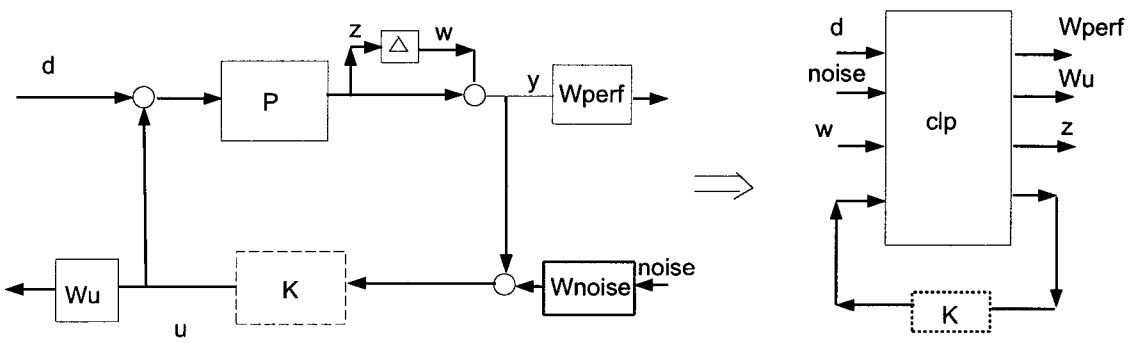

Figure 6.1 Robust LPV PSS setup.

synthesis offers an ability to emphasize different performance objectives depending on different operating conditions. By adjusting weighting functions according to different operating conditions, more flexibility can be achieved. This could be used to further reduce conservatism.

3. For large power systems, the special characteristic of sparsity can be used to reduce the computation burden in solving LMIs involved in LPV synthesis. Also mature model reduction techniques of large systems can be applied to power system. Further efforts can be made to make the LPV synthesis more applicable to large power systems.

4. Control design for other devices (i.e. FACTS devices such as SVC, TCSC, UPFC etc.) in power systems to damp the inter-area oscillations and improve system stability.

APPENDIX A. DETAILS OF SYSTEM LINEARIZATION

The details of 3.39-3.43 are given here.

In 3.39

for function f_{1_i} :

$$\frac{\partial f_{1i}}{\partial E'_{qj}} = \begin{cases} 0 & \text{for j} \neq i \\ -\dfrac{1}{\tau'_{d0i}} & \text{for j=i} \quad j = 1, \cdots, m \end{cases} \tag{A.1}$$

$$\frac{\partial f_{1i}}{\partial E_{FDj}} = \begin{cases} 0 & \text{for j} \neq i \\ \dfrac{1}{\tau'_{d0i}} & \text{for j=i} \quad j = 1, \cdots, m \end{cases} \tag{A.2}$$

for function f_{2_i} :

$$\frac{\partial f_{2i}}{\partial E'_{dj}} = \begin{cases} 0 & \text{for j} \neq i \\ -\dfrac{1}{\tau'_{q0i}} & \text{for j=i} \quad j = 1, \cdots, m \end{cases} \tag{A.3}$$

for function f_{3_i} :

$$\frac{\partial f_{3i}}{\partial E'_{qj}} = \begin{cases} 0 & \text{for j} \neq i \\ -\dfrac{I_{qi0}}{M_i} & \text{for j=i} \quad j = 1, \cdots, m \end{cases} \tag{A.4}$$

$$\frac{\partial f_{3i}}{\partial E'_{dj}} = \begin{cases} 0 & \text{j} \neq i \\ -\dfrac{I_{di0}}{M_i} & \text{for j=i and} \quad j = 1, \cdots, m \end{cases} \tag{A.5}$$

$$\frac{\partial f_{3i}}{\partial \omega_j} = \begin{cases} 0 & \text{for j} \neq i \\ -\dfrac{D_i}{M_i \omega_S} & \text{for j=i} \quad j = 1, \cdots, n \end{cases} \tag{A.6}$$

for function f_{4_i} :

$$\frac{\partial f_{4i}}{\partial \omega_j} = \begin{cases} -1 & \text{for j=1} \\ 1 & \text{for j=i, j} \neq 1 \quad j = 1, \cdots, n \\ 0 & \text{otherwise} \end{cases} \tag{A.7}$$

for function f_{5_i} :

$$\frac{\partial f_{5i}}{\partial \omega_j} = \begin{cases} 0 & \text{otherwise} \\ a_i a_{2i} a_{3i} \dfrac{K_{Ai}}{T_{Ai}} \dfrac{K_{Si}}{\omega_S} & \text{for j=i and} \quad j = 1, \cdots, m \end{cases} \tag{A.8}$$

$$where \;\; a_i = T_{Ci}/T_{Bi} \;\; a_{2i} = T_{1i}/T_{2i} \;\; a_{3i} = T_{3i}/T_{4i}$$

$$\frac{\partial f_{5i}}{\partial E_{FDj}} = \begin{cases} 0 & \text{for j} \neq i \\ -\dfrac{1}{T_{Ai}} & \text{for j=i} \quad j = 1, \cdots, m \end{cases} \tag{A.9}$$

$$\frac{\partial f_{5i}}{\partial X_{E1j}} = \begin{cases} 0 & \text{for j} \neq i \\ -a_i \dfrac{K_{Ai}}{T_{Ai}} & \text{for j=i} \quad j = 1, \cdots, m \end{cases} \tag{A.10}$$

$$\frac{\partial f_{5i}}{\partial X_{E2j}} = \begin{cases} 0 & \text{for j} \neq i \\ \dfrac{K_{Ai}}{T_{Ai}} & \text{for j=i} \quad j = 1, \cdots, m \end{cases} \tag{A.11}$$

for function f_{6_i} :

$$\frac{\partial f_{6i}}{\partial X_{E1j}} = \begin{cases} 0 & \text{for j} \neq i \\ -\dfrac{1}{T_{Ri}} & \text{for j=i} \quad j = 1, \cdots, m \end{cases} \tag{A.12}$$

for function f_{7_i} :

$$\frac{\partial f_{7i}}{\partial \omega_j} = \begin{cases} 0 & \text{otherwise} \\ a_{2i}a_{3i}\dfrac{1-a_i}{T_{Bi}}\dfrac{K_{Si}}{\omega_S} & \text{for i=j} \quad j=1,\cdots,m \end{cases} \tag{A.13}$$

$$\frac{\partial f_{7i}}{\partial X_{E1j}} = \begin{cases} 0 & \text{for j} \neq i \\ -\dfrac{1-a_i}{T_{Bi}} & \text{for j=i} \quad j=1,\cdots,m \end{cases} \tag{A.14}$$

$$\frac{\partial f_{7i}}{\partial X_{E2j}} = \begin{cases} 0 & \text{for j} \neq i \\ -\dfrac{1}{T_{Bi}} & \text{for j=i} \quad j=1,\cdots,m \end{cases} \tag{A.15}$$

In 3.40,

$$\text{where } \frac{\partial f_{5i}}{\partial V_{REFj}} = \begin{cases} 0 & \text{for j} \neq i \quad j=1,\cdots,m \\ a_i\dfrac{K_{Ai}}{T_{Aj}} & \text{for j=i} \end{cases} \tag{A.16}$$

$$\frac{\partial f_{7i}}{\partial V_{REFj}} = \begin{cases} 0 & \text{for j} \neq i \quad j=1,\cdots,m \\ (1-a_i)\dfrac{1}{T_{Bj}} & \text{for j=i} \end{cases} \tag{A.17}$$

In 3.41,

for function f_{1_i} :

$$\frac{\partial f_{1_i}}{\partial I_{dj}} = \begin{cases} 0 & \text{for j} \neq i \quad j = 1, \cdots, m \\ \frac{1}{\tau'_{d0i}}(x_{di} - x'_{di}) & \text{for j=i} \end{cases} \tag{A.18}$$

for function f_{2_i} :

$$\frac{\partial f_{2_i}}{\partial I_{qj}} = \begin{cases} 0 & \text{for j} \neq i \quad j = 1, \cdots, m \\ -\frac{1}{\tau'_{q0i}}(x_{qi} - x'_{qi}) & \text{for j=i} \end{cases} \tag{A.19}$$

for function f_{3_i} :

$$\frac{\partial f_{3_i}}{\partial I_{qj}} = \begin{cases} \frac{1}{M_i}[-E'_{qi0} + (x'_{qi} - x'_{di})I_{di0}] & \text{for j=i and} j = m+1, \cdots, n \\ 0 & \text{otherwise} \\ \frac{1}{-M_i}E'_i & \text{for j=i and} j = 1, \cdots, m \end{cases} \tag{A.20}$$

$$\frac{\partial f_{3_i}}{\partial I_{di}} = \begin{cases} 0 & \text{otherwise} \\ \frac{1}{M_i}[-E'_{di0} + (x'_{qi} - x'_{di})I_{qi0}] & \text{for j=i and} j = 1, \cdots, m \end{cases} \tag{A.21}$$

for function f_{6_i} :

$$\frac{\partial f_{6_i}}{\partial V_{Tj}} = \begin{cases} 0 & \text{for j} \neq i \quad j = 1, \cdots, m \\ \frac{1}{T_{Ri}} & \text{for j=i} \end{cases} \tag{A.22}$$

In 3.42

$$\frac{\partial I_{qi}}{\partial I_{qj}} = \begin{cases} 0 & \text{for j} \neq i \quad j = 1, \cdots, n \\ 1 & \text{for j=i} \end{cases} \tag{A.23}$$

$$\frac{\partial I_{di}}{\partial I_{dj}} = \begin{cases} 0 & \text{for j} \neq i \quad j = 1, \cdots, n \\ 1 & \text{for j=i} \end{cases} \tag{A.24}$$

$$\frac{\partial V_{Ti}}{\partial I_{qj}} = \begin{cases} 0 & \text{for j} \neq i \quad j = 1, \cdots, m \\ -\dfrac{1}{V_{Ti0}}(-V_{di0}x'_{qi} - rV_{qi0}) & \text{for j=i} \end{cases} \tag{A.25}$$

$$\frac{\partial V_{Ti}}{\partial I_{dj}} = \begin{cases} 0 & \text{for j} \neq i \quad j = 1, \cdots, m \\ -\dfrac{1}{V_{Ti0}}(V_{qi0}x'_{di} - rV_{di0}) & \text{for j=i} \end{cases} \tag{A.26}$$

$$\frac{\partial V_{Ti}}{\partial V_{Tj}} = \begin{cases} 0 & \text{for j} \neq i \quad j = 1, \cdots, m \\ 1 & \text{for j=i} \end{cases} \tag{A.27}$$

In 3.43

$$\frac{\partial I_{qi}}{\partial E_{qj}'} = F_{G+B}(\delta_{ij0}) \tag{A.28}$$

$$\frac{\partial I_{qi}}{\partial E_{dj}'} = -F_{B-G}(\delta_{ij0}) \tag{A.29}$$

$$\frac{\partial I_{qi}}{\partial \delta_{r1}} = \sum_{j=1}^{m} \frac{\partial \delta_{ij}}{\partial \delta_{r1}} [F_{G+B}(\delta_{ij0}) E_{dj0}' + F_{B-G}(\delta_{ij0}) E_{qj0}'] \tag{A.30}$$

$$+ \sum_{k=m+1}^{n} \frac{\partial \delta_{ik}}{\partial \delta_{r1}} [F_{G+B}(\delta_{ij0}) E_{k0}'] \tag{A.31}$$

$$j = 1, \cdots, m \qquad k = m+1, \cdots, n \qquad r = 2, \cdots, n$$

$$\frac{\partial I_{di}}{\partial E_{qj}'} = F_{B-G}(\delta_{ij0}) \tag{A.32}$$

$$\frac{\partial I_{di}}{\partial E_{dj}'} = F_{G+B}'(\delta_{ij0}) \tag{A.33}$$

$$\frac{\partial I_{di}}{\partial \delta_{r1}} = \sum_{j=1}^{n} \frac{\partial \delta_{ij}}{\partial \delta_{r1}} [F_{B-G}(\delta_{ij0}) E_{dj0}' - F_{G+B}(\delta_{ij0}) E_{qj0}'] \tag{A.34}$$

$$+ \sum_{k=m+1}^{n} \frac{\partial \delta_{ik}}{\partial \delta_{r1}} [F_{B-G}(\delta_{ij0}) E_{k0}'] \tag{A.35}$$

$$j = 1, \cdots, m \qquad k = m+1, \cdots, n \qquad r = 2, \cdots, n$$

$$\frac{\partial V_{Ti}}{\partial E_{qj}'} = \begin{cases} 0 & \text{for j} \neq i \quad j = 1, \cdots, n \\ \dfrac{V_{qi0}}{V_{Ti0}} & \text{for j=i} \end{cases} \tag{A.36}$$

$$\frac{\partial V_{Ti}}{\partial E_{dj}'} = \begin{cases} 0 & \text{for j} \neq i \quad j = 1, \cdots, n \\ \dfrac{V_{di0}}{V_{Ti0}} & \text{for j=i} \end{cases} \tag{A.37}$$

APPENDIX B. LPV CONTROLLER REPRESENTATION IN TSAT

There is no standard block in the TSAT (56) control block library which can represent a time variant controller. Neither does other power system simulation software such as ETMSP, EUROSTAG and PSS/E. Users have to define the model by themselves. In TSAT, dynamically linked controller blocks (DLB) provide a method of implementing control functions or control logic not available in the standard control block. A DLB is basically created by the user (by writing C code) and linked to TSAT at run-time by means of Dynamic-Link Library (DLL) with an Application Program Interface (API). In our research, DLB is employed to define LPV controllers in simulations.

In order to illustrate the use of DLB in TSAT, the LPV PSS installed at generator ♯93 is taken as an example. The state space matrices of the LPV controller could be well approximated by the first order polynomial in P_{93} at each of the gridding points through the least-squares estimation. The controller space matrices can be written as:

$$\begin{aligned} A_k(P_{93}) &= A_0 + P_{93}A_1 \\ B_k(P_{93}) &= B_0 + P_{93}B_1 \\ C_k(P_{93}) &= C_0 + P_{93}C_1 \\ D_k(P_{93}) &= D_0 + P_{93}D_1 \end{aligned} \tag{B.1}$$

The dynamics of the LPV controller can be expressed in the diagram as Fig. B.1. One thing needs to be clarified is that only P is used here as a scheduling variable instead both P and Q. It is because for the case we studied given a value for P, Q is determined

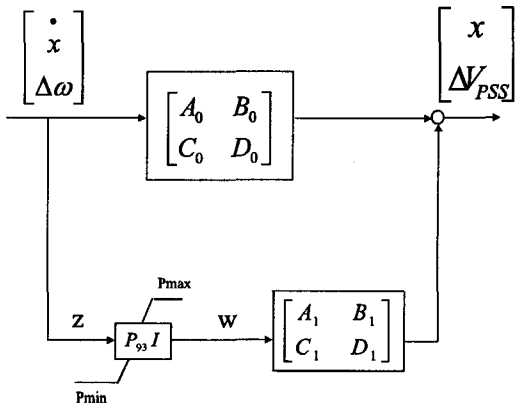

Figure B.1 Block diagram of the LPV PSS at generator 93.

since the system operating condition is characterized by setting the generation at Bus ♯93 and ♯110 to be some value. For a general case, both P and Q should be employed as scheduling variables.

The DLB code to implement this LPV PSS is shown below.

```
#include <windows.h>
#include <stdlib.h>
#include <stdio.h>
#include "udmface.h"
extern void __stdcall DLB_MSGSUB(char *msg,unsigned int lmsg);

const float a0[] =
   {-1.4406,-0.000, -0.3775,-72.6289,  -0.0000,-13.2213,  0.0000,
    0.0000,-0.8065,  0.0000,  0.0000,   0.0000,  0.0000, -0.0000,
   74.6533, 0.0000,-42.4269,302.6198,  -0.0000, 99.8703, -0.0002,
    8.1360,-0.0000,  0.0876,-61.0104,  -0.0000, -1.9761,  0.0000,
    0.0000, 0.0000, -0.0000, -0.0000,-100.0000, -0.0000, -0.0000,
```

```
   -0.0173,-0.0000,  0.0096, -0.0660,   0.0000, -1.0226,  0.0000,
   94.9946, 0.0000,-53.6934, 50.9139,  -0.0000, 70.3282, -40.0005};
const float a1[] =
   { 0.9151, 0.0000, -0.6032,  0.0901,  0.0000,   0.6137,  -0.0000,
   -0.0000,       0,  0.0000, -0.0000,  0.0000,  -0.0000,   0.0000,
   -1.2109,  0.0000,  0.6211, -0.1189, -0.0000,  -0.8274,   0.0000,
    0.0201, -0.0000, -0.0103,  0.0020,  0.0000,   0.0137,  -0.0000,
   -0.0000,  0.0000,  0.0000, -0.0000,       0,  -0.0000,   0.0000,
    0.0014, -0.0000, -0.0007,  0.0001,  0.0000,   0.0009,  -0.0000,
   -0.4033,  0.0000,  0.2069, -0.0396, -0.0000,  -0.2756,   0.0000};
const float b0[]=
   {207.0754, 0.0000, -117.6094, 19.8096,-0.0000,137.6040,  -21.263};
const float c0[]=
   {-86.9280, 0.0000, 354.2928, -13.1823, 0.0000,-6.4207 ,  50.0423};
const float d0[]={0,0,0};

const float Pmin=11.50,Pmax=17.50,Qmin=0,Qmax=10;

void __stdcall DLB_READ(struct udminfo *pinfo, char *buf,
   unsigned int lbuf, int *ninput, int *nstate, int *iret)
{
   *nstate=7;
   *ninput=3;
   *iret = 0;
}

void __stdcall DLB_INIT(struct udminfo *pinfo, struct udminputinfo
```

```
*pinput,   int *idir, float *valin, float *valout, float *x, int
*iret) {

    int i; x[0]=0; x[1]=0; x[2]=0; x[3]=0; x[4]=0; x[5]=0; x[6]=0;
    for(i=0;i<3;i++) {
        if (pinput[i].itype==3) {
            valin[i]=0.0f;
        }
    }
    if(strncmp(pinput[0].name,"PT",2)) {
        char* errorString = "***ERROR-IN READ PT";
        DLB_MSGSUB(errorString, strlen(errorString));
        *iret = 1;
        return;
    }
    if(strncmp(pinput[1].name,"QT",2)) {
        char* errorString = "***ERROR-IN READ QT";
        DLB_MSGSUB(errorString, strlen(errorString));
        *iret = 1;
        return;
    }
    if(strncmp(pinput[2].name,"DW",2)) {
        char* errorString = "***ERROR-IN READ DW";
        DLB_MSGSUB(errorString, strlen(errorString));
        *iret = 1;
        return;
    }
```

```
    *valout = 0;
    *iret = 0;
}

void __stdcall DLB_RESTART(struct udminfo *pinfo, int *iret) {
   *iret = 0;
}

void __stdcall DLB_DERIV(struct udminfo *pinfo, float *valin,
   float *valout, float *x, float *xdot, int *iret)
{
    float anew[49], bnew[21], cnew[7], dnew[3];
    float y=0;
    int i,j;
    if(valin[0]<Pmin)
    {
        int i;
        for ( i=0; i<49;i++)
            anew[i]=a0[i]-a1[i];
        for (i=0; i<7;i++)
        {bnew[i]=b0[i];
         bnew[i+7]=0;
         bnew[i+14]=0;
         cnew[i]=c0[i];
        }
        dnew[0]=dnew[1]=dnew[2]=0;
    }
```

```
else if (valin[0]>Pmax)
{
    int i;
    for (i=0; i<49;i++)
        anew[i]=a0[i]+a1[i];
    for (i=0; i<7;i++)
    {bnew[i]=b0[i];
     bnew[i+7]=0;
     bnew[i+14]=0;
     cnew[i]=c0[i];
    }
    dnew[0]=dnew[1]=dnew[2]=0;
}
else
{
    int i;
    for (i=0; i<49;i++)
        anew[i]=a0[i]+(valin[0]-14.5)/3*a1[i];
    for (i=0; i<7;i++)
    {bnew[i]=b0[i];
     bnew[i+7]=0;
     bnew[i+14]=0;
     cnew[i]=c0[i];
    }
    dnew[0]=dnew[1]=dnew[2]=0;
}
```

```
    for (i=0;i<7;i++) {
        xdot[i]=-b0[i]*valin[2];
        for (j=0;j<7;j++) {
            xdot[i]=xdot[i]+anew[i+j*7]*x[j];
        }
    }

    for( i=0;i<7;i++)
    {
        y=y+c0[i]*x[i];
    }
   *valout=y;
   *iret = 0;
}

void __stdcall DLB_NWLIMIT(struct udminfo *pinfo, float *x, int
*iret) {
   *iret = 0;
}

void __stdcall DLB_JACOB(struct udminfo *pinfo, float *valin,
float *x,
   float *a, float *b, float *c, float *d, int *iret)
{

    if(valin[0]<Pmin)
    {
```

```
    int i;
    for ( i=0; i<49;i++)
        a[i]=a0[i]-a1[i];
    for (i=0; i<7;i++)
        {b[i]=b0[i];
         b[i+7]=0;
         b[i+14]=0;
         c[i]=c0[i];
        }
    d[0]=d[1]=d[2]=0;
}
else if (valin[0]>Pmax)
{
    int i;
    for (i=0; i<49;i++)
        a[i]=a0[i]+a1[i];
    for (i=0; i<7;i++)
        {b[i]=b0[i];
         b[i+7]=0;
         b[i+14]=0;
         c[i]=c0[i];
        }
    d[0]=d[1]=d[2]=0;
}
else
{
    int i;
```

```
        for (i=0; i<49;i++)
            a[i]=a0[i]+(valin[0]-14.5)/3*a1[i];
        for (i=0; i<7;i++)
            {b[i]=b0[i];
             b[i+7]=0;
             b[i+14]=0;
             c[i]=c0[i];
            }
        d[0]=d[1]=d[2]=0;
    }

   *iret = 0;
}

void __stdcall DLB_CLOSE(struct udminfo *pinfo, int *iret) {
   *iret = 0;
}
```

The following is the sample data showing the use of this DLB. In this user-defined model, block ♯1is a DLB which requires a DLB DLL named $dlb_pss93.dll$, which is from the above code.

```
/ UD PSS START
       0.0       0.0    2
    0 / REMOTE BUS
    0 / REMOTE BRANCH
    1, 'STAB DLB', 'DLB', 'dlb_pss93' /CONTROL BLOCK 1
```

```
    2, 'STAB LIM', 'GN', 1.0, 0.2, -0.2 / CONTROL BLOCK 2
    1, 2 /BLOCK INTERCONNECTION
    1, 'PT', 1.0, 1 'QT', 1.0, 1, 'DW', 1.0 / BLOCK INPUT
    2 /BLOCK OUPUT
/ UD PSS ENDS
```

BIBLIOGRAPHY

[1] P. Kundur, "Power System Stability and Control" *New York: McGrawHill Inc.*, 1993.

[2] M. Klein, G. J. Rogers, and P.Kundur, "A fundermental study of inter-area oscillation in power systems," *IEEE Trans. Power Systems*, vol. 6, Aug. 1991, pp. 914-921.

[3] D. N. Koterev, C. W. Taylor, and W. A. Mittelstadt, "Model validation for the August 10, 1996 WSCC system outage," *IEEE Trans. Power Systems*, vol. 14, Aug. 1999, pp. 967-979.

[4] E. Khutoryansky and M. A. Pai, "Parametric Robust Stability of Power system Using Generalized Kharitonov's Theorem," *Proceedings of the 36th IEEE Conference on Decision and Control*, San Diego, California, 1997, pp. 3097-3099.

[5] S. Chen and O. P. Malik, "H_∞ Optimization Based Power System Stabilizer Design," *IEEE Proceedings*, Part C, vol.142, no.2, March 1995, pp.179-184.

[6] S. Chen and O. P. Malik, "Power System Stabilizer Design Uisng H_∞ Synthesis," *IEEE Trans. on Energy Conversion*, vol.10, no.1, March 1995, pp. 175-181.

[7] R. Asgharian, and S. A. Tavakoli, "Systematic Approach to Performance Weights Selection in Design of Robust H_∞ PSS Using Genetic Algorithms," *IEEE Trans. on Energy Conversion*, vol. 11, no. 1, March 1996, pp. 111-117.

[8] M. Klien, L. X. Le, G. J. Rogers, and S. Farrokhpay, "H_∞ Damping Controller Design in Large Power Systems," *IEEE Trans. on Power Systems*, vol. 10, no. 1, Feburary 1995, pp. 158-166.

[9] S. S. Ahmed, L. Chen, and A. Petroianu, "Design of Suboptimal H_∞ Excitation Controllers," *IEEE Trans. on Power Systems*, vol. 11, no. 1, February 1996, pp. 312-318.

[10] M. H. Khammash, V. Vittal, and C. D. Pawloski, "Analysis of Control Performance for Stability Robustness of Power Systems," *IEEE Trans. on Power Systems*, vol. 9, no. 4, November 1994, pp. 1861-1867.

[11] S. Venkataraman, M. H. Khammash, and V. Vittal, "Analysis and Synthesis of HVDC Controls for Stability of Power Systems," *IEEE Trans. on Power Systems*, vol. 10, no. 4, November 1995, pp. 1933-1939.

[44] V. Vittal, M. Khammash, and M. Djukanovic, " Robust Analysis and Design of Control in Power Systems," *ERPI TR-111922*, Dec. 1998.

[13] M. Djukanovic, M. Khammash, and V. Vittal, " Application of the Structured Singular Value Theory for Robust Stability and Control Analysis in Multimachine Power Systems, Part-I: Framework Development and Part II: Numerical Simulation and Results," *IEEE Transaction on Power systems*, vol. 13, Nov.1998, pp. 1311-1316.

[14] P. M. Anderson and A. A. Fouad, "Power System Control and Stability," *IEEE Press*, 1994.

[15] IEEE Commitee Report, "Excitation System Models for Power System Stability Studies," *IEEE Trans. on Power Apparatus and Systems*, vol. PAS-100, Feburary 1981, pp.494-509.

[16] G. E. Boukarim, S. Wang, J. H. Chow, G. N. Taranto, and N. Martins, "A Comparison of Classical, Robust, and Decentralized Control Designs for Multiple Power System Stabilizers," *IEEE Transactions on Power Systems*, Volume: 15, Issue: 4 , Nov. 2000, pp. 1287 -1292.

[17] M. J. Gibbard, N. Martins, J. J. Sanchez-Gasca, N. Uchida, V. Vittal, and L. Wang, "Recent applications of linear analysis techniques," *IEEE Transactions on Power Systems* , Vol. 16, Issue 1, Feb 2001, pp.154 -162.

[18] C. E. Grund, J. J. Paserba, J. F. Hauer, and S. L. Nilsson, "Comparison of Prony and Eigenanalysis for Power System Control design," *IEEE Transactions on Power Systems*, Volume: 8 Issue: 3, Aug. 1993 pp. 964 -971.

[19] J. S. Shamma and M. Athans, "Guaranteed Properties of Gain Scheduled Control for Linear Parameter Varying Plants," *Automatica*, vol. 27, 1991, pp.559-564.

[20] J. S. Shamma and M. Athans, "Gain Scheduling: Potential Hazards and Possible Remedies," *IEEE Contr. Sys. Mag.*, 12(3), 1992, pp.101-107.

[21] P. Gahinet, A. Nemivovskil, A. Laub, and M. Chilali, "LMI Control ToolBox," *Mathworks Inc*, Naha, MA 1995.

[22] G. Beck and A. K. Packard, "Robust Performance of Linear Parametriclaly Varying System Using Parameterially Dependent Linear Feed Back," *Syst. Contr. Lett.*, 23(3), 1994, pp. 205-215.

[23] G. Becker, "Additional Results on Parameter Dependent Controllers for LPV Systems," *Pro. 13th IFAC World Congress*, 1996, pp. 351-356.

[24] A.K. Packard, "Gain Scheduling Via Linear Fractional Transformatins," *Syst. Contr. Lett.*, 22(2): 1994, pp. 77-92.

[25] P. Apkarian , P. Gahinet. "A Convex Characterization of Gain Scheduled H_∞ controllers," *IEEE Trans. Automat. Contr.*, AC-40(5), 1995, pp. 853-864.

[26] F. Wu, X. H. Yong, A. K. Packard, and G. Becker. "Induced L_2 Norm Control for LPV Systems with Bounded Parameter Variation Rates," *Int. J. Robust Non. Contr.*, 6(9/10), 1996, pp. 983-1996.

[27] J. S. Shamma and M. Athans. "Analysis of Gian Scheduled Control for Nonlinear Plants," *IEEE Trans. Automat. Contr.*, AC-35 1990, pp. 898-907.

[28] J. Yu and A. Sideris "H_∞ Control with Parametric Lyapunov Functions," *Sys. Contr. Lett.*, Vol.30, 1997, pp. 57-69.

[29] P. Apkarian, P. Gahinet and G. Becker, "Self-scheduled H_∞ Control of Linear Parameter-varying systems: a Design Example," *Automatica*, 31(9): pp. 1251-1261, 1995.

[30] A.Rehm and F. Allgower , "Self-scheduled Nonlinear Output Feedback H_∞ Control of a Class of Nonlinear Systems," *Proceedings of Amcrican Control Conference*, New Mexico, 1997, pp. 386-390.

[31] G. J. Balas, I. Fialho, A. Packard, J. Renfrow, and C. Mullaney, "On the design of LPV controllers for the F-14 aircraft lateral-directional axis during powered approach," *Proceedings of the American Control Conference*, 1997, Volume: 1 pp. 123 -127.

[32] F. Wu, A. Packard, and G. Balas, "LPV Control Design for Pitch-axis Missile Autopilots," *Proceedings of the 34th IEEE Conference on Decision and Control*, Volume: 1, 1995, pp. 188 -193.

[33] F. Wu, "Switching LPV Control Design for Magnetic Bearing Systems," *Proceedings of the 2001 IEEE International Conference on Control Applications*, 2001, pp. 41 -46.

[34] N. C. Pahalawaththa and U. C. Annakkage, "An Optimum Gain Scheduling Power System Stabilizer," *Proceedings of the IEE International Conference on Advances in Power System Operation, Control, and Management*, November 1991, Hong Kong, pp. 211-215.

[35] F. Ghosh and I. Sen, "Design and Performance of a Local Gain Scheduling Power System Stabilizer for Inter-Connected System," *IEEE Region 10 International Conference on EC3-Energy, Computer, Communication and Control Systems*, 1991, Volume: 1, pp. 355 -359.

[36] A. M. Sharaf and T. T. Lie, "A Hybrid Neuro-Fuzzy Power System Stabilizer," *IEEE International Conference on Neural Networks*, Volume: 3, 1994, pp. 1760 -1765.

[37] J. Reeve and M. Sultan, "Gain Scheduling Adaptive Control Strategies for HVDC Systems to Accommodate Large Disturbance," *IEEE Transactions on Power Systems*, Vol 9, No. 1, February 1994. pp. 366-372.

[38] M. A. Pai, D. P. Sen Gupta and K. R. Padiyar, "Topics in Small Signal Analysis of Power Systems," *Final Report Project ♯ NSF INT 93-02565*, January 2003.

[39] S. Cui, et. al., "Design of Power System Stabilizer Based on Robust Gain Scheduling Control Theory," *PowerCon 2000. International Conference on Power System Technology*, Volume:3, 2000, pp. 1191 -1196.

[40] C. T. Pan and C. M. Liaw, "An Adaptive Controller for Power System Load Frequency Control," *IEEE Trans. on Power Sys.*, Vol.4, No.1, 1989, pp. 122-128.

[41] M. Djukanovic et.al., "Two Area Load Frequency Control with Neural Nets", *Proc. NAPS* , pp. 161-169.

[42] P. Kundur, G.J. Rogers, and D.Y. Wong, " Extended Transient Midterm Stability Program Package: Version 2.0, user's manuals," *ERPI EL-6648*, December 1989.

[43] P. Kundur, M. Klien, G. J. Rogers, and M. Zwyno, "Applications of Power System Stabilizers for Enhancement of Overall System Stability," *IEEE Trans. on Power Systems*, vol.4, No. 2, May, 1989, pp. 614-622.

[44] V. Vittal, M. Khammash, and M. Djukanovic, " Robust Analysis and Design of Control in Power Systems," *ERPI TR-111922*, Dec. 1998.

[45] G. J.Balas, J. C. Doyle, K. Glover, A. Packard and R. Smith, " μ Analysis and Synthesis Toolbox User's Guide," *Natick, Mass.:Mathwork*, 1993.

[46] Z. Lin, M. Khammash, "Robust gain-scheduled aircraft longitudinal controller design using an H_∞ approach," *Proceedings of the American Control Conference*, June, 2001 , Volume: 5 pp. 2724-2729

[47] W. Qiu, M. Khammash and V. Vittal, "Power System Stabilizer Design Using LPV Approach," *Proceedings of the 34th North American Power Symposium*, 2002, pp. 67-74.

[48] D. Silak, D. Stipanovic and A. Zecevic, "Robust Decentralized Turbine/Governor Control Using Linear Matrix Inequalities," *IEEE Transactions on Power Systems*, Vol. 17, No. 3, Aug. 2002, pp. 715-722.

[49] K. Ohtsuka and Y. Morioka, "A Decentralized Control System for Stabilizing a Longitudinal Power System Using Tieline Power Flow Measurements," *IEEE Transactions on Power Systems*, Vol. 12, No. 3, Aug. 1997, pp. 1202 -1209.

[50] V. Vittal, "Transient Stability Test Systems for Direct Stability Methods," *IEEE Transactions on Power Systems*, No.1, Feb. 1992, pp. 37-44.

[51] A. Felliachi, "Identification and Decentralized Control of Critical Modes in Electrical Power Systems," *EPRI Report TR-103900*, Octorber 1994.

[52] G. Rogers, " Power System Oscillations," *Kluwer Academic Publishers*, 2000.

[53] E.V. Larsen and D.A. Swann, " Applying Power System Stabilizers Part I,II,III," *IEEE Trans. on Power Systems*, vol. PAS-100, No.6 June 1981, pp. 3017-3046.

[54] P. Pourbeik and M. J. Gibbard, "Simultaneous Coordination of Power System Stabilizers and FACTS Device Stabilizers in a Multimachine Power System for Enhancing Dynamic Performance," *IEEE Trans. on Power Systems*, vol. 13 Issue 2, May 1998, pp. 473 -479.

[55] Fen Wu, "Control of Linear Parameter Varying Systems," *Ph.D. dissertation*, Universisty of California at Berkeley, 1995.

[56] "Transient Stability Assessment Tool," *Powertech Labs Inc.*, Surrey, British Columbia, Canada, March, 2003.